Capacity reservation for humanitarian relief: A logic-based Benders decomposition method with subgradient cut

Penghui Guo[a], Jianjun Zhu[a,*]

[a] *College of Economics and Management, Nanjing University of Aeronautics and Astronautics, Nanjing 211106, China*

Abstract

Prepositioning of relief supplies has been widely addressed to cover the demands of humanitarian emergencies. However, cost inefficiency, item type limitation, and damage risk make solely relying on prepositioning unrealistic. We develop two-stage stochastic models that incorporate prepositioning, physical capacity reservation, and production capacity reservation for reactive procurement. As an alternative to the traditional physical capacity reservation, the production capacity reservation is inspired by the practice of the automotive industry, garment industry, etc. for manufacturing personal protective equipment during the pandemic. Our models minimize the supply-side monetary costs and the demand-side social impacts, i.e., deprivation costs. The discretized deprivation cost function is introduced to handle the nonlinear deprivation cost function. The hierarchical nature of our stochastic models motivates us to utilize the logic-based Benders decomposition (LBBD). Our Benders master problem contains one set of nonbinary integer variables for prepositioning inventory and another set of continuous variables for estimating the second-stage costs, which differs from the existing LBBD works that typically contain binary and continuous variables in the master problem. Hence, a new type of logic-based Benders optimality cut, namely logic-based subgradient cut, is first introduced. To compute the cutting coefficients efficiently, heuristics that can lead to almost optimal solutions is developed. We also develop warm-start cutting planes, namely wait-and-see cuts and expected-value cuts, to help with better upper bounds and lower bounds. Extensive numerical results followed by a case study validate the efficiency of the solution method, the value of incorporating stochasticity, and the superiority of the capacity reservation.

Keywords: humanitarian logistics, capacity reservation, deprivation cost, two-stage stochastic programming, logic-based Benders decomposition

1. Introduction

From 2000 to 2021, 9869 recorded natural disasters caused over one million deaths, more than four billion people affected, and more than 3585 billion USD economic losses worldwide (CRED, 2022). Humanitarian logistics plays a vital role in the four phases (mitigation, preparedness, response, and recovery) of humanitarian relief (McLoughlin, 1985). The mission of humanitarian logistics is to alleviate human suffering by delivering aid to affected people under the situation of hazards. Humanitarian logistics is defined as "the process of planning, implementing and controlling the efficient, cost-effective flow and storage of goods and materials, as well as related information, from point of origin to point of consumption for the purpose of meeting the end beneficiary's requirements" (Thomas & Mizushima, 2005). For instance, the World Food Program (WFP) reached about 100 million of beneficiaries with 4.4 million metric tons of food to respond to 21 emergencies in 2019 (WFP, 2020). Humanitarian logistics accounts for up to 80% of total relief efforts (funds) (Hein et al., 2020). Furthermore, among activities in humanitarian logistics (e.g. warehousing, procurement, and transportation), procurement accounts for 65% expenditures and is the most costly (Falasca & Zobel, 2011). However, for humanitarian organizations that typically operate with a limited budget (Keshvari Fard et al., 2022), it is challenging to trade-off between suffering decrease and cost reduction.

We study the problem of inventory preparation, capacity reservation, and allocation for humanitarian relief. The goal is to balance the procurement before and after a disaster, such that human suffering and monetary cost can be minimized. In the preparedness phase, to be able to respond to a sudden onset disaster, it is common to prepare a certain amount of relief inventory for the vulnerable areas. This mechanism that procuring relief suppliers in advance of disasters strike is namely *prepositioning*. The major superiority of prepositioning to post-disaster procurement is the shorter lead time. Practically, the United Nations Humanitarian Response Depot (UNHRD) and the International Federation of Red Cross and Red Crescent Societies (IFRC) operate several facilities around the world that keep emergency stocks to provide immediate assistance to the affected areas (Balcik et al., 2019). The United Nations Office for the Coordination of Humanitarian Affairs (OCHA) allocates its 15% of funds for prepositioning to cover the demand of the first few weeks of an emergency. The prepositioning stock

*Corresponding author
Email addresses: guopenghui@outlook.com (Penghui Guo), zhujianjun@nuaa.edu.cn (Jianjun Zhu)

is determined by considering procurement lead times (OCHA, 2018). Studies on prepositioning can be traced back to more than ten years ago (Rawls & Turnquist, 2010; Salmerón & Apte, 2010; Sabbaghtorkan et al., 2020). However, there are some shortcomings of prepositioning. Firstly, prepositioning can be financially prohibitive (Balcik & Beamon, 2008). As mentioned before, procurement occupies the majority of humanitarian logistics costs. A higher level of prepositioning inventory implies less budget can be used for response activities. This is especially a matter of concern since humanitarian organizations usually do not have sufficient funds (Keshvari Fard et al., 2022). Secondly, certain types of relief suppliers that is perishable, e.g., prepared food, blood, and vaccine, cannot be stored for a long time before they are consumed. For example, the Federal Emergency Management Agency (FEMA) spoiled prepared meals worth more than 40 million USD due to insufficient refrigeration space (Hsu, 2007). Thirdly, the prepositioning inventory is at the risk of being damaged, since the location of warehouses can be near or in the affected areas for providing prompt response. Lastly, humanitarian organizations usually rely on donations to operate (Keshvari Fard et al., 2022). The donors can be less interested in providing funds for pre-disaster inventory than reactive replenishment (Eftekhar et al., 2022). In conclusion, it is usually impossible to solely rely on prepositioning to respond.

We integrate the post-disaster procurement into the well studied prepositioning problem. In the response phase, the procurement process is implemented within a capacity reservation framework that is negotiated between the suppliers and the buyer (humanitarian organization). The capacity reservation framework guarantees the buyer quantity and price, and allows the supplier to manage its capacity better (Akbalik et al., 2017; Serel et al., 2001). Procuring from the local spot market is neglected because of the limited quality and production capacity (Moshtari et al., 2021). There are some examples of capacity reservation in the humanitarian context. Firstly, the Doctors Without Borders (MSF) signs contracts with qualified potential suppliers a long time before a disaster, thus tendering can be completed within a relatively shorter period (two or three days) when in emergencies (Moshtari et al., 2021). Secondly, FEMA uses the advanced contracting strategy to award suppliers contracts of goods and services in advance of disaster declarations for rapid response. The contracts usually cover years (FEMA, 2022). Thirdly, to alleviate the conflict between overcapacity in usual and insufficient capacity in emergencies, China selects enterprises that produce certain types of productions (e.g., medicine, vaccine, and rescue equipment) for emergency capacity reservation (NDRC, 2021). Once upon emergency occurrence, these enterprises will produce and provide what is in need. We refer to all the previously mentioned capacity reservations as *physical capacity reservations* (PHCR). Although these examples demonstrate that the capacity reservation accelerates the delivery and improves the reliability of relief aids, capacity reservation for humanitarian relief has not been broadly addressed in the literature, which is inconsistent with its practice.

Unpredictability is one of the most crucial characteristics of humanitarian emergencies. The last two years (2020–2021) have witnessed an extreme shortage of personal protective equipment (PPE) caused by the unpredictable COVID-19 pandemic. The practice of the PPE manufacture during the pandemic inspires us with another type of capacity reservation, we call it *production capacity reservation* (PRCR), which reserves production capacity rather than physical suppliers. On February 10, 2020, the SAIC-GM-Wuling Automobile (SGMW), one of the major automobile manufacturers in China, converted its production capacity to produce face masks for combating the pandemic. Seven days later, on February 13, the first batch of face masks in a quantity of 0.5 million was accomplished. Actions similar to the SGMW were also taken by some others in the automotive industry in China. It is surprising that the automotive industry can produce distinct production after such a short period of conversion. The reasons that the automotive industry is able to manufacture PPE are two folds. Firstly, cleanrooms in the automotive industry for painting are capable of the requirement for PPE production. Secondly, the main raw material for automotive sound-absorbing foam is the same as that for face masks, i.e., polypropylene. Meanwhile, the United Nations International Children's Emergency Fund (UNICEF) helped manufacturers in the garment industry in South Asia to meet technical specifications for PPE. The long-term arrangements were finally established with a Sri Lanka manufacturer that can meet all the requirements for PPE, i.e., technical specifications, material availability, and regulatory performance standards (UNICEF, 2021). In Latin America and the Caribbean countries, during the first wave of the COVID-19 pandemic, adaptions and adjustments by the alcoholic beverages industries, textiles industries, household appliance industries, and research institutes converted their production capacities to hand sanitizer, masks, shields, and test kit, respectively (UNDRR, 2022; Haraguchi et al., 2022; ECLAC, 2020). Exploiting the similarities between industries is a promising way for PRCR. This strategy is especially useful for large-scale unpredictable emergencies. Compared with the PHCR, uncertainty of the lead time is involved, since there is usually not a time guarantee for transforming to a new type of item production.

Though this study is inspired by the need for PPE production capacity during the pandemic, its scope extends beyond this particular situation. The proposed PRCR is not limited to future pandemics, as it can also be used for other disasters that may result in unanticipatable demand and have long-lasting impacts. Reports by the government of China (NDRC, 2021), the United States government (Li et al., 2022a), as well as humanitarian organizations (UNDRR, 2022; Haraguchi et al., 2022; ECLAC, 2020) suggest that PRCR is a potential strategy for disaster preparedness. However, there is no agenda for deploying this emerging strategy, and it remains unclear how to implement this approach within existing prepositioning-based systems and what impact it may have on overall performance. While the PRCR has shown potential in certain circumstances, it is worth noting that it is not a universal solution for disaster relief. We propose that the PRCR be used in conjunction with prepositioning and PHCR. This study attempts to offer a possible way to integrate the PRCR into prepositioning and PHCR systems for building a versatile disaster response system. Different types of disasters require distinct relief systems based on

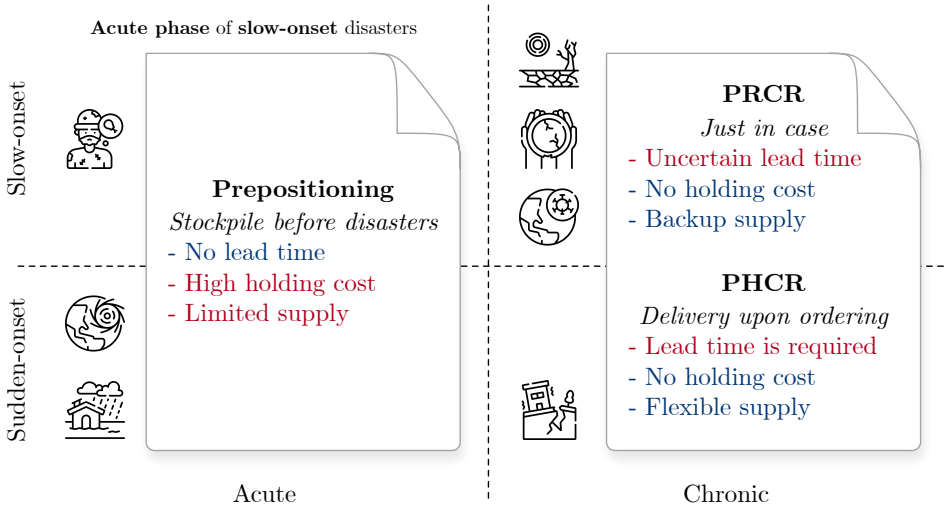

Figure 1: Relief systems for different types of disasters

their characteristics. Disasters can be classified into sudden-onset (e.g., hurricanes, floods, and earthquakes) or slow-onset (e.g., droughts, famines, and epidemics) based on the speed of onset. Based on the duration, severity, and impact, disasters can also be categorized as acute disasters, which typically last for hours or days; or chronic disasters, which can last for months or years and result in long-term impacts. The combination of these two characteristics results in four types of disasters as shown in Figure 1. Each relief system in this study is designed to fit one or several types of disasters within these four categories. Prepositioning is a reliable disaster relief strategy that requires no lead time and ensures timely delivery of relief items from warehouses to affected areas. However, the high cost of holding inventory limits the quantity of prepositioned items. Therefore, this strategy is best suited for sudden-onset acute disasters or the initial days (acute phase) following other types of disasters when external deliveries are not possible and total demand is relatively low. The PHCR is applicable for chronic disasters with long-lasting impacts. Additionally, it can be implemented before a slow-onset disaster strikes when the time from the early warning to the actual event is sufficient. Unlike prepositioning, the PHCR does not incur holding costs but requires lead time. It complements prepositioning by balancing cost and timeliness. The PRCR shares similarities with PHCR but faces uncertainty in lead time. It is preferable for slow-onset chronic disasters when demand quantity is unanticipatable. In addition to the examples of PPE mentioned earlier, PRCR has also been used for distributing drinking water, one of the most critical supplies in emergency responses, by several beverage factories [1] in the United States. This is possible because water purification is one of the initial steps in the production process of beverages. In disaster-prone areas, multiple types of disasters can occur. Decision-makers must balance lead time, quantity, and price to determine appropriate aid sources. Therefore, integrating prepositioning, PHCR, and PRCR can be beneficial because of the synergy they create.

In this study, aiming at decreasing suffering for affected people and reducing costs for humanitarian organizations, we develop a two-stage multi-phase stochastic programming model for the capacity reservation problem. The first stage determines the quantity of prepositioning relief suppliers. The second stage, which consists of multiple decision periods, procures relief suppliers from both PHCR suppliers and PRCR suppliers. The available relief supplies are distributed to affected areas that have uncertain demands. In order to coordinate the supplies with the buyer, we introduce the quantity-flexibility contract as a capacity reservation mechanism. The benefits of our capacity reservation problem are: (i) Compared with the pure prepositioning model, our model is more flexible because it allows decision-makers to allocate more budget towards the response phase. Additionally, our model is cost-efficient because it reduces inventory holding costs that arise from pre-disaster procurement. (ii) Compared with the pure response model, our model avoids a shortage of relief supplies in the initial days after a disaster strike. We investigate not only supply-side monetary costs but also demand-side social impacts for which the literature is still in its infancy (Sabbaghtorkan et al., 2020). Specifically, the demand-side social impacts in this study are measured by the *deprivation cost* (Holguín-Veras et al., 2013). The deprivation cost is used to evaluate the economic cost of human suffering associated with a lack of access to a good or service. The nonlinearity nature of the deprivation cost function adds computational complexity to the optimization model. Hence, we propose a discretization transformation, namely *discretized deprivation cost function* (DDCF), that can handle any form of deprivation cost function. Even with the DDCF, the stochastic programming model is still challenging to be solved exactly. A solution method based on the logic-based Benders decomposition (LBBD) (Hooker & Ottosson, 2003) is developed to solve the problem efficiently. The structure of our problem differs from existing works using LBBD. That is our Benders master problem contains one set of nonbinary integer variables for prepositioning inventory and another set of continuous variables for estimating the second-stage recourse cost. The existing literature using LBBD usually contains binary variables with continuous (or nonbinary integer) variables in the master problem. This difference calls for a new class of logic-based Benders cuts. The logic-based *subgradient cut*, which is a new class of logic-based Benders *optimality cut*, is thus first introduced to the LBBD. In summary, the contributions of this work lie in both modeling and solution methodology

as follows.

- We propose a stochastic capacity reservation model that incorporates prepositioning, PHCR, and the novel PRCR. As far as we know, capacity reservation has not been satisfactorily addressed, and we are the first that introduces PRCR to humanitarian operations management. Uncertainty of demand and lead time are involved in our two-stage stochastic model. Furthermore, the quantity-flexibility contract is introduced to coordinate the suppliers with the buyer.
- The DDCF is proposed to cope with the deprivation cost function that is usually nonlinear. This transformation is capable of any form of deprivation cost function. Since the practical decision making process of humanitarian operations management is usually in a discrete manner, i.e., in days or hours, the DDCF is general enough for practice. The DDCF is less computationally intractable compared with the original nonlinear (usually exponential) ones.
- We first introduce the logic-based subgradient cut, which is a new class of Benders optimality cut, to the LBBD algorithm. In the existing LBBD literature, the works that contain two sets of variables in the master problem always have one set of quantitative (continuous / nonbinary integer) variables and another set of combinatorial (binary) variables, while ours contains two sets of quantitative variables. Thus, the subgradient cut is distinct from existing logic-based Benders cuts in terms of the information delivered. The cutting coefficients for the subgradient cut are computed by an efficient heuristics. This heuristics leads to almost optimal solutions and requires far less computational effort. We believe that the subgradient cut can be adopted to other classes of problems, and this work can inspire future studies on the LBBD.

The remainder of this paper is organized as follows. Section 2 reviews related literature. Section 3 formulates the prepositioning, PHCR, and PRCR models. Section 4 develops an LBBD algorithm with subgradient cuts. Numerical results are reported in Section 5 before conclusions in Section 6.

2. Literature review

2.1. Prepositioning and post-disaster procurement

Humanitarian and disaster operations management activities can be categorized into four phases based on the life cycle of disaster: pre-disaster mitigation and preparedness, post-disaster response and recovery (McLoughlin, 1985; Çelik et al., 2012). We focus on the preparedness phase and response phase since WFP, the largest humanitarian organization in the world, demonstrated the importance of preparedness and response by "emergency preparedness and response is rooted within WFP policies". The preparedness activities focus on facility location, asset prepositioning, resource allocation, transportation planning, and contract designing, such that the response activities can be conducted efficiently. In the preparedness phase, prepositioning of relief supplies, e.g., water, food, and medicine, is one of the main activities to combat disaster impact (Sabbaghtorkan et al., 2020). Since one of the main factors for prepositioning is the uncertainty of the disaster impact, most of the works on prepositioning exploit the stochastic optimization (Alem et al., 2016; Noham & Tzur, 2018; Erbeyoğlu & Bilge, 2020; Ni et al., 2018; Torabi et al., 2018; Sanci & Daskin, 2019). For a sudden-onset disaster, prepositioning results in a short lead time and thus increases relief efficiency. However, financial expense prohibits many humanitarian organizations from storing relief supplies and it is usually impossible to solely rely on prepositioning inventory in the response phase (Balcik & Beamon, 2008). The response activities aim at distributing available relief supplies that are either prepared in the preparedness phase or replenishment in the response phase (through procurement, loan, or donation) to alleviate the suffering of affected areas. Studies in the response phase usually use dynamic models to capture the timeline of inventory management and supply distribution processes (Das & Hanaoka, 2014; Acar & Kaya, 2022; Hu et al., 2017; Loree & Aros-Vera, 2018; Zhang et al., 2022b; Liu & Xie, 2021; Zhang et al., 2021a; Boujemaa et al., 2020; Sakiani et al., 2020).

Researches on procurement are inconsistent with the role that procurement plays in humanitarian operations management (Moshtari et al., 2021). Relatively few studies are performed on both pre-disaster prepositioning and post-disaster procurement simultaneously. Specifically, the post-disaster procurement can be from the local spot market, within a PHCR framework, and within a PRCR framework. There are some works that consider one or combinations of procurement methods. Procurement of relief supplies from the local spot market is the most simple and easy to be implemented among all the three. Eftekhar et al. (2022) studied a mixed prepositioning and local purchasing problem with uncertain demand, supply, and budget. They demonstrated that the ability of prepositioning is limited by difficulty in determining item type and quantity, high holding cost, and donor preference. Alem et al. (2021) developed an optimization model for capacity planning, prepositioning, and local procuring. They pointed out that local procurement can suffer from the unavailability of goods. (Physical) Capacity reservation is a possible way to avoid spot market unavailability and it has been more widely studied in the commercial context in the past decade (Boulaksil et al., 2011; Park & Kim, 2014; Hou et al., 2017; Cheaitou & Cheaytou, 2019). To engage PHCR, negotiation with suppliers to achieve agreement is required. This makes the problem related to the supplier selection, readers may refer to Hu et al. (2022) for a literature review. Balcik & Ak (2014) considered a supplier selection problem for establishing framework agreement using two-stage stochastic programming. The first-stage determines the selection for supplies and the second-stage determines the amount of supplies to be purchased. Nevertheless, propositioning is not included in their model, and only the

initial phase after diaster is considered. Hu & Dong (2019) developed a stochastic model for procurement activities before and after a disaster. Their model aims at determining the location and size of relief facilities, achieving agreement frameworks with supplies, and optimizing the procurement quantity. Above are all PHCR, to the best of our knowledge, the PRCR has not been addressed in the humanitarian operations management literature, though it has shown great potential during the COVID-19 pandemic.

Contracting is essential for achieving agreement and implementing capacity reservation. In the humanitarian context, the option contract (Zhang et al., 2019; Wang et al., 2015; Liu et al., 2021; Liang et al., 2012; John et al., 2020; Hu et al., 2019; Devi Prasad Patra & Jha, 2022; Chen et al., 2017; Liu et al., 2019), quantity-flexibility contract (Nikkhoo et al., 2018; John & Gurumurthy, 2021), and their combination (Ghavamifar et al., 2022) are the most common approaches. Note that the majority of these papers used game theory. In the following, we detail works that involve contracting into mathematical programming models for humanitarian operations management. Both option contracts and quantity-flexibility contracts promise to deliver relief supplies according to agreement terms. Akbarpour et al. (2020) proposed a min-max robust model for pharmaceutical relief network design problem with option contract. Options with different prices and amounts are known in advance and are used as the parameters that determine the procurement price and maximum amount. They observed increasing option size can reduce prepositioning holding and procurement costs. Aghajani et al. (2020) designed a two-period option contract for stochastic prepositioning-inventory problem. Cost efficiency is improved by reducing the prepositioning inventory in the areas where there are sufficient supplies. Balcik & Ak (2014) developed a two-stage stochastic model for supplier selection. The contract criteria are initially provided by supplies as input parameters. In the first stage, the humanitarian organization determines which supplier is selected. In the second stage, the humanitarian organization determines the quantity to be purchased. The first-stage agreement fee as well as the expected second-stage procurement cost and penalty cost of unmet demand is minimized. Torabi et al. (2018) proposed a two-stage stochastic model for pre-disaster prepositioning and post-disaster procurement. The second-stage procurement process is based on the quantity-flexibility contract determined in the first stage. Existing studies suggest that contracting, as a coordination mechanism between supplier and buyer for capacity reservation, is promising in terms of reducing prepositioning costs. However, it remains a topic that has not been well addressed in the humanitarian context. Furthermore, the aforementioned works with contracting neglect the timeline of post-disaster procurements and distributions for relief supplies, i.e., current decisions can have impacts on future decisions, which is crucial for effective response.

2.2. Deprivation cost

The objective of this study consists of not only supply-side monetary costs but also demand-side social impacts as suggested by Sabbaghtorkan et al. (2020). Specifically, the social impacts considered in this study are the *deprivation cost*. The deprivation cost was first introduced by Holguín-Veras et al. (2013) to evaluate the economic cost of the human suffering associated with a lack of access to goods or services. The deprivation cost is a monotonic, non-linear, and convex function with respect to deprivation time. The natural questions for incorporating deprivation cost into humanitarian logistics problems are how to formulate the deprivation cost function and how to evaluate the parameters of the deprivation cost function. Holguin-Veras et al. (2016) estimated the deprivation cost function of drinkable water using contingent valuation. They concluded that the deprivation cost has non-linear relation with the deprivation time and the exponential function fits the data better. After this work, there are other estimates for deprivation cost using the Box-Cox transformations (Cantillo et al., 2018; Macea et al., 2018; Fernandez Pernett et al., 2022) and exponential function fittings (Cantillo et al., 2018; Macea et al., 2018). It is worth noting that all the works that specialized in deprivation cost estimation demonstrate the nonlinearity of the deprivation cost function. In the following, we focus on studies that formulate the objective function based on the deprivation cost. Works that use proxy measures for deprivation cost, e.g., penalty-based formulations and models that minimize unmet demand are neglected. Readers may refer to Shao et al. (2020) for a literature review on deprivation cost.

The literature on deprivation cost typically deals with location, allocation, inventory, transportation, and routing problems (Table 1). The resulting optimization problems can be deterministic (Perez-Rodriguez & Holguin-Veras, 2016; Zhu et al., 2019), dynamic (Yu et al., 2018, 2019; Ismail, 2021; Loree & Aros-Vera, 2018), robust (Wang & Paul, 2020; Paul & Wang, 2019; Ni et al., 2018), and stochastic (Rafiei et al., 2022; Moreno et al., 2018; Pradhananga et al., 2016; Jamali et al., 2021; Paul & Zhang, 2019). In terms of the deprivation cost functions used for numerical study, it is not surprising that the exponential is the majority (9 in 14, Table 1), which is aligned with the aforementioned studies on deprivation cost function estimation. However, involving nonlinearity adds computational difficulties to the optimization problems, hence some works adopted to piecewise-linear functions (Jamali et al., 2021; Paul & Zhang, 2019; Wang & Paul, 2020; Paul & Wang, 2019) or linear functions (Ni et al., 2018). In order to avoid the nonlinearity, Yu et al. (2018, 2019) introduced a metric namely starting state-based deprivation cost (SSDC) for discretized time periods. They developed a dynamic programming algorithm to solve the problem. Another way to handle the nonlinearity is the heuristics that was first introduced by Perez-Rodriguez & Holguin-Veras (2016) and applied by Loree & Aros-Vera (2018). The specialized exact solution methods in sense of proven optimality have not been widely addressed for problems with deprivation cost. Most existing works addressing the problem rely on either heuristics or off-the-shelf solvers (Table 1), particularly those utilizing two-stage stochastic programming. However, heuristics always cannot guarantee solution

Table 1: Literature using the deprivation cost

Paper	Problem	Model	DCF	Solution method
Perez-Rodriguez & Holguin-Veras (2016)	Inventory-allocation-routing	DT	E	Heuristics
Zhu et al. (2019)	Routing	DT	E	Ant colony algorithm
Yu et al. (2018)	Allocation	DN	E*	Dynamic programming
Yu et al. (2019)	Allocation	DN	E*	Dynamic programming
Ismail (2021)	Inventory-transportation	DN	E	Rolling horizon
Loree & Aros-Vera (2018)	Location-inventory-allocation	DN	E	Outer approximation
Rafiei et al. (2022)	Procurement and cash transfer	2SS	E	SAA & CPLEX
Moreno et al. (2018)	Location-transportation	2SS	E	Heuristic
Pradhananga et al. (2016)	Resource allocation	2SS	E	CPLEX
Jamali et al. (2021)	Location-transportation	2SS	PL	Goal Programming & GAMS
Paul & Zhang (2019)	Location-transportation	2SS	PL	CPLEX
Wang & Paul (2020)	Preparation	RB	PL	CPLEX
Paul & Wang (2019)	Location-allocation	RB	PL	CPLEX
Ni et al. (2018)	Location-inventory	RB	L	CPLEX (Benders decomposition)
This paper	Preparation-inventory-allocation	2SS	E*	LBBD

[1] `DCF`: deprivation cost function; `DT`: deterministic; `DN`: dynamic; `2SS`: two-stage stochastic; `RB`: robust; `E`: exponential; `PL`: piecewise-linear; `L`: linear; `*`: discretized.

quality while uncertainty and nonlinearity challenge the off-the-shelf solvers by the scale of the problem that can be handled. We contribute to the deprivation cost literature by introducing the DDCF that can handle exponential deprivation cost function directly without loss of accuracy. Indeed, the DDCF is capable of any form of deprivation cost function.

2.3. Benders decomposition

The solution method for the proposed capacity reservation problem is based on the LBBD (Hooker & Ottosson, 2003), which is a generalization of the classic Benders decomposition (BD) (Benders, 1962). BD is an outer approximation technique that uses cutting planes to approximate the true objective function of the original problem. BD decomposes a mathematical programming problem into a master problem and subproblems that use trail solutions and *Benders cuts* to exchange information. Before convergence, the master problem feeds trail solutions to subproblems and subproblems generate Benders cuts to exclude suboptimal solutions. The hierarchical nature of stochastic programming implies the potential of BD. For the stochastic problem with a huge number of constraints in the *deterministic equivalent*, the BD does not have to add all the constraints before the searching begins, consequently, the computational burden is reduced. Note that the BD for stochastic programming is known as the L-shaped method (Van Slyke & Wets, 1969). The classic BD relies on the dual subproblem, thus subproblems must be linear programming (LP), which limits the ability of the classic BD method. Hence there emerged some variants of BD, including the combinatorial Benders decomposition (CBD) (Codato & Fischetti, 2006), the generalized Benders decomposition (GBD) (Geoffrion, 1972), and the integer L-shaped method (Laporte & Louveaux, 1993) that each supports specific types of problems (Table 2). Readers may refer to Rahmaniani et al. (2017) for a literature review on Benders decomposition. The LBBD is the latest advance in the Benders methods. The advantage of the LBBD compared with others is it can be applied to any class of optimization problems, e.g., mixed integer linear programming (MILP), non-linear programming (NLP), and feasibility-checking problem (Hooker & Ottosson, 2003; Rahmaniani et al., 2017). However, the LBBD approach for generating Benders cuts differs from other methods. Specifically, the Benders cuts must be customized to suit the specific problem being addressed.

The LBBD has been used for solving problems such as planning (Roshanaei & Naderi, 2021; Barzanji et al., 2020; Hooker, 2007; Martínez et al., 2022; Leutwiler & Corman, 2022; Elçi & Hooker, 2022), scheduling (Naderi & Roshanaei, 2022; Zhang et al., 2022c; Naderi & Roshanaei, 2020; Restrepo et al., 2018; Tran et al., 2016; Roshanaei et al., 2017; Zhang et al., 2022a; Gedik et al., 2016; Riise et al., 2016; Guo et al., 2021), location (Li et al., 2022b; Fazel-Zarandi & Beck, 2012; Fazel-Zarandi et al., 2013; Wheatley et al., 2015), routing (Fachini & Armentano, 2020; Kloimüllner & Raidl, 2017), and network designing (Baloch & Gzara, 2020; Enayaty-Ahangar et al., 2019). In the context of humanitarian and disaster operations management, Erbeyoğlu & Bilge (2020) is the only one. Additionally, works that solve stochastic programming with LBBD are emerging these years (Lombardi et al., 2010; Fazel-Zarandi et al., 2013; Wheatley et al., 2015; Erbeyoğlu & Bilge, 2020; Guo et al., 2021; Elçi & Hooker, 2022). Hooker (2019) reviewed works with LBBD comprehensively. The Benders cuts, subproblem, and master problem are the key components of LBBD. Unlike other BD variants that have a standard way to generate Benders cut and only allow a certain class of subproblem and master problem, the LBBD Benders cuts, subproblem, and master problem can vary with problems. In terms of Benders cuts, the logic-based Benders cuts can be classified into *optimality cut* and *feasibility cut*. Implementing LBBD requires one or both types of logic-based Benders cut depending on the problem structure. When the subproblem is always feasible, e.g., stochastic programming with *relatively complete* recourse (Guo et al., 2021; Elçi & Hooker, 2022), only optimality cuts are required. When the subproblem is a feasibility problem, only feasibility cuts are required. When the subproblem has an objective function and can be infeasible with certain master problem decision variable values, both optimality and feasibility cuts are required. In terms of the master problem, the majority of LBBD literature formulate the master problem using either continuous variables or general integer variables with binary variables (see papers with $\mathbb{R}, \mathbb{B}$

Table 2: Benders method variants and LBBD applications

Paper	Problem	Master	Sub	OC	FC	WS
Benders method variants:						
BD (Benders, 1962)	MILP	$\mathbb{Z}, \mathbb{R}$	LP	√	√	-
GBD (Geoffrion, 1972)	NLP	$\mathbb{R}$	Convex	√	×	-
CBD (Codato & Fischetti, 2006)	MILP	$\mathbb{R}, \mathbb{Z}, \mathbb{B}$	Linear system	×	√	-
L-shaped (Van Slyke & Wets, 1969)	Stochastic LP	LP	LP	√	√	-
Integer L-shaped (Laporte & Louveaux, 1993)	Stochastic MILP	$\mathbb{R}, \mathbb{B}$	$\mathbb{R}, \mathbb{B}$	√	×	-
LBBD (Hooker & Ottosson, 2003)	Any	Any	Any	√	√	-
LBBD for deterministic problems:						
Li et al. (2022b)	Scheduling and location	$\mathbb{R}^*$, $\mathbb{B}$	$\mathbb{R}$, $\mathbb{B}$	√	√	√
Zhang et al. (2022c)	Scheduling	$\mathbb{R}^*$, $\mathbb{B}$	$\mathbb{R}$, $\mathbb{B}$	√	×	×
Roshanaei & Naderi (2021)	Planning and scheduling	$\mathbb{R}^*$, $\mathbb{B}$	$\mathbb{R}$, $\mathbb{B}$	√	√	×
Fachini & Armentano (2020)	Vehicle routing	$\mathbb{R}^*$, $\mathbb{B}$	$\mathbb{R}$, $\mathbb{B}$	√	√	√
Naderi & Roshanaei (2020)	Scheduling	$\mathbb{R}^*$, $\mathbb{B}$	$\mathbb{R}$, $\mathbb{B}$	√	×	×
Barzanji et al. (2020)	Planning and scheduling	$\mathbb{R}^*$, $\mathbb{B}$	$\mathbb{R}$, $\mathbb{B}$	√	×	×
Hooshmand et al. (2020)	Contamination detection	$\mathbb{R}^*$, $\mathbb{B}$	$\mathbb{R}$, $\mathbb{B}$	√	√	√
Baloch & Gzara (2020)	Network design	$\mathbb{R}^*$, $\mathbb{B}$	$\mathbb{R}$, $\mathbb{B}$	√	×	×
Heching et al. (2019)	Healthcare delivery scheduling	$\mathbb{R}^*$, $\mathbb{B}$	$\mathbb{R}$, $\mathbb{B}$	√	√	×
Naderi & Roshanaei (2022)	Scheduling	$\mathbb{R}^*$, $\mathbb{B}$	$\mathbb{R}$, $\mathbb{B}$	√	×	√
Restrepo et al. (2018)	Scheduling	$\mathbb{R}^*$, $\mathbb{B}$	$\mathbb{R}$, $\mathbb{Z}$	√	×	×
Tran et al. (2016)	Scheduling	$\mathbb{R}^*$, $\mathbb{B}$	TSP	√	×	×
Kloimüllner & Raidl (2017)	Route planning	$\mathbb{R}$, $\mathbb{B}$	TSP	√	√	×
Polyakovskiy & M'Hallah (2021)	Bin packing	$\mathbb{R}$, $\mathbb{B}$	Feasibility	×	√	√
Enayaty-Ahangar et al. (2019)	Network interdiction	$\mathbb{R}$, $\mathbb{B}$	Feasibility	×	√	×
Delorme et al. (2017)	Stock cutting	$\mathbb{R}$, $\mathbb{B}$	Feasibility	×	√	×
Caglar Gencosman & Begen (2022)	Shelf space allocation	$\mathbb{Z}$, $\mathbb{B}$	$\mathbb{Z}$, $\mathbb{B}$	√	√	×
Zhang et al. (2021b)	Package consolidation	$\mathbb{Z}^*$, $\mathbb{B}$	$\mathbb{Z}$, $\mathbb{B}$	√	×	×
Roshanaei et al. (2017)	Scheduling	$\mathbb{Z}^*$, $\mathbb{B}$	$\mathbb{B}$	√	√	×
Fazel-Zarandi & Beck (2012)	Location	$\mathbb{Z}^*$, $\mathbb{B}$	Algorithmic	√	√	×
Hooker (2007)	Planning and scheduling	$\mathbb{R}^*$ ($\mathbb{Z}^*$), $\mathbb{B}$	$\mathbb{Z}$	√	√	×
Zhang et al. (2022a)	Scheduling	$\mathbb{B}$	$\mathbb{Z}$, $\mathbb{B}$	√	×	×
Martínez et al. (2022)	Production planning	$\mathbb{B}$	Feasibility	×	√	×
Roshanaei et al. (2020)	Planning and scheduling	$\mathbb{B}$	Feasibility	×	√	×
Riedler & Raidl (2018)	Dial-a-ride problem	$\mathbb{B}$	Feasibility	×	√	×
Gedik et al. (2016)	Scheduling	$\mathbb{B}$	Feasibility	×	√	×
Riise et al. (2016)	Scheduling	$\mathbb{B}$	$\mathbb{B}$	×	√	×
Leutwiler & Corman (2022)	Timetable planning	$\mathbb{R}$	$\mathbb{R}$	×	√	×
LBBD for stochastic problems:						
Guo et al. (2021)	Scheduling	$\mathbb{R}^*$, $\mathbb{B}$	$\mathbb{B}$	√	×	√
Erbeyoğlu & Bilge (2020)	Disaster preparedness	$\mathbb{R}$, $\mathbb{B}$	Feasibility	×	√	×
Elçi & Hooker (2022)	Planning and scheduling	$\mathbb{R}^*$ ($\mathbb{Z}^*$), $\mathbb{B}$	$\mathbb{Z}$	√	×	√
Lombardi et al. (2010)	Allocation and scheduling	$\mathbb{B}$	Feasibility	×	√	×
Fazel-Zarandi et al. (2013)	Facility location	$\mathbb{B}$	Feasibility	×	√	×
Wheatley et al. (2015) (Chance constrained)	Inventory-location	$\mathbb{B}$	$\mathbb{B}$	×	√	×
This paper	Humanitarian relief	$\mathbb{R}^*$, $\mathbb{Z}$	$\mathbb{R}$, $\mathbb{Z}$, $\mathbb{B}$	√	×	√

[1] `OC`: optimality cut; `FC`: feasibility cut; `WS`: warm-start; `*`: variables are estimators for the subproblem objective.

and $\mathbb{Z}, \mathbb{B}$ master problem in Table 2). Continuous variables and nonbinary integer variables are typically used to estimate the subproblem cost (see papers with * in the master problem in Table 2). For instance, the scheduling papers usually contain continuous variables in the master problem to represent the makespan that is minimized in the subproblems (Hooker, 2007; Elçi & Hooker, 2022). Logic-based Benders cuts are expressed with the master problem variables, hence, in the existing works, the logic-based Benders cuts contain continuous (or nonbinary integer) variables and binary variables. That is the logic-based Benders cuts say the current master objective value (expressed with continuous or nonbinary integer variables) can be improved when the combinatorial decisions (expressed with binary variables) are modified. However, as far as we know, there is no work containing two sets of quantitative (continuous / nonbinary integer) variables in the master problem, in which one set for subproblem cost estimating and the other set for master problem decision making. In this condition, the logic-based Benders cuts express the relationship between the objective and quantitative variables. To be more specific, let us put the facility location problem as an example. The logic-based Benders cuts in the existing works typically answer questions like "what if more facility is opened?" and "what if the assignment is changed?" to the master problem, but cannot answer "what if more inventory is prepared?". We call the logic-based Benders cuts, that describe the marginal contribution of certain continuous or nonbinary integer variables to the objective, logic-based subgradient cuts. The term "subgradient" rather than "gradient" is used since the objective function can be nonsmooth with respect to the continuous or nonbinary integer variables. Readers familiar with the GBD may recognize that it resembles the concept of *generalized Benders cuts* (Geoffrion, 1972; Fischetti et al., 2017). Nevertheless, the GBD requires convex subproblems (Lee et al., 2021; Geoffrion, 1972), whereas our subproblems are mixed integer programming (MIP), which are nonconvex. Hence, our LBBD method is novel because it introduces subgradient cuts to handle a new class of problems and bridges the gap between LBBD and GBD. Additionally, we develop warm-start cuts to strengthen upper and lower bounds in initial iterations. We believe the LBBD with subgradient cuts can provide new insights into the LBBD method.

3. Problem description and formulation

3.1. Problem description

The prepositioning, capacity reservation, and allocation problem aim at determining a reasonable level of prepositioning inventories, placing reactive orders at the right time in the right quantity, and allocating available relief supplies to affected individuals. The goal is to minimize monetary costs associated with prepositioning and capacity reservation, and humanitarian costs by insufficient and delayed response. The humanitarian relief network of interest contains three main components: (i) local distribution centers (LDCs) that paly the role of relief facilities, (ii) external suppliers who provide supplies after an emergency, and (iii) affected areas. The prepositioning inventories are prepared at LDCs before disasters. Although prepositioning allows immediate response, there are some shortcomings of it as demonstrated in Section 1, i.e., financially prohibitive, item type limitations, risk of damage, and donor preference. To overcome the shortcomings of prepositioning, we introduce the PHCR and PRCR in Section 3.4 and Section 3.5, respectively. Compared with the pure prepositioning model, both PHCR model and PRCR model involve external suppliers to provide relief supplies in the response to emergencies. The PRCR is proposed for extreme cases that require enormous relief items. Unlike PHCR, the PRCR suppliers are not necessarily producing exactly what is needed in emergencies but will produce what is required by the buyer after setting up workshops and training for personnel. Both PHCR and PRCR suppliers require lead time between the order placement and delivery. For PHCR suppliers, the lead time is certain. While for PRCR suppliers, the lead time for delivering the first order is uncertain due to their lack of experience in producing the required goods. The prepositioning inventory and reactive supplies from capacity reservation suppliers are the available resources that can be allocated to affected individuals.

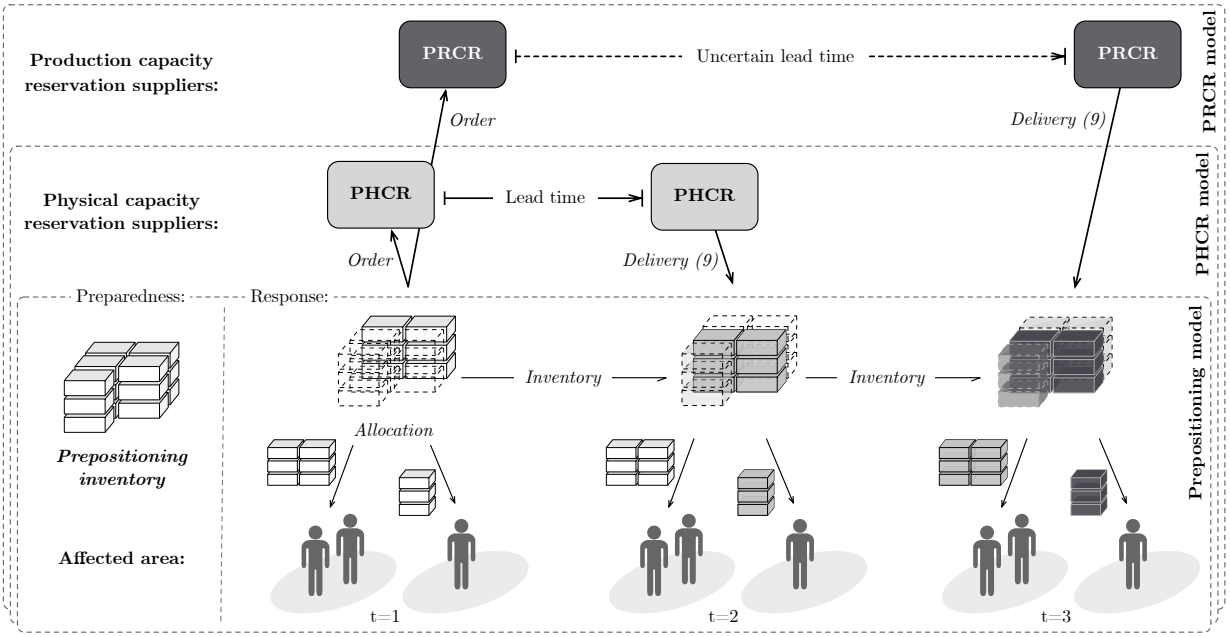

Figure 2: Prepositioning and capacity reservation

Figure 2 is an illustrative example that compares pure prepositioning with the capacity reservation enhanced prepositioning. The illustrative example has two affected areas (each has two and one affected individuals, respectively) and three periods. We assume that 15 units of relief items are prepositioned before the disaster occurs, and the demand is three units of items for each affected individual in each period. That is the total prepositioning inventory (15) cannot fully meet the demands of affected individuals during the response phase (27). This can be true in practice since holding too much inventory make humanitarian organizations less financially flexible and it is always difficult to prepare the right item at the right place in the right quantity. Without capacity reservation, i.e., PHCR and PRCR, there will be undersupply in the second and third periods. Alternatively, the decision-makers can evenly distribute the prepositioning inventory throughout the whole response phase. That is five units of relief items are allocated to three individuals in each period, although the demand is nine for three individuals. In both cases, the undersupply can result in the suffering of affected individuals. With the capacity reservation, a PHCR order and a PRCR order are placed the first time after the disaster strike ($t = 1$), and the orders are delivered ($t = 2$ and $t = 3$) after the lead time. Then at $t = 2$ and $t = 3$, the capacity reservation supplies, as well as the prepositioning inventories, are delivered to affected areas sufficiently. There is no human suffering incurred with capacity reservation. As presented in Figure 2, the PHCR model is an extension of the prepositioning model, and the PRCR model further extends the PHCR model.

Our problems take the following as inputs: (i) the unit prepositioning price, (ii) the capacity of LDCs and the maximum amount of unused relief items that can be stored in each affected area, (iii) the demand and population of affected areas, (iv) characteristics of capacity reservation suppliers (unit price, lead time, production capacity, and contract-related parameters), and (v) the deprivation cost function. In Figure 2, the italic letters represent decisions. Decisions related to emergency preparation

and response can be classified into preparedness decisions and response decisions. The preparedness decisions are mainly prepositioning inventory levels of LDCs. The response decisions include: PHCR and PRCR order quantity and timing, quantity of relief items delivered to each LDC from PHCR and PRCR suppliers, and quantity of relief items delivered to each affected area from LDCs. The objective is to minimize the summation of monetary costs and human suffering. This problem trade-off between the prepositioning cost, the reactive procurement cost, and the deprivation cost. Specifically, maintaining a high level of prepositioning inventory reduces human suffering through prompt response. However, on the other hand, prepositioning inventory is more expensive than the PHCR and PRCR supplies when the inventory holding cost is taken into account. The PHCR and PRCR supplies are more flexible than the prepositioning inventory, but the lead time makes human suffering can be incurred in the initial periods after an emergency. In summary, rather than solely relying on prepositioning or capacity reservation, combining them is more reliable.

3.2. Prepositioning model

We propose the multi-phase stochastic prepositioning model in this section as a baseline. In the following subsections, the baseline prepositioning model is extended to models with PHCR and PRCR. The prepositioning model that only involves prepositioning inventory is formulated as follows. We let R denotes the set of LDCs, D denotes the set of affected areas, and $T = \{1, 2, 3, \cdots, t_{\max}\}$ be the planning horizon. Before an emergency occurs ($t = 0$), relief items in a quantity of r_j and a unit price of u are prepared in each LDC $j \in R$. After an emergency strikes ($t \geq 1$), relief items are delivered from LDC $j \in R$ to affected areas $i \in D$ over all the period $t \in T$. For a particular realization of a scenario $s \in S$, the quantity of item delivered is denoted as f_{ji}^{ts} and the inventory level is denoted as y_i^{ts} for affected areas (y_j^{ts} for LDCs). There is not a simple rule to determine r_j and f_{ji}^{ts}, r_j and f_{ji}^{ts} can neither be too large nor too small. Large r_j and f_{ji}^{ts} may result in the capacity of LDCs (v_j) and affected areas (v_i) be exceeded. Smaller r_j and f_{ji}^{ts} may cause the demand of affected areas (d_i^{ts}) cannot be met. A set of binary variables ω_i^{ts} is introduced to indicate whether inventory at $i \in D$ at least meet the demand at $t \in T$ under scenario $s \in S$, $\omega_i^{ts} = 1$ if $y_i^{ts} \geq d_i^{ts}$ else $\omega_i^{ts} = 0$. We aim at minimizing the summation of prepositioning cost and expected deprivation cost. The mathematical model for our stochastic prepositioning-inventory problem (SPIP) is presented formally as follows. The notations are summarized in the supplementary material.

$$\text{[SPIP] minimize} \quad \sum_{j \in R} u \cdot r_j + \mathbb{E}_{s \in S}\left[\sum_{i \in D} \mathcal{D}_i^s(\phi_i^{ts}, y_i^{ts})\right] \tag{1.1}$$

$$\text{subject to} \quad \sum_{i \in D}\sum_{t \in T} f_{ji}^{ts} \leq r_j, \qquad \forall j \in R, s \in S \tag{1.2}$$

$$y_j^{0s} = r_j, \qquad \forall j \in R, s \in S \tag{1.3}$$

$$y_i^{0s} = 0, \qquad \forall i \in D, s \in S \tag{1.4}$$

$$y_j^{t-1,s} - \sum_{i \in D} f_{ji}^{ts} = y_j^{ts}, \qquad \forall j \in R, t \in T, s \in S \tag{1.5}$$

$$y_i^{t-1,s} + \sum_{j \in R} f_{ji}^{ts} - \omega_i^{t-1,s} d_i^{t-1,s} = y_i^{ts}, \qquad \forall i \in D, t \in T, s \in S \tag{1.6}$$

$$y_j^{ts} \leq v_j, \qquad \forall j \in R, t \in T, s \in S \tag{1.7}$$

$$y_i^{ts} \leq v_i, \qquad \forall i \in D, t \in T, s \in S \tag{1.8}$$

$$\omega_i^{ts} \in \{0, 1\}, \qquad \forall i \in D, t \in T, s \in S \tag{1.9}$$

$$r_j, y_j^{ts}, y_i^{ts}, f_{ji}^{ts} \in \mathbb{Z}_0^+, \qquad \forall i \in D, j \in R, t \in T, s \in S \tag{1.10}$$

$$(2.2) - (2.8), (3.1) - (3.7), \tag{1.11}$$

(1.1) minimizes the social cost, which is defined as the sum of prepositioning inventory cost and expected deprivation cost. The first term is the prepositioning inventory cost. It is worth noting that the coefficient u includes both procurement cost and holding cost. The second term is the expected deprivation cost that is formulated later in (2.1)–(2.8). (1.2) limits the total quantity of relief items that can flow out of an LDC during the planning horizon T to be less than or equal to the quantity of prepositioned items. (1.3) and (1.4) are the initial inventory of LDCs and affected areas, respectively. At the beginning of the planning horizon, inventory at each LDC is equal to the quantity of items prepositioned and we assume no inventory is prepared at affected areas. (1.5) calculates inventory level for LDCs. This equation subtracts the quantity of relief items that flow out from the previous period's inventory to determine the current period's inventory level for each LDC. (1.6) calculates inventory level for affected areas similar to (1.5). For each affected area, (1.6) substrates the consumed relief item from the sum of the previous period's inventory and incoming relief items. (1.6) does not include allocating supplies to individuals but ensures demands of individuals in each affected area can be met or not without any discrimination, which promotes fairness and equality. However, if the definition of D is based on geographical location alone, this assumption may be unrealistic due to potential heterogeneity among individuals in each $i \in D$, since individuals can have varying levels of urgency for supplies. In this case, sub-classifications can be applied within each $i \in D$, grouping together homogeneous individuals such as children,

adults, or seniors. (1.6) would then be more appropriate for geographically close and homogeneous groups. (1.7) and (1.8) limit the inventory by the capacity of LDCs and affected areas, respectively. (1.9) and (1.10) are domains of decision variables where "$\in \mathbb{Z}_0^+$" is equivalent to "≥ 0 and integer". The constraints in (1.11) are related to the deprivation cost.

To trade-off between the monetary costs and the human suffering, traditionally, there are two possible ways. Firstly, the unmet demands are penalized in the objective. In this case, it is difficult to assign weights to the unmet demands reasonably, such that the penalty costs can be at the same scale as the monetary cost. Secondly, the recourse quantities are modeled as parameters in constraints. To make actionable decisions, it is more desired that resource quantities can be decision variables. To overcome the shortcomings of the traditional methods, the deprivation cost that was first introduced by Holguín-Veras et al. (2013) is utilized to directly evaluate human suffering in the objective. The deprivation cost is defined as "the economic value of the human suffering caused by lack of access to a good or service" (Holguín-Veras et al., 2013). The method with deprivation cost avoids subjective parameters and the resources (relief supplies) quantities are modeled as decision variables. The deprivation cost with a general deprivation cost function is formulated formally as follows (Perez-Rodriguez & Holguin-Veras, 2016). Recall that y_i^{ts} be the total quantity of relief items that are available at time t for affected area i in scenario s, and d_i^{ts} be the demand of i at t in scenario s. Then let ϕ_i^{ts} denotes whether there is a delivery arrived at i at t in scenario s (if there is a delivery arrived then $\phi_i^{ts} = 1$ otherwise $\phi_i^{ts} = 0$), ω_i^{ts} denotes whether the inventory level is sufficient for affected area i at time t in scenario s ($\omega_i^{ts} = 1$ if $y_i^{ts} \geq d_i^{ts}$ else $\omega_i^{ts} = 0$), and l_i^{ts} denotes the most recent time that affected area i consumed relief items before time t in scenario s. Given the population of affected areas $w_i, \forall i \in D$, and the deprivation cost function $\gamma(\cdot)$, the deprivation cost of affected area i in the scenario s can be calculated as

$$[\text{DC}]\ \mathcal{D}_i^s(\phi_i^{ts}, y_i^{ts}) = \sum_{t \in T} w_i \cdot \phi_i^{ts} \cdot (1 - \omega_i^{t-1,s}) \cdot \gamma(t - l_i^{t-1,s}) + w_i \cdot (1 - \omega_i^{t_{\max} s}) \cdot \gamma(t_{\max} - l_i^{t_{\max} s}) \qquad \forall i \in D, s \in S \quad (2.1)$$

$$\text{subject to } d_i^{ts} - M \cdot (1 - \omega_i^{ts}) \leq y_i^{ts} \leq M\omega_i^{ts} + d_i^{ts} - \epsilon, \qquad \forall i \in D, t \in T, s \in S \quad (2.2)$$

$$d_i^{ts}\phi_i^{ts} \leq \sum_{j \in R} f_{ji}^{ts} \leq M\phi_i^{ts}, \qquad \forall i \in D, t \in T, s \in S \quad (2.3)$$

$$l_i^{ts} = l_i^{t-1,s} + \omega_i^{ts} \cdot (t - l_i^{t-1,s}), \qquad \forall i \in D, t \in T, s \in S \quad (2.4)$$

$$l_i^{ts} \geq l_i^{t-1,s}, \qquad \forall i \in D, t \in T, s \in S \quad (2.5)$$

$$l_i^{0s} = 0, \qquad \forall i \in D, s \in S \quad (2.6)$$

$$\phi_i^{ts} \in \{0, 1\}, \qquad \forall i \in D, t \in T, s \in S \quad (2.7)$$

$$l_i^{ts} \in \mathbb{Z}_0^+, \qquad \forall i \in D, t \in T, s \in S. \quad (2.8)$$

An illustrative example that helps to understand how to calculate the deprivation cost is provided in the supplementary material. (2.1) defines the overall deprivation cost where $t - l_i^{t-1,s}$ and $t_{\max} - l_i^{t_{\max} s}$ are deprivation time. The first term of (2.1) corresponds to the summation of deprivation costs incurred when a delivery is made for all the $t \in T$. The second term of (2.1) is the deprivation cost that occurred in the last period. (2.2) transforms the if statement, $\omega_i^{ts} = 1$ if $y_i^{ts} \geq d_i^{ts}$ else $\omega_i^{ts} = 0$, into a linear expression where M is a sufficiently large number and ϵ is a small number. (2.3) ensures relief item flow into affected area i if and only if $\phi_i^{ts} = 1$, i.e., a delivery is made. (2.4) links the binary variable ω_i^{ts} with integer variable l_i^{ts}. If the total supply is sufficient ($\omega_i^{ts} = 1$), (2.4) becomes $l_{it} = t$. Otherwise, if the total supply is insufficient ($\omega_i^{ts} = 0$), (2.4) becomes $l_i^{ts} = l_i^{t-1,s}$. In other words, l_i^{ts} will remain the same as that of the previous time $l_i^{t-1,s}$ when there is not enough supply but increase to t when the demand of i at t is totally met. (2.5) is a valid inequality that strengthens the formulation. Note that $l_i^{0s} = 0$ as shown in (2.6). (2.7) and (2.8) are domains of decision variables.

3.3. Discretized deprivation cost function

The deprivation cost function $\gamma(\cdot)$ is a function of deprivation time. In previous literature, the deprivations cost function was usually formulated as a monotonic, non-linear, and convex function (Holguín-Veras et al., 2013; Holguin-Veras et al., 2016). Directly solving the model with nonlinear $\gamma(\cdot)$ is extremely challenging, although nonlinear terms can be handled by piecewise linearization. When accuracy is expected, conducting such an approximation can be expensive in terms of both implementation and computation. Our initial attempts using piecewise linearization failed to find a feasible solution for small-scale problems. In order to tackle computational intractability, we introduce the DDCF. The core idea of the DDCF is: to calculate the value of deprivation cost, we only need to know some discrete points on the deprivation cost function. For example, if we let $T = \{1, 2, 3\}$ be the planning horizon, it is sufficient to only know the value of $\gamma(1), \gamma(2)$ and $\gamma(3)$ for deprivation cost calculation. Since the planning horizon is discrete, we do not have to know any $\gamma(dt)$ values for $1 < dt < 2$ and $2 < dt < 3$. This observation allows us to solve a discrete model rather than the nonlinear continuous one. To formulate the DDCF, we introduce sets of binary indicator variables $\pi_i^{ts}(dt)$ that denote whether the deprivation time of affected area i under scenario s at t is dt, binary indicator variables $\pi_i^{'t_{\max} s}(dt)$ that denote whether the deprivation time of affected area i under scenario s at the last period of planning horizon $t_{\max}$ is dt, continuous variable Γ_i^{ts} that denote the deprivation cost incurred for each (i, t, s) triple, and continuous variable $\Gamma_i^{'t_{\max} s}$ that denote the deprivation cost incurred for each $(i, t_{\max}, s)$ triple. Then let $\gamma(dt)$ be the value of

deprivation cost with particular deprivation time dt. (2.1) can be reformulated to

$$[\text{DDCF}]\ \mathcal{D}_i^s(\phi_i^{ts}, y_i^{ts}) = \sum_{t\in T} w_i \cdot \phi_i^{ts} \cdot (1-\omega_i^{t-1,s}) \cdot \Gamma_i^{ts} + w_i \cdot (1-\omega_i^{t_{\max} s}) \cdot \Gamma_i^{'t_{\max} s} \qquad \forall i \in D, s \in S \quad (3.1)$$

$$\text{subject to } \pi_i^{ts}(dt) = 0 \Rightarrow |t - l_i^{t-1,s} - dt| \geq 1, \qquad \forall i \in D, t \in T, dt \in T(dt \leq t), s \in S \quad (3.2)$$

$$\pi_i^{ts}(dt) = 1 \Rightarrow \Gamma_i^{ts} = \gamma(dt), \qquad \forall i \in D, t \in T, dt \in T(dt \leq t), s \in S \quad (3.3)$$

$$\pi_i^{'t_{\max} s}(dt) = 0 \Rightarrow |t_{\max} - l_i^{t_{\max} s} - dt| \geq 1, \qquad \forall i \in D, dt \in T(dt \leq t), s \in S \quad (3.4)$$

$$\pi_i^{'t_{\max} s}(dt) = 1 \Rightarrow \Gamma_i^{'t_{\max} s} = \gamma(dt), \qquad \forall i \in D, dt \in T(dt \leq t), s \in S \quad (3.5)$$

$$\pi_i^{ts}(dt), \pi_i^{'t_{\max} s}(dt) \in \{0,1\}, \qquad \forall i \in D, t \in T, dt \in T(dt \leq t), s \in S \quad (3.6)$$

$$\Gamma_i^{ts}, \Gamma_i^{'t_{\max} s} \in \mathbb{R}_0^+, \qquad \forall i \in D, t \in T, dt \in T(dt \leq t), s \in S. \quad (3.7)$$

(3.1) replaces the deprivation cost function $\gamma(\cdot)$ in (2.1) with continuous variable Γ_i^{ts} and $\Gamma_i^{'t_{\max} s}$. (3.2)–(3.5) are indicator constraints. An indicator constraint consists of a binary variable and another constraint. The constraint is enforced when the binary variable takes a certain value. For example, $b = 1 \Rightarrow cx \leq d$, where $b \in \{0,1\}$, is an indicator constraint. $cx \leq d$ is enforced when $b = 1$. When $b = 0$, either $cx \leq d$ or $cx > d$ can hold. However, one can explicitly use $b = 0 \Rightarrow cx \geq d$ to enforce $cx \geq d$ when $b = 0$. Note that the indicator constraint is an alternative for big-M formulation and the indicator constraint is known to be more numerically stable. The indicator constraint is supported by modern solvers, e.g., Gurobi, CPLEX, and SCIP. (3.2) and (3.3) are formulated as follows. For each pair of (t, dt) that $t \in T, dt \in T$, and $dt \leq t$, $\pi_i^{ts}(dt) = 1$ if and only if ($\Leftrightarrow$) the deprivation time (calculated as $t - l_i^{t-1,s}$) at t is dt. Otherwise, $\pi_i^{ts}(dt) = 0$. (3.2) and (3.3) are for the case that $t - l_i^{t-1,s} \neq dt$ and $t - l_i^{t-1,s} = dt$, respectively. For the former case, $|t - l_i^{t-1,s} - dt| \geq 1$ in (3.2) is equivalent to $(t - l_i^{t-1,s} < dt) \vee (t - l_i^{t-1,s} > dt)$ since t, $l_i^{t-1,s}$, and dt are all nonnegative integers. For the latter case, the deprivation cost incurred is $\gamma(dt)$, i.e., $\Gamma_i^{ts} = \gamma(dt)$ in (3.3). We can express the core idea of our DDCF by substituting the contrapositive proposition of (3.2) to (3.3): $t - l_i^{t-1,s} = dt \Rightarrow \Gamma_i^{ts} = \gamma(dt)$. However, if $t - l_i^{t-1,s}$ is not equal to dt, then Γ_i^{ts} is unconstrained, but it will be pushed towards zero by the model. (3.4) and (3.5) are counterparts of (3.2) and (3.3), which restrict $\pi_i^{'ts}(dt)$ and $\Gamma_i^{'t_{\max} s}$ for the last period. (3.6) and (3.7) are domain of decision variables where "$\in \mathbb{R}_0^+$" is equivalent to "≥ 0". Note that all the indicator constraints like (3.2) can be linearized by introducing big M as $t - l_i^{t-1,s} \leq dt - 1 + M\pi_i^{ts}(dt)$ where $M = T$. For ease of understanding, we leave all the indicator constraints in the original forms.

The advantages of our DDCF are as follows. Firstly, no additional intractability is involved. Our models are MIP, which is the most common for humanitarian operations management modeling. MIP itself is discrete and requires branch-and-bound solvers, our discretization-based method does not introduce any other intractability, e.g., nonlinearity. Secondly, unlike ones that use heuristics (Perez-Rodriguez & Holguin-Veras, 2016) or proxy (Holguín-Veras et al., 2013) method, which usually causes losing of accuracy, our method does not lose any accuracy compared with the nonlinear-deprivation-function model. Lastly and most importantly, the DDCF can be adapted to any other form of deprivation cost function.

3.4. Physical capacity reservation model

The disaster situation makes the normal market failure. That is insufficient supply of certain goods may occur in the local market due to high demand, leading to a potential increase in prices and moral hazard. Thus a contract is required to coordinate the PHCR suppliers with the buyer (humanitarian organization). The term PHCR suppliers denote the suppliers that will provide items that they supply routinely after a disaster. A contract ensures the buyer desired supplies, however, the huge demand can make suppliers be stretched to the limit. Thus, in the contract, ensuring a manufacturing balance over time for suppliers should be included. The idea of the quantity-flexibility contract, which is extended to a multi-phase fashion in this study, meets the above requirements. Under the standard quantity-flexible contract, the supplier and buyer reach an agreement that the buyer purchases in quantity between $(1-\alpha)q$ and $(1+\beta)q$ where q is a predictive quantity and (α, β) controls the minimal and maximal order quantity (John & Gurumurthy, 2021). In addition to factors in SPIP, the PHCR model mainly focus on ordering at the right time in the right quantity, such that they can be distributed timely and sufficiently. In the following, we let K be the set of PHCR suppliers, each supplier provides $(\alpha_k, \beta_k, p_k, L_k, \eta_k)$ (quantity-flexibility lower limit parameter, quantity-flexibility upper limit parameter, unit price, lead time, and production capacity) to the buyer in advance of disasters. In other words, $(\alpha_k, \beta_k, p_k, L_k, \eta_k), \forall k \in K$ are parameters. The multi-phase quantity-flexibility contract and lead time are two main aspects of modeling. They are discussed in detail as follows.

Modeling the contract: Let q_k^{-ts} be the quantity of order placed (in the following, q^- and q denote the order placed and delivered, respectively) at time t from supplier k in scenario s, and assume that $q_k^{-t's}$ be quantity ordered at time t' and from time t to t' there is not other order be placed from supplier k. Under our multi-phase quantity-flexibility contract, the inequality $(1-\alpha_k)q_k^{-ts} \leq q_k^{-t's} \leq (1+\beta_k)q_k^{-ts}$ should hold. This inequality makes the future order size "predictable" and "stable" for the suppliers, and it guarantees the buyer order in the size that is bounded by (α_k, β_k). In uncertain and stressful humanitarian contexts, this approach helps to counterbalance the tendency to overestimate and provides a buffer for the buyer beyond its estimates. Nevertheless, inequalities in this form cannot be directly used as constraints, since there can be orders placed from

t to t'. To formulate the quantity-flexibility constraints, we introduce auxiliary variables $o_k^{ns}, \forall k \in K, n \in T, s \in S$ that denote the quantity of the nth order and binary variables $\lambda_k^{nts}, \forall k \in K, n \in T, t \in T, s \in S$ that indicate whether the nth quantity (o_k^{ns}) is actually placed by an order at time t. Since the nth quantity o_k^{ns} can be non-zero only if all the $o_k^{n's}, \forall n' \leq n-1$ are non-zero, a set of binary auxiliary variables $\psi_k^{ns}, \forall k \in K, n \in T, s \in S$ is introduced to control the length of the quantity series. If $\psi_k^{ns} = 1$, o_k^{ns} can be > 0 and the successor $\psi_k^{\{n'|n'>n\}s}$ can be $= 1$, otherwise, $o_k^{ns} = 0$ and $\psi_k^{\{n'|n'>n\}s} = 0$. Thus the quantity-flexibility constraints can be formulated as $(1-\alpha_k) \cdot \psi_k^{ns} \cdot o_k^{n-1,s} \leq o_k^{ns} \leq (1+\beta_k) \cdot \psi_k^{ns} \cdot o_k^{n-1,s}$. And all the o_k^{ns} for each pair of (k, s) is assigned to an actual order by $q_k^{-ts} = \sum_{n \in T} \lambda_k^{nts} o_k^{ns}$. Constraints associated with the capacity reservation contract are presented in (4.2)–(4.9).

Modeling the lead time: Recall the L_k be the lead time of the supplier k and q_k^{-ts} be the quantity of order placed at t from supplier k in scenario s. The lead time is determined by the production time and the transportation time from the supplier to the affected area. In the PHCR model, we assume the lead time is deterministic for the following reasons. Firstly, since the supplier is required to provide what it supplies routinely, the production time is deterministic. Secondly, since the geographical locations of both sides are predetermined, the transportation time is deterministic. Let q_k^{ts} be the relief item delivered at time t by supplier k in scenario s, $q_k^{ts} = \sum_{t' \in \{T|t'<t, t'+L_k=t\}} q_k^{-t's}, \forall k \in K, t \in T, s \in S$. This equality links the order placement variables to the order delivery variables. However, the equality is not linear due to $t' \in \{T|t' < t, t' + L_k = t\}$ that contains a conditional statement, we present the linearization for it in the supplementary material. Constraints associated with lead time and relief item allocation are detailed in (4.11)–(4.13). In addition, let $f_{kj}^{'ts}, \forall k \in K, j \in R, t \in T, s \in S$ be the allocation variables that allocate q_k^{ts} to relief facilities, the PHCR model is as follows.

$$\text{[PHCR] minimize } (1.1) + \mathbb{E}_{s \in S}\left(\sum_{t \in T}\sum_{k \in K} p_k q_k^{-ts}\right) \tag{4.1}$$

$$\text{subject to } \psi_k^{ns} \leq \psi_k^{n-1,s}, \qquad \forall k \in K, n \in T, s \in S \tag{4.2}$$

$$o_k^{ns} \leq M\psi_k^{ns}, \qquad \forall k \in K, n \in T, s \in S \tag{4.3}$$

$$(1-\alpha_k) \cdot o_k^{n-1,s} \cdot \psi_k^{ns} \leq o_k^{ns}, \qquad \forall k \in K, n \in T, s \in S \tag{4.4}$$

$$o_k^{ns} \leq (1+\beta_k) \cdot o_k^{n-1,s} \cdot \psi_k^{ns}, \qquad \forall k \in K, n \in T, s \in S \tag{4.5}$$

$$q_k^{-ts} = \sum_{n \in T} \lambda_k^{nts} o_k^{ns}, \qquad \forall k \in K, t \in T, s \in S \tag{4.6}$$

$$\sum_{t \in T} \lambda_k^{nts} = 1, \qquad \forall k \in K, n \in T, s \in S \tag{4.7}$$

$$\sum_{n \in T} \lambda_k^{nts} \leq 1, \qquad \forall k \in K, t \in T, s \in S \tag{4.8}$$

$$\lambda_k^{n't's} + \lambda_k^{nts} + \psi_k^{ns} + \psi_k^{n's} \leq 3, \qquad \forall k \in K, n, n', t, t' \in T(n' > n, t' < t), s \in S \tag{4.9}$$

$$q_k^{-ts} \leq \eta_k, \qquad \forall k \in K, t \in T, s \in S \tag{4.10}$$

$$q_k^{ts} = \sum_{t' \in \{T|t'<t, t'+L_k=t\}} q_k^{-t's}, \qquad \forall k \in K, t \in T, s \in S \tag{4.11}$$

$$\sum_{j \in R} f_{kj}^{'ts} \leq q_k^{ts}, \qquad \forall k \in K, t \in T, s \in S \tag{4.12}$$

$$y_j^{t-1,s} + \sum_{k \in K} f_{kj}^{'ts} - \sum_{i \in D} f_{ji}^{ts} = y_j^{ts}, \qquad \forall j \in R, t \in T, s \in S \tag{4.13}$$

$$\lambda_k^{nts}, \psi_k^{ts} \in \{0, 1\}, \qquad \forall k \in K, n \in T, t \in T, s \in S \tag{4.14}$$

$$o_k^{ns}, q_k^{-ts}, q_k^{ts}, f_{kj}^{'ts} \in \mathbb{Z}_0^+, \qquad \forall k \in K, j \in R, n \in T, t \in T, s \in S \tag{4.15}$$

$$(1.3), (1.4), (1.6) - (1.10), (2.2) - (2.8), (3.1) - (3.7) \tag{4.16}$$

(4.1) minimizes the social cost. The first term is the same as (1.1), which minimizes the prepositioning cost and expected deprivation cost. The second term is the expected PHCR procurement costs. (4.2)–(4.9) are capacity reservation contract constraints (see the supplementary material for an illustrative example). The idea of quantity-flexibility contract constraints is as follows. Firstly, make at most $t_{\max}$ quantity decisions with respect to the contract parameter (α_k, β_k). Then assign each quantity to an actual order, such that orders with specific quantities with respect to the multi-phase flexibility-quantity contract are placed. Since there are at most $t_{\max}$ "opportunities" to place an order, binary variable ψ_k^{ns} is introduced to denote whether the nth ($n \in T$) opportunity is used, o_k^{ns} is the decided quantity of the nth opportunity, and λ_k^{nts} assign o_k^{ns} to an actual order. For example, $\psi_k^{ns} = [1, 1, 0, 0, 0]$, $o_k^{ns} = [10, 5, 0, 0, 0]$, $\lambda_k^{0,0s} = 1, \lambda_k^{1,4s} = 1$, and $q_k^{-ts} = [10, 0, 0, 5, 0]$ is a feasible solution representation for an instance with $t_{\max} = 5$. (4.2) ensures an opportunity is used only if its previous one is used. (4.3) ensures quantity is incurred only if an opportunity is used. (4.4) and (4.5) are the quantity-flexibility constraints. If an opportunity is used, $\psi_k^{ns} = 1$, (4.4) and (4.5) control the variation of quantity between o_k^{ns} and $o_k^{n-1,s}$ by α_k and β_k. (4.6)–(4.8) assign a series of quantities that meet the flexibility-quantity contract requirement to actual orders.

(4.6) calculates the actual order quantity of time t. (4.7) ensures each quantity o_k^{ns} must be assigned to an actual order. (4.8) ensures an actual order can only have at most one value among all the o_k^{ns}. (4.9) enforces for all the (k,s) pairs at least one of $\lambda_k^{n't's}, \lambda_k^{nts}, \psi_k^{ns}, \psi_k^{n's}, n, n', t, t' \in T(n' > n, t' < t)$ is zero. To be more straightforward, (4.9) make sure the actual order quantity series meet the quantity-flexibility contract requirement. Consider a quantity series defined by o_k^{ns} as $[10, 11, 12.1, 0, 0]$ and $\psi_k^{ns} = [1, 1, 1, 0, 0]$, which is valid with $\alpha_k = 0$ and $\beta_k = 0.1$. Without (4.9), there exist a possible actual order quantity series $[10, 12.1, 11, 0, 0]$ with $\lambda_k^{1,3} = \lambda_k^{3,1} = \psi_k^1 = \psi_k^3 = 1$, which violates the quantity-flexibility contract since $12.1 > 10 \times (1+0.1)$. Note that $[10, 0, 11, 12.1, 0]$ is valid because there is no order placed at $t = 1$. (4.9) can be explained by two cases: (i) if $\psi_k^{ns} = 1$ and $\psi_k^{n's} = 1$, at least one of $\lambda_k^{n't's}, \lambda_k^{nts}$ must be zero. Otherwise, the quantity o_k^{ns} that appears before $o_k^{n's}$ in a valid quantity series can be placed after $o_k^{n's}$ in an actual order series, resulting quantity-flexibility-related infeasibility similar to the aforementioned example. (ii) if both $\lambda_k^{n't's} = 1$ and $\lambda_k^{nts} = 1$, then either o_k^{ns} or $o_k^{n's}$ must be zero. This means that either $\psi_k^{ns} = 0$ or $\psi_k^{n's} = 0$, as suggested by the relationship between o_k^{ns} and ψ_k^{ns} in (4.3). (4.10) is the production capacity constraint. (4.11) calculates the quantity of relief items delivered at t based on the quantity of orders placed. (4.11) is nonlinear but can be transformed into a linear form (see the supplementary material). (4.12) links the PHCR model with the prepositioning model using external source variable $f_{kj}^{'ts}$. The external sources are the PHCR supplies. (4.13) is a counterpart of (1.5), which is an inventory balance constraint. (4.14) and (4.15) are domains of decision variables. (4.16) copies constraints from the prepositioning model.

In the quantity-flexibility contract, each supplier provides α_k and β_k while the buyer determines o_k^{ns}. o_k^{0s} is feedback to the supplier once the response begins. From the buyer's perspective, using different values of o_k^{0s}, the buyer can determine whether purchase more items at the beginning stages or not. The buyer has no incentive to set extreme large or small o_k^{0s} since the former can cause inventory burden while the latter may lead to undersupply. From the suppliers' perspective, given (α_k, β_k) and o_k^{0s}, future order quantities are predictable and stable. In summary, the capacity-reservation contract allows the buyer to determine when to receive more supplies and provides the suppliers with valuable demand information for production planning.

3.5. Production capacity reservation model

The PRCR serves as a backup to the PHCR during times of high demand, particularly in extreme events. This section does not consider the quality-flexibility contract in Section 3.4, reasons are two folds. Firstly, in extreme events, humanitarian organizations desire to purchase as many as possible items. Secondly, from the perspective of suppliers, since the PRCR is designed for highly unpredictable events, suppliers should anticipate the consequences of being activated as a PRCR supplier. Suppliers are motivated to produce at their maximum capacity due to high demand, which means that production capacity is the only limiting factor for PRCR. Similar to the PHCR model, the PRCR model also focuses on ordering and distribution. However, unlike the PHCR model, the PRCR model deals with uncertain lead times. In the following, we let K' be the set of PRCR suppliers, each supplier provides $(p_k, L_k^s, L_k, \eta_k)$ (unit price, stochastic lead time of the first order, lead time of orders after the first one, and production capacity) to the buyer in advance of disasters. $(p_k, L_k^s, L_k, \eta_k)$ are parameters used as inputs for the PRCR model. The uncertain lead time is the main aspect of modeling compared with the PHCR model. It is discussed in detail as follows.

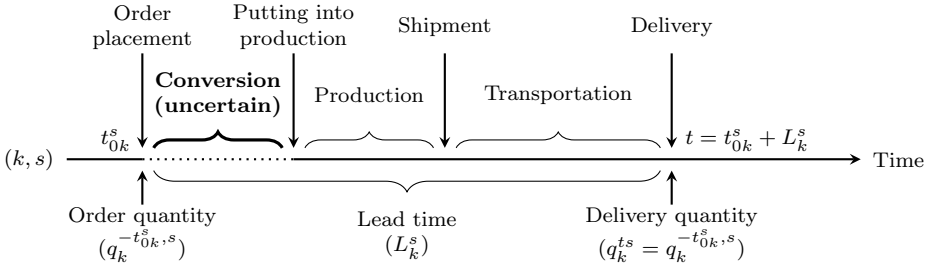

Figure 3: Ordering timeline with uncertain conversion time

Modeling the stochastic lead time: This part can be seen as an extension of "Modeling the lead time" in Section 3.4 that with deterministic lead time $L_k, \forall k \in K$. The timeline from an order is placed to it is delivered is presented in Figure 3. In addition to the production time and transportation time for PHCR, the uncertain conversion time is also included. The conversion time is uncertain due to that the PRCR suppliers typically lack the experience to produce a certain type of item. The conversion time can include the time for acquiring certification, preparing machines, buying raw materials, and training personnel. We assume that the lead time uncertainty only influences the first order, since the conversion is not necessary for subsequent orders. Therefore, we have $L_k^s, \forall k \in K', s \in S$ be the uncertain lead time of the first order and $L_k, \forall k \in K'$ be the deterministic lead time of orders after the first one. Let $q_k^{-ts}, \forall k \in K', t \in T, s \in S$ be quantity of item ordered at t, $q_k^{ts}, \forall k \in K', t \in T, s \in S$ be quantity of item delivered at t, and $q_k^{-t_{0k}^s s}, \forall k \in K', s \in S$ be the quantity of the first order where t_{0k}^s is the time that the first order is received by k. The order delivered at t from k consists of two parts, i.e., the order placed at t_{0k}^s and the orders placed after t_{0k}^s. The first part is calculated by introducing auxiliary variables g_k^{ts} that denote the quantity of the first placed order that is delivered at t from k in scenario s, i.e., $g_k^{ts} = q_k^{-t_{0k}^s s}$ if $t_{0k}^s + L_k^s = t$ else $g_k^{ts} = 0$. The second

part is calculated as $\sum_{t' \in \{T | t^s_{0k} < t' < t, t'+L_k = t\}} q_k^{-t's}$. The overall PRCR model is as follows.

$$\text{[PRCR] minimize } (4.1) + \mathbb{E}_{s \in S} \left(\sum_{t \in T} \sum_{k \in K'} p_k q_k^{-ts} \right) \tag{5.1}$$

$$\text{subject to } q_k^{-ts} \leq 0, \qquad \forall k \in K', t \in \{T | t \leq t^s_{0k} - 1\}, s \in S \tag{5.2}$$

$$q_k^{ts} = g_k^{ts} + \sum_{t' \in \{T | t^s_{0k} < t' < t, t'+L_k = t\}} q_k^{-t's}, \qquad \forall k \in K', t \in T, s \in S \tag{5.3}$$

$$g_k^{ts} = \begin{cases} q_k^{-t^s_{0k} s}, & \text{if } t^s_{0k} + L^s_k = t \\ 0, & \text{otherwise} \end{cases}, \qquad \forall k \in K', t \in T, s \in S \tag{5.4}$$

$$q_k^{-t^s_{0k} s} \leq \eta_k, \qquad \forall k \in K', s \in S \tag{5.5}$$

$$q_k^{-ts} \leq \eta_k, \qquad \forall k \in K', t \in T, s \in S \tag{5.6}$$

$$\sum_{j \in R} f'^{ts}_{kj} \leq q_k^{ts}, \qquad \forall k \in K', t \in T, s \in S \tag{5.7}$$

$$y_j^{t-1,s} + \sum_{k \in K \cup K'} f'^{ts}_{kj} - \sum_{i \in D} f^{ts}_{ji} = y_j^{ts}, \qquad \forall j \in R, t \in T, s \in S \tag{5.8}$$

$$q_k^{-ts}, t^s_{0k}, q_k^{-t^s_{0k} s}, g_k^{ts}, q_k^{ts}, f'^{ts}_{kj} \in \mathbb{Z}_0^+, \qquad \forall k \in K', t \in T, s \in S \tag{5.9}$$

$$(1.3), (1.4), (1.6) - (1.10),$$
$$(2.2) - (2.8), (3.1) - (3.7), \tag{5.10}$$
$$(4.2) - (4.12), (4.14) - (4.15)$$

(5.1) includes the procurement cost of PRCR, which is not present in (4.1). (5.2) allows to accept orders only after t^s_{0k}. (5.3) calculates the quantity of relief item delivered at t after several order have been placed at t'. In the right-hand side of (5.3), the first term, which is detailed in (5.4), is the quantity of relief item delivered at t by the first order placed at t^s_{0k} from k, the second term is similar to (4.11). (5.2)–(5.4) contain if statements and they are linearized in the supplementary material. (5.5) and (5.6) limit the maximum order sizes based on suppliers' capacity. (5.7) links the PRCR model, the PHCR model, and the prepositioning model similar to (4.12). (5.8) is a counterpart of (4.13), which is an inventory balance constraint. The difference between (5.8) and (4.13) is (5.8) takes PRCR suppliers K' into consideration. (5.9) are domains of decision variables. (5.10) copies constraints from the prepositioning model and PHCR model.

Our models' structure and the nature of two-stage stochastic programming present two computational challenges. Firstly, the nonbinary integer prepositioning variables in the first-stage problem result in a large decision space. The Benders decomposition is known to be promising for stochastic programming. Nevertheless, the nonbinary integer variables in the first-stage problem and the integer variables in the second-stage problem require new type of Benders cuts. Secondly, the recourse problem is noncontinuous and nonconvex, which complicates the evaluation of the second-stage recourse cost. These challenges motivate us to develop a specialized algorithm for solving the problem efficiently.

4. Logic-based Benders decomposition

Our SPIP, PHCR, and PRCR models are two-stage stochastic programming models. To solve two-stage stochastic programming models, Monte Carlo Sampling can be utilized. The Monte Carlo sampling uses a finite number of *scenarios* to represent the random parameters. The resulting approximation model is namely *deterministic equivalent*. With a sufficiently large scenario size, the deterministic equivalent can yield the true optimal solution of the original stochastic model. However, the deterministic equivalent is usually too huge to be tackled directly by off-the-shelf solvers. The hierarchical nature of two-stage stochastic programming inspired the stage-wise decomposition techniques. That is, when the first-stage variables are fixed to certain values there are $|S|$ (scenario number) scenario-specified problems that can be solved independently. And the objective values (or proof for infeasibility) of scenario-specified problems can in turn guide searching for the optimal first-stage variable values. One of the decomposition methods that follow this scheme is known as BD (Benders, 1962; Van Slyke & Wets, 1969; Geoffrion, 1972; Codato & Fischetti, 2006). However, the ability of BD is usually limited by the type of problem that can be handled. For example, the classical BD requires the decomposed subproblems to be LP. The LBBD (Hooker & Ottosson, 2003) generalized the existing Benders methods and it can be applied to any class of optimization problems (Rahmaniani et al., 2017). Similar to other Benders methods, the LBBD decomposes the original problem into a master problem and subproblems. *Benders cuts* are generated to link the master problem and subproblems. Unlike other BDs that follow standard ways to decompose the problem and have templates for generating Benders cuts, LBBD does not follow standard methods for problem decomposition or cuts generation.

In the following subsections, the original problem is decomposed in Section 4.1. The prepositioning variables in the resulting master problem are nonbinary integers, requiring a new class of LBBD Benders cuts. Section 4.2 introduces the logic-based

subgradient cuts and the cutting coefficients calculation method. To accelerate convergence, warm-start enhancements for the LBBD are presented in Section 4.3 followed by the overall implementation.

4.1. Decomposition

The difference between PRCR, PHCR, and SPIP models is that the PRCR model involves not only prepositioning but also PHCR suppliers and PRCR suppliers, hence the PRCR model is more general than the PHCR and SPIP models. If we set $f_{kj}^{'ts} = 0, \forall k \in K'$ for the PRCR model, the PRCR model becomes PHCR model. Similarly, if we set $f_{kj}^{'ts} = 0, \forall k \in K \cup K'$ for the PRCR model, the PRCR model becomes SPIP model. In this section, we show how the original PRCR be decomposed into a master problem and a set of subproblems. Note that this decomposition can also be adapted to the PHCR and SPIP models, and the LBBD method is capable of the PHCR and SPIP models. Before proceeding, we rewrite PRCR in a more compact and general way as

$$\text{[CPRCR]} \quad \min_{X \in \mathcal{X}} c^\top X + \mathbb{E}_\xi \left[Q(X, \xi) = \min_{Y \in \mathcal{Y}} q(Y, \xi) \right] \tag{6}$$

where $X = \{r_j\}$ is the first-stage decisions, $\mathcal{X}$ is the set for all feasible X, and $c = \{u\}$ is the cost coefficient. $Q(X, \xi)$ is the second-stage recourse cost. $Y = \{f_{kj}^{'ts}, f_{ji}^{ts}, \lambda_k^{nts}, \psi_k^{ts}, q_k^{-ts}, g_k^{ts}, q_k^{ts}, y_j^{ts}, y_i^{ts}, \phi_i^{ts}, \omega_i^{ts}, l_i^{ts}\}$ is the second-stage decisions, $\mathcal{Y}$ is the set for all feasible Y, and $q(Y, \xi)$ is the second-stage objective function. $\xi = \{d_i^{ts}, L_k^s\}$ is the random variable vector. (6) minimizes the sum of the first-stage cost and the expected second-stage cost. Let S be set of samples of the random variable vector ξ, ξ_s denotes the corresponding revelation of random vector of $s \in S$, and θ_s be an estimator for the second-stage cost of $s \in S$. The deterministic equivalent of (6): $\min_{X \in \mathcal{X}} c^\top X + \sum_{s \in S} \mathbb{P}_s \left[Q(X, \xi_s) = \min_{Y \in \mathcal{Y}} q(Y, \xi_s) \right]$ where $\mathbb{P}_s = 1/|S|$, can be decomposed into a master problem and set of subproblems. The master problem is

$$\text{[CPRCR-MP]} \quad \text{minimize} \quad \sum_{j \in R} u \cdot r_j + \sum_{s \in S} \mathbb{P}_s \theta_s \tag{7.1}$$

$$\text{subject to} \quad (12), (13) \qquad \text{[Warm-start cuts]} \tag{7.2}$$

$$(9.1), (9.2) \qquad \text{[Benders cuts]} \tag{7.3}$$

$$r_j \in \mathbb{Z}_0^+, \qquad \forall j \in R \tag{7.4}$$

$$\theta_s \in \mathbb{R}_0^+, \qquad \forall s \in S \tag{7.5}$$

where (7.1) minimizes the sum of the first-stage cost and the expected second-stage cost. (7.2) is the warm-start cuts introduced in Section 4.3. The role of the warm-start cuts is to provide tightened bounds for the LBBD, especially in initial iterations. (7.3) is the Benders cuts in Section 4.2. The role of the Benders cuts is to let the master problem use information obtained from subproblems with specific $\bar{X}$. The Benders cuts guide searching for the value of globally optimal second-stage cost θ_s^*. (7.4) and (7.5) are domains of the master problem decision variables. With $\bar{X}$ yielded by the master problem there are $|S|$ subproblems

$$\text{[CPRCR-SP]} \quad Q(\bar{X}, \xi_s) = \min_{Y \in \mathcal{Y}} \sum_{t \in T} \sum_{k \in K \cup K'} p_k q_k^{-ts} + \sum_{i \in D} w_i \left[\sum_{t \in T} \phi_i^{ts} \cdot (1 - \omega_i^{t-1,s}) \cdot \Gamma_i^{ts} + (1 - \omega_i^{t_{\max} s}) \cdot \Gamma_i^{'t_{\max} s} \right] \tag{8}$$

that minimize the second-stage recourse cost with given first-stage decision variable values $\bar{X}$ and realization of stochastic parameters ξ_s. $\mathcal{Y}$ denotes the feasible set for all second-stage decision variables. The set of constraints in $\mathcal{Y}$ can be divided into two categories: (i) Constraints from the PRCR model that do not include any first-stage variables are simply duplicated. (ii) Constraints from the PRCR model that involve first-stage variables are also duplicated, but with their values in $\bar{X}$ substituted for the original variables.

4.2. Logic-based subgradient cuts

A new type of logic-based Benders optimality cut, namely logic-based subgradient cut, is the key element of our solution method. The logic-based subgradient cuts are added to CPRCR-MP when CPRCR-SP solution indicates CPRCR-MP does not reach the global optimum. Note that feasibility cuts are not required as the subproblems are always feasible. Let $\hat{Q}(\bar{X}, \xi_s)$ be the optimal second-stage objective obtained with the master problem decisions $\bar{X} = \{\bar{r}_j, \bar{\theta}_s\}$ and revelation of random parameters ξ_s by solving CPRCR-SP. If $\bar{\theta}_s < \hat{Q}(\bar{X}, \xi_s)$, which implies that θ_s under estimates the true second-stage objective, we have the logic-based subgradient cuts $\mathcal{O}_s \left(\theta_s, \bar{X}, \hat{Q}(\bar{X}, \xi_s), \hat{Y} \right) \geq 0$ where $\hat{Y}$ is the subproblem decisions variable values as

$$\text{[Benders cuts]} \quad \sum_{j \in R} r_j \geq \sum_{j \in R} \bar{r}_j \Rightarrow \theta_s \geq \hat{Q}(\bar{X}, \xi_s) - \nabla_1^s \cdot \sum_{j \in R} (r_j - \bar{r}_j) \tag{9.1}$$

$$\sum_{j \in R} r_j \leq \sum_{j \in R} \bar{r}_j - 1 \Rightarrow \theta_s \geq \hat{Q}(\bar{X}, \xi_s) + \nabla_2^s \cdot \sum_{j \in R} (\bar{r}_j - r_j). \tag{9.2}$$

(9.1) and (9.2) approximate θ_s from below using a piecewise linear function that has a changepoint at $\sum_{j \in R} \bar{r}_j$. Since by definition r_j is integer, (9.1) and (9.2) omit the interval $(\sum_{j \in R} \bar{r}_j - 1, \sum_{j \in R} \bar{r}_j)$, which does not contain any integer point. (9.1)

imposes the second-stage cost reduction caused by adding additional prepositioning inventory in future iterations. (9.2) imposes the second-stage cost increase caused by reducing prepositioning inventory in future iterations. ∇_1^s and ∇_2^s are coefficients of cost reduction and increase respectively, i.e., they are *subgradients* of the value function $Q(X, \xi_s)$ at $X = \bar{X}$. Hence, (9) is namely *subgradient cuts*, which is a new variant of logic-based Benders cuts. (9) is transformed into indicator constraints, which are supported by the modern solvers, in the supplementary material. There are three cases in total, with the first two corresponding to (9.1) and the last one corresponding to (9.2).

- In a future iteration v, if $\sum_{j\in R} r_j^v = \sum_{j\in R} \bar{r}_j$, (9.1) becomes $\theta_s \geq \hat{Q}(\bar{X}, \xi_s)$. When the quantity of prepositioning relief items in a future iteration is exactly the same as $\sum_{j\in R} \bar{r}_j$, current solution $\bar{\theta}_s$ is excluded by the inequality $\theta_s \geq \hat{Q}(\bar{X}, \xi_s)$ since the optimality cut is added only if $\bar{\theta}_s < \hat{Q}(\bar{X}, \xi_s)$.
- In a future iteration v, if $\sum_{j\in R} r_j^v \geq \sum_{j\in R} \bar{r}_j + 1$, (9.1) becomes $\theta_s \geq \hat{Q}(\bar{X}, \xi_s) - \nabla_1^s \cdot \sum_{j\in R}(r_j^v - \bar{r}_j)$ where ∇_1^s denotes the second-stage cost reduction either by purchasing fewer supplies from PHCR and PRCR supplier or by deprivation cost reduction. To calculate ∇_1^s, let $\sum_{j\in R}(r_j^v - \bar{r}_j)$ be the increased quantity of prepositioning relief items, then there are three sub-cases: (i) purchasing $\sum_{j\in R}(r_j^v - \bar{r}_j)$ units less relief item from PHCR suppliers, the resulting unit cost reduction is $\max_{k\in K} p_k \sum_{j\in R}(r_j^v - \bar{r}_j)$; (ii) purchasing $\sum_{j\in R}(r_j^v - \bar{r}_j)$ units less relief item from PRCR suppliers, the resulting cost reduction is $\max_{k\in K'} p_k \sum_{j\in R}(r_j^v - \bar{r}_j)$; and (iii) purchasing the same quantity of relief item form PHCR and PRCR suppliers as the previous iteration, then the deprivation cost may be reduced. Calculating the unit contribution of prepositioning inventory on deprivation cost reduction denoted as ν^s is a little bit involved, we detail it later. The maximum possible second-stage cost reduction by prepositioning inventory increase is the largest among the aforementioned three cases, i.e., $\nabla_1^s = \max\{\max_{k\in K\cup K'} p_k, \nu^s\}$.
- In a future iteration v, if $\sum_{j\in R} r_j^v \leq \sum_{j\in R} \bar{r}_j - 1$, (9.2) becomes $\theta_s \geq \hat{Q}(\bar{X}, \xi_s) + \nabla_2^s \cdot \sum_{j\in R}(\bar{r}_j - r_j^v)$ where ∇_2^s denotes the second-stage cost increase caused either by purchasing more supplies from PHCR and PRCR suppliers or by deprivation cost increase. Since (9.2) provides lower bound to θ_s, we simply let $\nabla_2^s = 0$ without loss of validity.

A valid logic-based Benders optimality cut is a logic expression over master problem variables that has two properties (Chu & Xia, 2004; Guo et al., 2021): (i) it must exclude the current master problem solution if it is not globally optimal; (ii) it must not remove any globally optimal solution. Property (i) guarantees finite convergence if the master problem variables have a finite domain and property (ii) guarantees optimality because globally optimal solutions are never cut off. The properties (i) and (ii) ensure the LBBD converges to the optimal solution in finite iterations. The validity of (9) is presented in Theorem 1.

Theorem 1. *There exists a ν^s that let (9) be a valid logic-based Benders optimality cut.*

Proof. See the supplementary material. □

The proof for Theorem 1 in brief is: the property (i) holds with any ν^s; the property (ii) holds with a "large enough" ν^s that makes $Q(X, \xi_s) \leq \max\{\max_{k\in K\cup K'} p_k, \nu^s\} \cdot \sum_{j\in R}(r_j - \bar{r}_j)$ holds for any $X = \{r_j\}$. The choosing for ν^s is of great importance for the efficiency of LBBD. With an sufficiently but arbitrarily large ν^s, (9.1) can be equivalent to $\sum_{j\in R} r_j \geq \sum_{j\in R} \bar{r}_j \Rightarrow \hat{Q}(\bar{X}, \xi_s) - \infty \cdot \sum_{j\in R}(r_j - \bar{r}_j)$. Benders cuts in this form do not provide any useful information but simply let the master problem try another solution. An efficient Benders cut should provide more information than that. To be more specific, the Benders cut should be able to answer questions like: when the prepositioning inventory is increased, how much the second-stage costs can be reduced in maximum? It is desired that ν^s can be as small as possible but preserve the validity of Benders cuts, since smaller ν^s results in a smaller feasible region for the master problem. We answer the above question by an exact method and a heuristics for calculating ν^s.

We first present the exact method for calculating ν^s. To make sure the resulting Benders cuts are valid, the ν^s must ensures $Q(X, \xi_s) \leq \max\{\max_{k\in K\cup K'} p_k, \nu^s\} \cdot \sum_{j\in R}(r_j - \bar{r}_j)$ as mentioned. Making this inequality a constraint, the minimal ν^s that let (9) be valid can be computed from (10.1) to (10.3).

$$\text{minimize } \nu^s \tag{10.1}$$

$$\text{subject to } Q(X, \xi_s) \leq \max\left\{\max_{k\in K\cup K'} p_k, \nu^s\right\} \cdot \sum_{j\in R}(r_j - \bar{r}_j) \tag{10.2}$$

$$\begin{aligned} Q(X, \xi_s) = \min & \sum_{t\in T}\sum_{k\in K\cup K'} p_k q_k^{-ts} + \sum_{i\in D} w_i \left[\sum_{t\in T} \phi_i^{ts} \cdot (1 - \omega_i^{t-1,s}) \cdot \Gamma_i^{ts} + (1 - \omega_i^{t_{\max} s}) \cdot \Gamma_i^{'t_{\max} s}\right] \\ \text{s.t.} & \sum_{i\in R} r_j \geq \sum_{i\in R} \bar{r}_j \\ & Y \in \mathcal{Y} \end{aligned} \tag{10.3}$$

(10) is a bi-level programming model, in which the inner problem minimizes $Q(X, \xi_s)$ and the outer problem minimizes ν^s. (10.1) minimizes the cutting coefficient ν^s. (10.2) ensures the validity of the resulting Benders cuts. (10.3) is the inner problem that calculating the recourse cost $Q(X, \xi_s)$. Solving (10) is difficult. Firstly, the class of bi-level optimization problems is known to be computationally challenging. Secondly, (10.2) contains the maximization term and production of variables.

Thirdly, even when the values of X are fixed, the problem (10.3) has the same structure as the CPRCR-SP, which requires pretty computational effort. Hence, directly solving (10) for the cutting coefficient ν^s is unrealistic. Therefore, we are motivated to develop efficient alternative approaches that reasonably approximate the cutting coefficients.

Algorithm 1 is developed as an alternative for (10.1)–(10.3). The main idea is as follows. If there is no deprivation cost incurred (Line 2), then $\nu^s = 0$, since the deprivation cost cannot be reduced further. On the other hand, if the deprivation cost is incurred (Line 3), we can allocate the additional relief items in the future iterations to the (i,t) pair with the highest marginal contribution to deprivation cost reduction (denoted as i_Δ, t_Δ). To determine the (i_Δ, t_Δ) pair, assume that i is fulfilled with the relief supplies in the quantity of exactly the coming period's demand, we can calculate the marginal contribution of added inventory as shown in Line 7 and Line 9. The (i_Δ, t_Δ) is chosen among all the (i,t) pairs (Line 5–Line 11), and it allows additional prepositioning inventory to make the highest deprivation cost reduction. After the (i_Δ, t_Δ) is determined, we modify the value of the variable $\hat{\phi}_i^{ts}$, $\hat{\omega}_i^{ts}$, and $\hat{y}_i^{ts}$ such that there is a delivery in quantity of $d_{i_\Delta}^{t_\Delta-1,s} - \hat{y}_{i_\Delta}^{t_\Delta-1,s}$ (or $d_{i_\Delta}^{t_\Delta-1,s} + d_{i_\Delta}^{t_{\max}s} - \hat{y}_{i_\Delta}^{t_\Delta-1,s} - \hat{y}_{i_\Delta}^{t_{\max}s}$ for the last period $t_{\max}$) that is made at $t_\Delta - 1$ to i_Δ (Line 12–Line 16). This modification results in the maximum marginal changes in deprivation cost. Let $\mathcal{D}^s$ (Line 17) and $\mathcal{D}^{'s}$ (Line 18) denote the original and modified deprivation cost that can be computed by substituting values of ω_i^{ts} (implied by values of y_i^{ts} by (2.2)), l_i^{ts} (implied by values of ω_i^{ts} by (2.4)), and ϕ_i^{ts} to (2.1), the ν^s is calculated from Line 19 to Line 22. Although Algorithm 1 potentially results in ν^s that is not "sufficiently" large, i.e., globally optimal solutions may be cut off, the numerical results in Section 5 reveal that solutions yielded by this heuristics are almost optimal for most of the instances, which validates the effectiveness of Algorithm 1.

Algorithm 1: Calculating the cutting coefficient

Data: The CPRCR-SP solutions $\hat{\phi}_i^{ts}, \hat{\omega}_i^{ts}, \hat{y}_i^{ts}, \forall i \in R, t \in T$ of scenario s of iteration v.
Result: The cutting coefficient ν^s

1 **def** `calcAlpha`$(\hat{\phi}_i^{ts}, \hat{\omega}_i^{ts}, \hat{y}_i^{ts}, \forall i \in R, t \in T)$**:**
2 $\quad \nu^s \leftarrow 0$;
3 $\quad$ **if** $\sum_{t\in T} \hat{\phi}_i^{ts} \cdot (1 - \hat{\omega}_i^{t-1,s}) \cdot \Gamma_i^{ts} + (1 - \hat{\omega}_i^{t_{\max}s}) \cdot \Gamma_i^{'t_{\max}s} \neq 0$ **:**
4 $\quad\quad \Delta^{s(v)} \leftarrow 0$, $i_\Delta \leftarrow$None, $t_\Delta \leftarrow$None;
5 $\quad\quad$ **for** $i, t \in D \times T$ **:**
6 $\quad\quad\quad$ **if** $t \neq t_{\max}$ **:**
7 $\quad\quad\quad\quad \Delta \leftarrow \hat{\phi}_i^{ts} \cdot (1 - \hat{\omega}_i^{t-1,s}) \cdot \Gamma_i^{ts} / \left(d_i^{t-1,s} - \hat{y}_i^{t-1,s}\right)$;
8 $\quad\quad\quad$ **else:**
9 $\quad\quad\quad\quad \Delta \leftarrow \left[\hat{\phi}_i^{ts} \cdot (1 - \hat{\omega}_i^{t-1,s}) \cdot \Gamma_i^{ts} + (1 - \hat{\omega}_i^{t_{\max}s}) \cdot \Gamma_i^{'t_{\max}s}\right] / \left(d_i^{t-1,s} + d_i^{t_{\max}s} - \hat{y}_i^{t-1,s} - \hat{y}_i^{t_{\max}s}\right)$;
10 $\quad\quad\quad$ **if** $\Delta > \Delta^{s(v)}$ **:**
11 $\quad\quad\quad\quad \Delta^{s(v)} \leftarrow \Delta$, $i_\Delta \leftarrow i$, $t_\Delta \leftarrow t$;
12 $\quad\quad$ **for** $i, t \in D \times T$ **:**
13 $\quad\quad\quad$ **if** $i, t \neq i_\Delta, t_\Delta - 1$ **:**
14 $\quad\quad\quad\quad \hat{\phi}_i^{'ts} \leftarrow \hat{\phi}_i^{ts}, \hat{y}_i^{'ts} \leftarrow \hat{y}_i^{ts}$;
15 $\quad\quad\quad$ **else:**
16 $\quad\quad\quad\quad \hat{\phi}_i^{'ts} \leftarrow 1, \hat{y}_i^{'ts} \leftarrow d_i^{ts}$;
17 $\quad\quad \mathcal{D}^s \leftarrow \sum_{i\in D} \mathcal{D}_i^s \left(\hat{\phi}_i^{ts}, \hat{y}_i^{ts}\right)$;
18 $\quad\quad \mathcal{D}^{'s} \leftarrow \sum_{i\in D} \mathcal{D}_i^s \left(\hat{\phi}_i^{'ts}, \hat{y}_i^{'ts}\right)$;
19 $\quad\quad$ **if** $t_\Delta \neq t_{\max}$ **:**
20 $\quad\quad\quad \nu^s = \left(\mathcal{D}^s - \mathcal{D}'^s\right) / \left(d_{i_\Delta}^{t_\Delta-1,s} - \hat{y}_{i_\Delta}^{t_\Delta-1,s}\right)$;
21 $\quad\quad$ **else:**
22 $\quad\quad\quad \nu^s = \left(\mathcal{D}^s - \mathcal{D}'^s\right) / \left(d_{i_\Delta}^{t_\Delta-1,s} + d_{i_\Delta}^{t_{\max}s} - \hat{y}_{i_\Delta}^{t_\Delta-1,s} - \hat{y}_{i_\Delta}^{t_{\max}s}\right)$;
23 $\quad$ **return** ν^s

There are other methods that are relevant to our LBBD with logic-based subgradient cuts. In the context of Benders method, as mentioned in Section 2.3, the GBD also involves subgradient into the optimality cut to approximate the value function, e.g. Lin & Tian (2021); Angulo et al. (2016); Fischetti et al. (2017). However, their subproblems are linear or at least convex, and the subgradient is always computed on the binary variables. In contrast, our subproblems are nonconvex and the subgradient is computed on the nonbinary integer variables, both are more general than the GBD. In the *bundle method* for nonsmooth optimization, there are also some similarities. The idea of the bundle method is to approximate an unconstrained function from the bellow using piecewise-linear functions (Mäkelä, 2002). In terms of our Benders method, in the first iteration (the case without warm-start cuts), the master problem is unconstrained. However, after the first Benders cut is added to the master problem, the subsequent master problems are solved in a constraint optimization manner. Contrarily, the bundle method relies on the *line search* procedure (Mäkelä, 2002; Bagirov et al., 2014), which is for unconstrained problems.

4.3. Warm-start and implementation

The warm-start is an accelerating technique for solving mathematical programming problems. In the context of branch-and-bound methods for MIP, warm-start is used to feed an initial feasible solution to a solver. Since the objective value of the initial feasible solution is a valid upper bound (in the case of minimization), it can be used for *pruning*. However, simply feeding an

initial feasible solution to our LBBD master problem is unhelpful, since the initial solution will soon be proved to be suboptimal as in the first iteration all the recourse costs are zero. Consequently, the initial feasible solution has no contribution to searching for the optimum. To enhancements the convergence performance of LBBD, we derive warm-start cuts from inequalities of stochastic programming. Given set of samples S, we know that (Madansky, 1960; Keshvari Fard et al., 2022)

$$\mathbb{E}_{\xi_s} \min_{X\in\mathcal{X}}[c^\top X + Q(X,\xi_s)] \leq c^\top X^* + \mathbb{E}_{\xi_s} Q(X^*,\xi_s) \leq \mathbb{E}_{\xi_s}[c^\top X_{EXP} + Q(X_{EXP},\xi_s)]. \tag{11}$$

In (11), $c^\top X^* + Q(X^*,\xi_s)$ is objective value of the true optimal solution X^* given the stochastic parameters $\xi_s, \forall s \in S$. The first term $\mathbb{E}_{\xi_s} \min_{X\in\mathcal{X}}[c^\top X + Q(X,\xi_s)]$ is the expected value of the wait-and-see (WS) solution. To derive the WS, $|S|$ independent deterministic problems $\min_{X\in\mathcal{X}}[c^\top X + Q(X,\xi_s)]$ are solved with the scenario specified parameters ξ_s. Then the expected objective values of all the scenario-specific problems are computed. The last term $\mathbb{E}_{\xi_s}[c^\top X_{EXP} + Q(X_{EXP},\xi_s)]$ is the expected value of the expected value solution (EEV) where X_{EXP} is referred to as the expected value (EV) solution. The EV solution is obtained by solving the deterministic problem that replaces the stochastic parameters with their expected value. Then the first-stage decision variables are fixed to the value of the EV solution, and EEV is obtained by solving this problem. Inspired by (Kůdela & Popela, 2017), we use (11) to generate an initial set of cutting planes that strengthen the master problem.

The first set of warm-start cuts, namely *wait-and-see cuts*, is introduced to provide lower bounds. Recall that X be the first-stage variables and c is the cost coefficient, θ_s be the recourse cost estimator for scenario $s \in S$, and $\min_{X\in\mathcal{X}}[c^\top X + Q(X,\xi_s)]$ be the WS solution of scenario $s \in S$. For each scenario $s \in S$, we have the wait-and-see cut as

$$\text{[Wait-and-see cuts] } c^\top X + \theta_s \geq \min_{X\in\mathcal{X}}[c^\top X + Q(X,\xi_s)]. \tag{12}$$

The idea of (12) is when $\mathbb{E}_{\xi_s}(\cdot)$ are removed from the first two terms of (11) "$\leq$" still holds, since $\min_{X\in\mathcal{X}}[c^\top X + Q(X,\xi_s)]$ is the minimum cost that is incurred through a perfect information problem. (12) ensures objective values of the master problem in the initial iterations do not be too small. The second set of warm-start cuts, namely *expected-value cuts*, is introduced to provide upper bounds and it is formulated as

$$\text{[Expected-value cuts] } c^\top X + \sum_{s\in S} \mathbb{P}_s \theta_s \leq \mathbb{E}_{\xi_s}[c^\top X_{EXP} + Q(X_{EXP},\xi_s)]. \tag{13}$$

(13) replaces $\mathbb{E}_{\xi_s} Q(X,\xi_s)$ in the second term of (11) with $\sum_{s\in S} \mathbb{P}_s \theta_s$. (13) provides a valid upper bound for the objective function of the original problem. (12) is more valuable than (13). When there is not any warm-start cuts added, in initial iterations, $\theta_s, \forall s \in S$ are close to zero, thus (13) may not be activated. Adding (12) to the master problem improves the lower bounds significantly. Specifically, according to our experiments, with (12), the initial lower bounds have the same order of magnitude as the optimal objective. When (12) is removed, the initial lower bounds can be several orders of magnitude lower than the optimal objective.

Algorithm 2: Solving the PRCR model with LBBD

Data: CPRCR-MP$_0$ generated from (7.1), (7.4), and (7.5); time limit (*Lmt.*); relative tolerance (*Tol.*).
Result: Optimal PRCR solution or proof of infeasibility.

```
def LBBD(CPRCR-MP_0, Lmt., Tol.):
    Gap ← +∞, BestUB ← +∞, v ← 0;
    Solve the wait-and-see problem and add (12) to the CPRCR-MP_0;
    Solve the expected-value problem and add (13) to the CPRCR-MP_0;
    while Gap > Tol. and Runtime ≤ Lmt. :
        Solve the CPRCR-MP_v to get X̄ and θ̄_s;
        if CPRCR-MP_v is optimal :
            for s ∈ S :
                Solve the CPRCR-SP (8) with X̄ yielded by CPRCR-MP_v to get Q̂(X̄, ξ_s);
            LB ← c^⊤ X̄ + Σ_{s∈S} P_s θ̄_s;
            UB ← c^⊤ X̄ + Σ_{s∈S} P_s Q̂(X̄, ξ_s);
            if UB < BestUB :
                BestUB ← UB;
            Gap = |BestUB − LB|/|BestUB|;
            if Gap > Tol. :
                for s ∈ S :
                    if θ̄_s < Q̂(X̄, ξ_s) :          // Add Benders optimality cut to CPRCR-MP
                        Call the Algorithm 1 to calculate the cutting coefficient;
                        CPRCR-MP_v ← CPRCR-MP_v + (9);
            else:                                   // The PRCR model is optimized
                CPRCR-MP* ← CPRCR-MP_v, CPRCR-SP* ← CPRCR-SP;
        else:                                       // The PRCR model is infeasible
            return PRCR is infeasible;
        v ← v + 1;
    return CPRCR-MP*, CPRCR-SP*, Gap
```

The overall implementation of the LBBD is presented in Algorithm 2, which takes CPRCR-MP, time limit, and relative tolerance as inputs. The output of the Algorithm 2 is the optimal solution of the PRCR when it is not proved to be infeasible.

For the CPRCR-MP in a certain iteration, the objective of the first-stage problem plus the expected value of the second-stage problem estimator ($\bar{\theta}_s$) provides a lower bound (Line 10) for the original problem. The objective of the first-stage problem plus the expected value of the actual second-stage cost ($\hat{Q}(\bar{X}, \xi_s)$) provides an upper bound (Line 11–Line 13) for the original problem. The LBBD reaches the optimum when the lower bound meets the upper bound, otherwise, the logic-based subgradient cuts are added to the CPRCR-MP (Line 15–Line 19). The Algorithm 2 is terminated whenever the optimality gap is below the tolerance or the time limit is hit (Line 5). Note that to apply Algorithm 2 to the SPIP model, let $\nabla_1^s = \nu^s$ for (9); to apply Algorithm 2 to the PHCR model, let $\nabla_1^s = \max\{\max_{k\in K} p_k, \nu^s\}$ for (9). We implemented the algorithm with Gurobi 9.1's Python API, the version of Python is 3.8.11. The machine that our code running on is an Aliyun Elastic Compute Service instance with 8 cores of Intel Xeon Platinum 8369 (3.3 gigahertz, Turbo Boost speed of 3.8 gigahertz) vCPU and 16 gigabyte RAM. The operating system is CentOS 7.9.

5. Numerical experiments

5.1. Instance design and sampling

Since there is not standard benchmark instance for our problems, instances are designed in this section. Our instances characterize factors of realistic emergencies. Through them, both computational performances and managerial insights can be analyzed. The parameters for instance generation are divided into variable ones, stochastic ones, and deterministic ones. The variable parameters are mainly the size of sets, e.g., the number of affected areas, length of the planning horizon, and patterns of consumption rate (for generating demands). The stochastic parameters are probability distributions of consumption rate and lead time. The deterministic parameters are capacity- and cost-related parameters. Let $|D|$-$|T|$-$\mathcal{C}$ denote an instance, where $|D|$ is the number of affected areas, $|T|$ is the length of the planning horizon, and $\mathcal{C}$ is the consumption rate pattern, which is introduced later, there are totally $|\{5, 10\} \times \{3, 5\} \times \{0, 1, 2\}| = 12$ instances.

Among all the stochastic parameters, demand is the most crucial. Since the problem is multi-phase, a question raise naturally: how the demand increases or decreases over the planning horizon? We introduce an auxiliary parameter namely consumption rate, which is the quantity of items that are consumed per individual per period of an affected area. Given the population of affected areas, the aforementioned question then becomes: how the consumption rate varies from one period to another? We assume three consumption rate patterns according to the type of emergency: (i) a monotonic increasing one for public health emergencies like pandemics; (ii) a monotonic decreasing one for natural disasters; and (iii) a steady one. Hence, we generate three series of consumption rates: $\mathcal{C}_0(t) \sim N(1.75/(1+e^{-0.4t}) - 0.75, 0.05^2)$, $\mathcal{C}_1(t) \sim N(1.50/(1+e^{0.6t}) + 0.25, 0.05^2)$, and $\mathcal{C}_2(t) \sim N(0.5, 0.05^2)$. $N(\mu, \sigma^2)$ denotes the truncated normal distribution where μ and σ are the expected value and standard deviation, respectively. The consumption rates are truncated at $\mu - 3\sigma$ and $\mu + 3\sigma$. The expected value terms in the consumption rates are adopted from the sigmoid function. For a sigmoid function $f(x) = L/(1+e^{-kx})$, $f(0) = L/2$, L is the limit of $f(x)$, i.e., $\lim_{x\to\infty} f(x) = L$, and k is the logistic growth rate or steepness of the curve. Under our parameter settings, $\mathbb{E}\mathcal{C}_0(0) = 0.125$ and $\lim_{t\to\infty} \mathbb{E}\mathcal{C}_0(t) = 1$, i.e., the expected consumption rate increases from 0.125 and gradually reaches 1; $\mathbb{E}\mathcal{C}_1(0) = 1$ and $\lim_{t\to\infty} \mathbb{E}\mathcal{C}_1(t) = 0.25$, i.e., the expected consumption rate decreases from 1 and gradually reaches 0.25; $\mathbb{E}\mathcal{C}_2(0) = 0.5$ and $\lim_{t\to\infty} \mathbb{E}\mathcal{C}_2(t) = 0.5$, i.e., the expected consumption rate is 0.5 through the planning horizon. $\mathcal{C}_0(t)$, $\mathcal{C}_1(t)$, and $\mathcal{C}_2(t)$ are designed to capture demand patterns in different types of disasters, including pandemics with rapidly increasing demand, acute disasters with higher initial consumption, and chronic disasters such as droughts and famines. These series are illustrated in the supplementary material. The demand of certain affected area $i \in D$ in the period t is calculated with $\lceil w_i \mathcal{C}_*(t) \rceil$ where w_i is the population of i and $*$ can be 0, 1, or 2. Though we assume normal distribution demand that is consistent with the literature, e.g., Ni et al. (2018), it is worth noting that our models and solution method are capable of any other probability distributions.

Among all the deterministic parameters, the deprivation cost function and value of life are of great importance. The deprivations cost function is defined as a monotonic, non-linear, and convex function with respect to the deprivation time for individuals under specific socio-economic conditions (Holguín-Veras et al., 2013; Holguin-Veras et al., 2016). The most commonly used deprivation cost functions are exponential, piecewise-linear, and linear (Section 2.2). The piecewise-linear and linear deprivation cost functions are usually compromises to the exponential ones for computational tractability. Since our DDCF can handle any form of deprivation cost function, we select the exponential deprivation cost function. Estimate for the deprivation cost function and value of life are out of the scope of this study. We use the deprivation cost estimated by Holguin-Veras et al. (2016) as $\gamma(t') = 0.2354 \times e^{0.1129\times t'}$ where t' is the deprivation time in unit of hour. We set $\gamma^{\max} = \$1,000,000$ based on estimates of the value of life in various countries (Australia, Austria, Canada, Chile, Colombia, India, Japan, Korea, the United Kingdom, and the United States) which range from \$0.5 million to over \$20 million, while in most of these countries, it is estimated in millions (Holguin-Veras et al., 2016; Dore & Singh, 2013). We assume that the minimal time unit is two days (48 hours) and the deprivation cost at the time $t = 0$ is zero, hence the deprivation cost function used in this study is $\gamma(t) = \min\{1 \times 10^6, 0.2354 \times e^{0.1129\times 48\times t} \text{ if } t \geq 1 \text{ else } 0\}$ in dollars. Other parameters, e.g., unit acquiring cost, lead time,

facility capacity, and production capacity, are presented in detail in the supplementary material. The dataset used in this study is available at https://guo.ph/data/cap_res.

The Monte Carlo sampling allows us to solve the stochastic programming problem with continuous random variables through a discrete counterpart. The resulting sample is one of the most critical factors that influence the solution quality. We call the instance that is used to find the solution in-sample instance and the instance that is used to validate the solution quality out-of-sample instance. In the context of humanitarian relief, it is particularly desired that the solution better not bring unexpected costs under the realization of stochastic parameters. That is the out-of-sample objective value should be close to the in-sample objective value. We say the problem is out-of-sample stable when the difference between the in-sample objective and the out-of-sample objective is small. The crude Monte Carlo sampling can be out-of-sample instable by failing to capture some extreme cases. To enhance the out-of-sample performance, other sampling methods, e.g., the Latin hypercube sampling (LHS), the quasi-Monte Carlo sampling, and the importance sampling, can be applied (Shapiro et al., 2021; Linderoth et al., 2006). These methods generate (partially) artificially designed samples rather than independent and identically distributed samples as in the crude Monte Carlo sampling, such that extreme but "crucial" cases with lower probability can be captured. We use "crucial" to describe cases that can result in high unexpected costs if they are not included in the in-sample instance. The LHS is used in this study since it is easy to implement and it performs well on our problem (validated in Section 5.2 and Section 5.4). From the in-sample perspective, the LHS is also known as a variance reduction technique, so it enhances the rate of convergence. Moreover and most importantly, the LHS is unbiased. Readers may refer to Shapiro et al. (2021) for the LHS in detail.

5.2. Analysis for scenario size

A larger sample size $|S|$ tends to result in a better approximation for the underlying continuous distribution, thus resulting in a better solution and a better approximation for the true objective. Nevertheless, a large value of $|S|$ can lead to computational burden as each LBBD iteration necessitates solving $|S|$ subproblems. There has to be a trade-off between solution quality and computational tractability. The *stochastic bound* was suggested by (Norkin et al., 1998) and developed by (Mak et al., 1999) to control the sample size for stochastic programming (Shapiro, 2013). In order to determine the sample size, we derive stochastically valid lower bound and upper bound that can be combined to bound the optimality gap. We chose the minimum $|S|$ that can yield a satisfactory stochastic optimality gap.

The method to generate the stochastic lower bound is pretty straightforward. In the following, we let $z^* = c^\top X^* + \mathbb{E}_{\tilde{\xi}} Q(X^*, \tilde{\xi})$ denotes the true optimal objective value where X^* is the true optimal solution. Given a certain sample size $|S|$, we solve $|N|$ CPRCR (6), each with a sample size of $|S|$. Let S^n ($|S^n| = |S|$) be the sample of the nth problem for all the $n \in N$, the resulting optimization problem is $\min_{X\in\mathcal{X}} c^\top X + 1/|S^n| \sum_{s\in S^n} Q(X, \xi_s^n)$. Since $\mathbb{E}\left[\min_{X\in\mathcal{X}} c^\top X + 1/|S^n| \sum_{s\in S^n} Q(X, \xi_s^n)\right] \leq z^*$ (Mak et al., 1999), $\min_{X\in\mathcal{X}} c^\top X + 1/|S^n| \sum_{s\in S^n} Q(X, \xi_s^n)$ is the stochastic lower bound of the true optimal objective value. Then we introduce the method to generate the stochastic upper bounds. Let X'^* be a "good enough" solution (detailed later) for CPRCR (6) and we generate $|S_U|$ samples. For all $s \in S_U$ we solve the second-stage problem $Q(X'^*, \xi_s)$ with the first-stage decision variables X be fixed to X'^*. $c^\top X'^* + 1/|S_U| \sum_{s\in S_U} Q(X'^*, \xi_s)$ is an unbiased estimator for $c^\top X'^* + Q(X'^*, \tilde{\xi})$, i.e., $\mathbb{E}\left[c^\top X'^* + 1/|S_U| \sum_{s\in S_U} Q(X'^*, \xi_s)\right] = c^\top X'^* + \mathbb{E}_{\tilde{\xi}} Q(X'^*, \tilde{\xi})$ (Mak et al., 1999). Since $c^\top X'^* + \mathbb{E}_{\tilde{\xi}} Q(X'^*, \tilde{\xi}) \geq z^*$, $c^\top X'^* + 1/|S_U| \sum_{s\in S_U} Q(X'^*, \xi_s)$ is a stochastic upper bound of the true optimal objective value. In summary, we have the inequality as follows. Note that (11) and (14) are equivalent when $|N| = 1, S_U = S^n$, and $X_{EXP} = X'^*$.

$$\mathbb{E}\left[\min_{X\in\mathcal{X}} c^\top X + \frac{1}{|S^n|}\sum_{s\in S^n} Q(X, \xi_s^n)\right] \leq z^* \leq \mathbb{E}\left[c^\top X'^* + \frac{1}{|S_U|}\sum_{s\in S_U} Q(X'^*, \xi_s)\right] \tag{14}$$

To derive a sample of the stochastic lower bound, we solve $|N|$ stochastic programming problems each with the sample size be $|S|$. Considering the computational resources limit, $|N|$ should not be too large, so we set $|N| = 30$. After all the $|N|$ problems are solved, let X_n denote the optimal solution of the nth problem, we obtain the "good enough" X'^* using the method inspired by Guo et al. (2021) as follows. A relatively larger scenario set S' ($|S'| = 300$) is generated, and the selected "good enough" solution is $X'^* = \arg_{X_n, n\in N} \min\left\{c^\top X_n + \frac{1}{|S'|}\sum_{s\in S'} Q(X_n, \xi_s)\right\}$. This requires $|N||S'|$ second-stage problems to be solved. To derive a sample of the stochastic upper bound, $|S_U|$ problems with the first stage decision variables be fixed to X'^* are needed to be solved. Since the resulting problems are deterministic, $|S_U|$ can be relatively larger, so we set $|S_U| = 3000$. Finally, 95% confidence intervals (CIs) are built from the lower bound sample and the upper bound sample. Let LB_{Mean}, LB_{Width}, UB_{Mean}, and UB_{Width} be the mean value of lower bound CI, width of lower bound CI, mean value of upper bound CI, and width of upper bound CI, the stochastic optimality gap is defined as $\left[(UB_{Mean} + UB_{Width}) - (LB_{Mean} - LB_{Width})\right] / (UB_{Mean} + UB_{Width})$.

Experiments are conducted on the instance 05-03-1 using crude Monte Carlo and LHS. In Table 3, "S.Gap" represents an overall measure of each sampling method, with "UB" reflecting out-of-sample stability and "LB" reflecting in-sample stability. The results show that for all sample sizes, both methods achieve stochastic optimality gaps of less than 5% based on "S.Gap". However, the trends of "S.Gap" with increased sample sizes are different for LHS and crude Monte Carlo. The "S.Gap" of LHS monotonously decreases with increased $|S|$, while the stochastic optimality gap for crude Monte Carlo fluctuates (4.28%) at $|S| =$ 100. Thus, LHS is more promising when the sample size is relatively large. The "UB" columns reflect the quality of the solution

Table 3: Stochastic bounds of different scenario size

$\|S\|$	LB (95% CI)			UB (95% CI)			S.Gap (%)
	Mean	Width	$\frac{\text{Width}}{\text{Mean}}$ (%)	Mean	Width	$\frac{\text{Width}}{\text{Mean}}$ (%)	
Crude							
5	49823388.33	487231.10	0.98	51565745.73	160235.15	0.31	4.62
10	50455015.67	267302.25	0.53	51645767.39	239805.56	0.46	3.27
25	50681657.33	242631.37	0.48	51694432.22	189790.81	0.37	2.79
50	50925201.49	188632.95	0.37	51826631.06	216934.97	0.42	2.51
100	51234509.83	118527.52	0.23	52808050.46	594800.45	1.13	4.28
150	51310677.01	130870.68	0.26	51829646.83	301455.52	0.58	1.82
LHS							
5	50186861.33	170168.01	0.34	52144322.46	430299.71	0.83	4.87
10	50724832.23	176945.82	0.35	51767318.50	189619.49	0.37	2.71
25	50842947.05	85649.82	0.17	51928468.44	347957.43	0.67	2.91
50	51095298.75	78642.19	0.15	51725294.03	157844.32	0.31	1.67
100	51342627.87	73482.64	0.14	51761916.37	216864.35	0.42	1.37
150	51487887.81	61958.82	0.12	51730161.33	189658.75	0.37	0.95

[1] `LB`: lower bound; `UB`: upper bound; `CI`: confidence interval; `Mean`: mean value of CI; `Width`: width of CI; `S.Gap`: stochastic optimality gap.

obtained (in sample) when applied to instances that are not used for optimization (out of sample). For $|S| \in \{50, 100, 150\}$, compared to crude Monte Carlo, LHS yields lower mean values of UB (as shown in "Mean"), and the CIs are narrower, both absolutely (as shown in "Width") and relatively (as shown in "$\frac{Width}{Mean}$"). This indicates that LHS can yield solutions with better out-of-sample performance when the sample size is relatively large. Detailed out-of-sample stability performance is discussed in Section 5.4. The "LB" columns reflect the quality of estimation for the true objective value. LHS yields narrower LB CIs with all $|S|$ compared to crude Monte Carlo. Overall, LHS is found to be superior to crude Monte Carlo in terms of both out-of-sample and in-sample stability, and it does not introduce any additional computational burden or implementation difficulties. Therefore, for all subsequent experiments in the following subsections, $|S| = 100$ is used with LHS, unless otherwise specified. Furthermore, even with $|S| = 5$, the "S.Gap" remains below 5%, which suggests that when the problem is extremely hard, a relatively small sample size can be used to reduce the computational burden without sacrificing much accuracy.

5.3. Efficiency of logic-based Benders decomposition

In Table 4, we compare the computational efficiency among solving the PRCR model directly with Gurobi (columns GRB), LBBD without warm-start (columns LBBD), and LBBD with warm-start (columns LBBD-W). For each instance with a certain solution method, the "Obj." denotes the best-known solution founded by the solution method, and the "Gap" is defined as (Obj. - LB) / Obj. LB for GRB is the objective value of the linear relaxation, while LB for LBBD and LBBD-W is the objective value of the master problem with an incomplete set of Benders cuts. The columns "Time'" are the time that the best-known solution is found and the columns "Time" are the overall runtime. For hard instances where the optimality cannot be proved but feasible solutions can be found, it is desired that a good quality solution can be found with less "Time'". We set a time limit of 3600 seconds (one hour) for all the instances and solution methods. Since we found that some of the subproblems can be hard to be optimized, we set a time limit of 600 seconds (ten minutes) for solving subproblems. The 600 seconds limit is also applied to the warm-start problems considering that the wait-and-see warm-start problems and the expected-value warm-start problems are as difficult as subproblems in the LBBD iterations.

Table 4: Computational performance

Instance	GRB				LBBD					LBBD-W				
	Obj. ($\times 10^6$)	Gap (%)	Time' (s)	Time (s)	Obj. ($\times 10^6$)	Gap (%)	Dif. (%)	Time' (s)	Time (s)	Obj. ($\times 10^6$)	Gap (%)	Dif. (%)	Time' (s)	Time (s)
05-03-0	25.26	59.61	434	3600	25.35	0.00	0.35	306	306	25.26	0.00	0.00	132	326
05-03-1	51.25	0.01	12	12	51.70	0.00	0.88	221	221	51.25	0.00	0.00	224	224
05-03-2	70.74	21.07	348	3600	72.17	0.04	1.97	212	212	70.74	0.00	0.00	118	222
05-05-0	1979.66	99.97	3595	3600	75.87	0.00	-2509.29	2476	2476	77.84	0.00	-2443.17	1320	1320
05-05-1	48.69	5.60	1526	3600	48.97	0.00	0.56	492	492	48.69	0.00	0.00	222	502
05-05-2	2293.61	99.68	3468	3600	54.84	0.00	-4082.19	637	637	-	-	-	-	-
10-03-0	170.92	85.79	1181	3600	66.85	0.00	-155.68	785	785	66.79	0.05	-155.92	304	849
10-03-1	106.92	0.01	35	36	107.01	0.00	0.09	475	475	107.53	0.05	0.57	302	535
10-03-2	95.99	20.37	3587	3601	96.10	0.00	0.12	656	656	95.99	0.00	0.00	237	599
10-05-0	105.59	84.56	123	3600	465.84	94.04	77.33	5776	5776	1897.43	99.02	94.44	6112	6112
10-05-1	124.22	0.01	5	5	1173.51	94.11	89.41	4049	4050	1173.51	94.11	89.41	5292	5292
10-05-2	91.48	38.55	1582	3600	2279.29	98.91	95.99	3620	3620	5270.48	100.00	98.26	3622	3622

[1] `GRB`: Gurobi; `LBBD(-W)`: LBBD (with warm-start); `Obj.`: objective value; `Gap`: $(Obj. - LB)/Obj.$; `Time'`: time that the best-known solution is found; `Time`: time that the algorithm is terminated; `Dif.`: $(LBBD(-W)_{Obj.} - GRB_{Obj.})/LBBD(-W)_{Obj.}$.

Results are presented in Table 4, from which there are several observations. Firstly, though the runtime of GRB is usually significantly longer than that of LBBD(-W), the GRB solutions are not significantly better than the LBBD(-W) solutions. In 7

out of 12 instances, the LBBD-W solutions are no worse than the GRB solutions, and the runtime of LBBD-W is usually shorter than that of GRB. For some of the instances (e.g. 05-05-0, 05-05-2, and 10-03-0), the GRB solutions can be significantly worse than the LBBD(-W) solutions. Secondly, in terms of optimality proof, GRB cannot prove optimality for most of the instances within 3600 seconds and the optimality gap can go up to 99%, while LBBD(-W) can prove optimality for 9 instances within 3600 seconds. The first and second observations reflect the LBBD(-W) can provide stronger lower bounds than the linear relaxation. Thirdly, among all the solution methods, LBBD-W requires the shortest time to find the best-known solutions. The value of warm-start cuts is validated. Lastly, the LBBD(-W) uses heuristics to calculate the cutting coefficients, it is worthwhile to verify whether the heuristics yield a subgradient that is close to the true one. For instance 05-03-1 and 10-03-1, the optimality gap by GRB is 0.01%, i.e., they are almost optimized. The relative differences between the LBBD solutions and the GRB solutions (Dif.) for 05-03-1 and 10-03-1 are 0.88% and 0.09%, respectively. The relative differences between the LBBD-W solutions and the GRB solutions (Dif.) for 05-03-1 and 10-03-1 are 0.00% and 0.57%, respectively. All the relative differences are significantly less than the S.Gap = 1.37% with $|S| = 100$ in Table 3. We can conclude the heuristics performs well since the error caused by cutting coefficients heuristics is less than the error caused by sampling (less than 1.00% versus 1.37%).

We find that instances 10-05-0, 10-05-1, and 10-05-2 cannot be solved within hours. The causes of computational difficulties are two folds. Firstly, scenario number 100 is too large for hard instances. Secondly, the decomposed subproblems themselves are difficult. Since Table 3 in Section 5.2 suggests that for hard instances we can use a relatively small scenario number, e.g. 10, 25, and 50, without losing too much accuracy. Therefore, in Table 4, we set $|S| = 10$ for solving 10-05-0, 10-05-1, and 10-05-2. This modification reduces the number of subproblems from 100 to 10 in each iteration, for each instance. On the other hand, since the resulting subproblems each contains 10 affected areas and 5 time period that can be hard to prove optimality, we set a time limit of 600 seconds and a MIP gap of 10% whichever is first reached. In the following, we analyze the validity of Benders cuts with suboptimal subproblems. Recall that $\hat{Q}(\bar{X}, \xi_s)$ be the optimal subproblem solution with fixed $\bar{X}$ and let $\hat{Q}_U(\bar{X}, \xi_s)$ be an upper bound of $\hat{Q}(\bar{X}, \xi_s)$, that is $\hat{Q}_U(\bar{X}, \xi_s) \geq \hat{Q}(\bar{X}, \xi_s)$ holds. Whenever Benders cut is generated by $\hat{Q}(\bar{X}, \xi_s)$, which implies $\bar{\theta}_s < \hat{Q}(\bar{X}, \xi_s)$, Benders cut is also generated by $\hat{Q}_U(\bar{X}, \xi_s)$ since $\bar{\theta}_s < \hat{Q}(\bar{X}, \xi_s) \leq \hat{Q}_U(\bar{X}, \xi_s)$ holds. The resulting Benders cuts by $\hat{Q}_U(\bar{X}, \xi_s)$ exclude the current master problem solution (property (i)) but cannot guarantee that any globally optimal solution will not be removed (property (ii)). Hence, sub-optimal subproblems lead to an upper bound for the original problem. Note that solving the warm-start problems is as hard as the aforementioned subproblems, so the same limits (600 seconds, 10% MIP gap) are also set for the warm-start problems for LBBD-W. In the warm-start cuts (12) and (13), only (13) is applied as it remains valid when the right-hand side of it is an upper bound. The results of 10-05-0, 10-05-1, and 10-05-2 in Table 4 suggest that to successfully apply the LBBD, the subproblems should not be too difficult. It is worth mentioning that when we set $|S| = 100$ for 10-05-0, 10-05-1, and 10-05-2, Gurobi returns out-of-memory errors and cannot find feasible solutions. In contrast, LBBD(-W) can yield feasible solutions but requires more than 3600 seconds of computational time. This indicates that our LBBD(-W) is more scalable than the deterministic equivalent. Observations from our instances suggest that: (i) Off-the-shelf solvers are suitable for deterministic equivalents with small scenario sizes. (ii) LBBD(-W) is promising for instances with large scenario sizes. (iii) LBBD-W is the best choice when high-quality feasible solutions are needed in a short runtime.

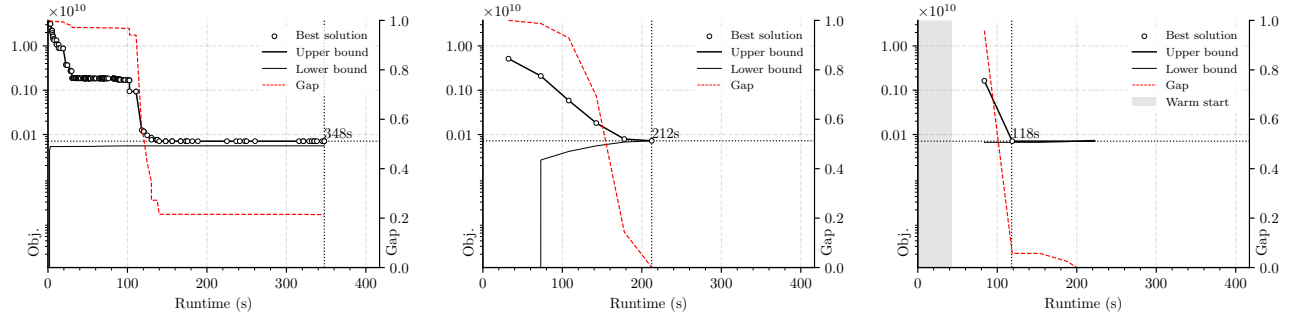

(a) GRB (b) LBBD (c) LBBD-W

Figure 4: Convergence curve

In order to analyze the convergence behaviors differences of all the solution methods, Figure 4 illustrates bounds during iterations for 05-03-2, which is typical among all the instances. In Figure 4, the circle represents the best solution that is found till a certain time, the thick and thin black lines represent the upper bound and lower bound respectively, and the red dashed lines denote the optimality gap. The definitions for the upper bound, lower bound, and gap is the same as that in Table 4. Additionally, for LBBD-W there is a shaded area that represents the process of warm-start. There are some observations from Figure 4. Firstly, all three solution methods can find solutions with similar objective values within 400 seconds. Secondly, although the GRB gets better lower bounds than both LBBD and LBBD-W before around 100 seconds, the GRB lower bound increases very slowly. As a result, the GRB optimality gap stops decreasing after a certain iteration. Thirdly, though LBBD-W takes more time to find the first feasible solution than both GRB and LBBD and the overall runtime for LBBD-W is slightly

longer than that for LBBD, the first feasible LBBD-W solution is better than that of GRB and LBBD. Furthermore, the LBBD-W takes less time to find the optimal solution (118 seconds versus 348 seconds for GRB and 212 seconds for LBBD), which validates the value of our warm-start enhancements. In summary, both LBBD and LBBD-W converge faster than GRB (the GRB even does not converge after 3600 seconds), and the warm-start helps to find better solutions in the initial iterations.

5.4. Value of incorporating stochasticity and out-of-sample stability

Incorporating stochasticity adds computational difficulties to the mathematical programming model. So we discuss the value of using stochastic models rather than deterministic ones in this section. We derive indicators from WS and EEV that have been introduced in Section 4.3 to measure the performance of stochastic programming. Furthermore, since our solution method uses LHS samples to approximate the true underlying stochastic parameters, it is worthwhile to analyze the out-of-sample performance of the optimal solutions. Before discussing numerical results in Table 5, we first describe the stochastic programming indicators as follows.

Firstly, the expected value of the perfect information (EVPI) (Raiffa & Schlaifer, 1961) is defined as $EVPI = SP - WS$ and $EVPI(\%) = (SP - WS)/SP$ where the WS is the expected value of the wait-and-see problem as mentioned in Section 4.3 and the SP is the value of the stochastic problem. EVPI measures the cost of the inability to perfectly predict the demand and lead time. EVPI also reflects the highest acceptable price for perfect information prediction. The WS are obtained from solving $|S|$ independent deterministic problems in which the stochastic parameters are replaced with the scenario-specified realization. Secondly, the value of the stochastic solution (VSS) (Birge, 1982) is defined as $VSS = EEV - SP$ and $VSS(\%) = (EEV - SP)/SP$ where the EEV it the expected value of the expected value solution as mentioned in Section 4.3 and the SP is the value of the stochastic problem. The VSS measures the cost saving when solving a stochastic problem rather than an expected value problem. The expected value problem replaces the stochastic parameters in the stochastic problem with their expected values. In Table 5, the column EVPI(%) reveals that the costs of imperfect prediction range from 1.98% to 23.29%. Since for most of the instances, the SP is not 10% larger than the WS, the quality of stochastic model solutions is also validated. The column VSS(%) ranges from 58.71% to 85.71%, that is when the decision-maker adopts the simpler expected value problem to replace the stochastic model, the resulting additional cost can go up to 85.71% higher than the stochastic model solution on average. Thus we can conclude that the benefit of using stochastic models is significant.

Table 5: Value of incorporating stochasticity

Instance	WS			SP	EEV		
	Obj.	EVPI	EVPI (%)	Obj.	Obj.	VSS	VSS (%)
05-03-0	2.37e+07	1.64e+06	6.45	2.54e+07	1.68e+08	1.42e+08	84.88
05-03-1	4.96e+07	2.09e+06	4.04	5.17e+07	1.57e+08	1.05e+08	67.03
05-03-2	6.73e+07	4.91e+06	6.80	7.22e+07	5.05e+08	4.33e+08	85.71
05-05-0	5.82e+07	1.77e+07	23.29	7.59e+07	2.81e+08	2.05e+08	72.99
05-05-1	4.80e+07	9.70e+05	1.98	4.90e+07	1.40e+08	9.13e+07	65.09
05-05-2	5.18e+07	3.09e+06	5.64	5.48e+07	2.89e+08	2.35e+08	81.05
10-03-0	6.26e+07	4.22e+06	6.31	6.69e+07	3.86e+08	3.19e+08	82.68
10-03-1	1.02e+08	4.73e+06	4.42	1.07e+08	2.59e+08	1.52e+08	58.71
10-03-2	9.16e+07	4.49e+06	4.67	9.61e+07	3.55e+08	2.59e+08	72.91

[1] `WS`: expected value of the wait-and-see problem; `SP`: value of the stochastic problem; `EEV`: expected value of the expected value solution; `EVPI`: $SP - WS$; `EVPI(%)`: $(SP - WS)/SP$; `VSS`: $EEV - SP$; `VSS(%)`: $(EEV - SP)/SP$.
[2] Results of 10-05-0, 10-05-1, and 10-05-2 are not presented since they cannot be optimized.

Practically, there may be unexpected disturbances in the stochastic parameters, which may result in disappointment with the stochastic programming solution, especially in the context of humanitarian relief. To measure how good are the obtained solutions when disturbances are added to the stochastic parameters, we conduct the out-of-sample stability test (Kaut & Wallace, 2007). To be more specifically, given an optimal solution X^* with the set of samples S_{in}, the value of $\mathbb{E}_{s' \in S_{out}} Q(X^*, \xi^{s'})$ with another sample S_{out} should be approximately the same as $\mathbb{E}_{s \in S_{in}} Q(X^*, \xi^s)$. The term "out-of-sample" is used as the stability that is judged on a different sample S_{out} rather than the S_{in} that is used for finding solutions. The experiments are conducted on instance 05-03-0, 05-03-1, and 05-03-2 with the following steps: (i) For each original instance, we generate additional 100 instances $S^j_{out}, j \in \{1, 2, \cdots, 100\}$ with increased standard deviations of the consumption rate as $\sigma := \sigma(1 + \delta_\sigma), \delta_\sigma \in \{0.00, 0.10, 0.30\}$. Note that the sample size is $|S^j_{out}| = 100$, and other parameters remain the same as that for the original instance. (ii) The 100×3 instances are solved with the first-stage variables being fixed to the solution of the original instance solved in Section 5.3. (iii) The relative differences between the in-sample objective value and out-of-sample objective value are computed with $\left[\mathbb{E}_{s' \in S^j_{out}} Q(X^*, \xi^{s'}) - \mathbb{E}_{s \in S_{in}} Q(X^*, \xi^s)\right] / \mathbb{E}_{s' \in S^j_{out}} Q(X^*, \xi^{s'}), \forall j \in \{1, 2, \cdots, 100\}$, namely out-of-sample bias. (iv) Additionally, we compute $\left[Q(X^*, \xi^{s'}) - \mathbb{E}_{s \in S_{in}} Q(X^*, \xi^s)\right] / Q(X^*, \xi^{s'}), \forall \xi^{s'} \in \bigcup_{j=1}^{100} S^j_{out}$, namely scenario-specific bias, to reflect the bias between estimated expected objective value and the actual objective value of a certain scenario realization. The relative differences in step (iii) and step (iv) are fitted with probability density functions (PDFs) using the Gauss Kernel Estimation and the PDFs are illustrated in Figure 5. Figure 5(a), Figure 5(b), and Figure 5(c) reflect the quality of objective value estimation

considering that the standard deviations may be underestimated in the instances for finding solutions. Figure 5(d), Figure 5(e), and Figure 5(f) reflect how good are the solutions when they are actually used for unexpected events.

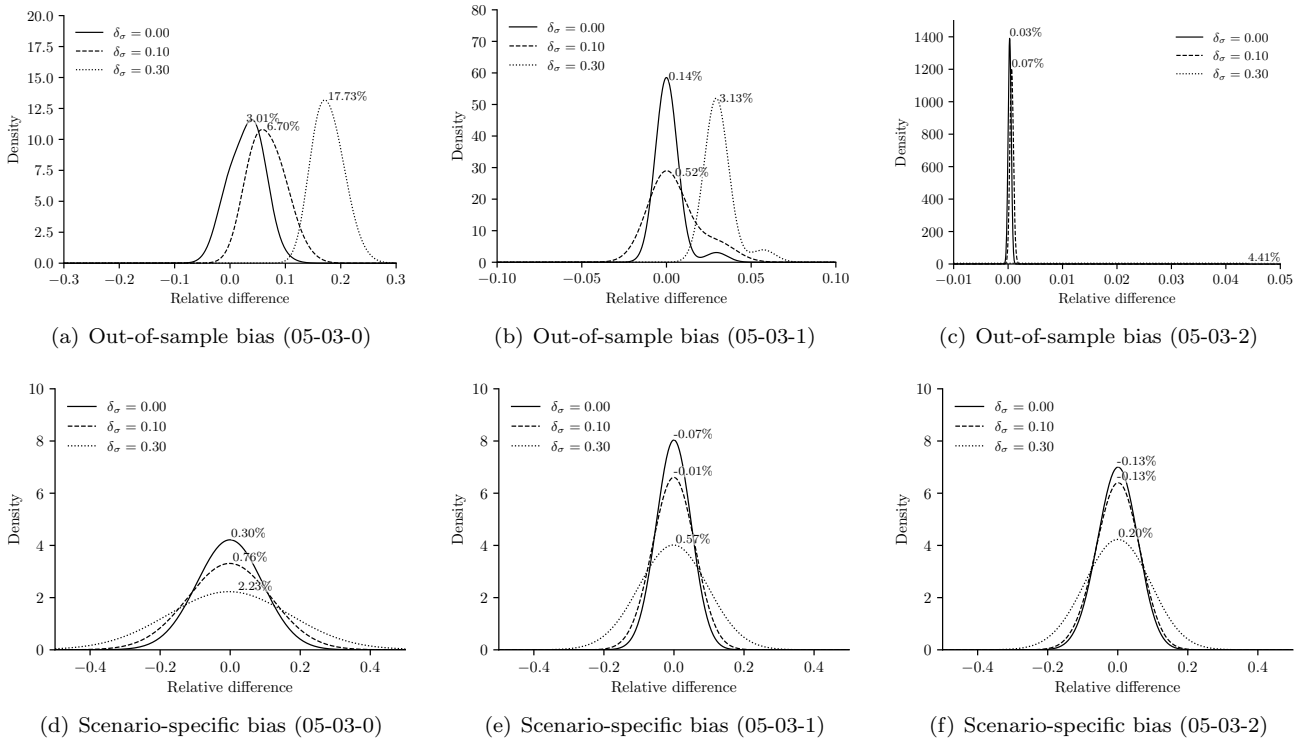

(a) Out-of-sample bias (05-03-0) (b) Out-of-sample bias (05-03-1) (c) Out-of-sample bias (05-03-2)

(d) Scenario-specific bias (05-03-0) (e) Scenario-specific bias (05-03-1) (f) Scenario-specific bias (05-03-2)

Figure 5: Out-of-sample performance under different disturbance

From Figure 5(a) to Figure 5(c), we can see that the average out-of-sample biases are at most 17.73% (Figure 5(a), $\delta_\sigma = 0.30$) and the mean objective values of out-of-sample instances without standard deviation increasing are at most 3.01% (Figure 5(a), $\delta_\sigma = 0.00$). When different samples of the same size are used to estimate the objective of the stochastic model, it is not likely that the differences in samples will significantly influence the estimated objective value, so our method is out-of-sample stable. Additionally, for all the instances, it is not surprising to observe the average out-of-sample biases increase with the standard deviations increase and the average out-of-sample biases are always positive, since the solutions are not optimized with the out-of-sample instances. In Figure 5(c), $\delta_\sigma \in \{0.00, 0.10\}$ result in nearly zero out-of-sample biases, which demonstrate the value of LHS. From Figure 5(d) to Figure 5(f), we can see that for all the instances and δ_σ, the average scenario-specific biases are no more than 2.23% (Figure 5(d), $\delta_\sigma = 0.30$). Even in the large variability cases ($\delta_\sigma = 0.30$), the maximum scenario-specific bias is around 30% to 40%, which is less than the VSS(%) in the Table 5 (58.71% to 85.71%). Hence, the value of using the stochastic model is justified. In other words, using stochastic models can yield solutions better than the expected value problem, even when there is something unexpected involved in the problem.

5.5. Value of capacity reservation

In this section, we compare the performance of the SPIP, PHCR, and PRCR models. The experiments are conducted on the instance 10-03-02. However, the insights can be generalized to other instances and more general cases. Apart from the three models, we also analyze the impact of prepositioning inventory on the overall cost. Since the prepositioning inventory is used to satisfy the sudden onset demand in the initial response phases, the prepositioning inventory level potentially influences the deprivation cost significantly. To conduct experiments, for the three models, we add an additional prepositioning inventory level constraint to them. The prepositioning inventory level constraint is defined as $\sum_{j\in R} r_j \leq \rho \cdot \sum_{t\in T} \left[\left(\sum_{i\in D} w_i\right) \cdot \mathcal{C}_2(t)\right]$ where $\sum_{j\in R} r_j$ is the total prepositioning inventory, $\rho \in \{0.25, 0.50, 1.00\}$ is the ratio of prepositioning inventory to total expected demand, and $\sum_{t\in T} \left[\left(\sum_{i\in D} w_i\right) \cdot \mathcal{C}_2(t)\right]$ is the total expected demand for all the affected areas through the planning horizon. The results are presented in Table 6 and illustrated in Figure 6.

We first compare the cost of SPIP, PHCR, and PRCR under the same ρ. For $\rho = 0.25$ and $\rho = 0.50$, the prepositioning procurement costs are the same for the SPIP, PHCR, and PRCR. For $\rho = 1.00$, the SPIP purchases more prepositioning inventory than PHCR and PRCR. It can be explained as in order to avoid potential stockout that can incur deprivation costs, the SPIP has to prepare as much as possible prepositioning inventory since there is no other procurement chance in the future periods. On the contrary, for all the ρ, the overall procurement cost of SPIP is lower than that of PHCR and PRCR (Figure 6(a)). It can be explained as the procurement cost of SPIP is limited by the prepositioning inventory level constraint with ρ, but PHCR and PRCR can purchase additional supplies in future periods. As a result of prepositioning inventory level limit, SPIP results in higher deprivation cost than PHCR and PRCR even when $\rho = 1$, since the true total demand can be

Table 6: Value of capacity reservation

ρ	Obj.	PC_1	PC_2		PC_3		DC	
			$\mathbb{E}(PC_2)$	$\mathbb{D}(PC_2)$	$\mathbb{E}(PC_3)$	$\mathbb{D}(PC_3)$	$\mathbb{E}(DC)$	$\mathbb{D}(DC)$
SPIP:								
0.25	3.73e+11	2.17e+07	-	-	-	-	3.73e+11	4.34e+10
0.50	1.66e+11	4.34e+07	-	-	-	-	1.66e+11	8.63e+10
1.00	4.15e+09	8.69e+07	-	-	-	-	4.07e+09	7.62e+09
PHCR:								
0.25	4.39e+09	2.17e+07	4.73e+07	6.63e+06	-	-	4.32e+09	2.66e+08
0.50	1.77e+09	4.34e+07	3.91e+07	3.84e+06	-	-	1.69e+09	5.29e+08
1.00	1.71e+08	6.27e+07	3.17e+07	4.03e+06	-	-	7.70e+07	1.84e+08
PRCR:								
0.25	4.38e+09	2.17e+07	3.06e+07	5.95e+06	9.76e+06	7.64e+06	4.32e+09	2.66e+08
0.50	1.77e+09	4.34e+07	2.48e+07	6.21e+06	9.34e+06	7.65e+06	1.69e+09	5.29e+08
1.00	9.61e+07	7.15e+07	1.24e+07	7.31e+06	9.32e+06	7.82e+06	0	0

[1] `Obj.`: objective value; PC_1: prepositioning procurement cost; PC_2: procurement cost for PHCR supplies; PC_3: procurement cost for PRCR supplies; DC: deprivation cost; $\mathbb{E}(\cdot)$: mean; $\mathbb{D}(\cdot)$: standard deviation.

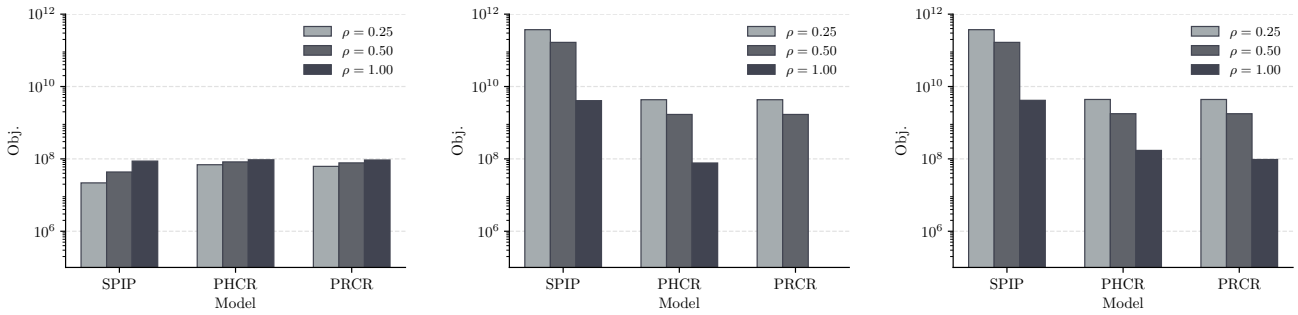

(a) Procurement cost (b) Deprivation cost (c) Total cost

Figure 6: Value of capacity reservation

higher than the expected value $\sum_{t\in T}\left[\left(\sum_{i\in D} w_i\right)\cdot \mathcal{C}_2(t)\right]$. It is worth noting that between components of the total cost, i.e., procurement cost and deprivation cost, the deprivation cost plays a dominating role, which highlights the negative impact of stockout. Then we compare the cost under different ρ with the same model. It is apparently from Figure 6, for all the models, an increase on ρ results in an increase in the procurement cost but a decrease in the deprivation cost. This can be explained by the trade-off between relief item purchasing and human suffering alleviating. Specifically, in instance 10-03-2, the unit cost for buying relief items ranges from 50 dollars to 100 dollars, the expected consumption rate is 0.5, and the deprivation cost is $\gamma(0) = 0, \gamma(1) = 54, \gamma(2) = 11,992, \gamma(3) = 1,000,000$. For a certain individual, the cost for satisfying the demands of two periods is at most \$25 ($= 0.5 \times 2 \times 100$), while two periods of deprivation are equivalent to \$11,992, so it is reasonable to purchasing relief items for alleviating deprivation. Finally, Figure 6(b) reveals that among all the experiments, only PRCR can result in zero deprivation. PRCR outperforms PHCR since PRCR order quantity is only limited by the suppliers' production capacity while PHCR requires the order quantity series to obey the quantity-flexibility contract. In summary, the results suggest that compared with using the traditional prepositioning strategy solely, integrating the capacity reservation to prepositioning can alleviate human suffering significantly, especially when the funds that can be used for prepositioning are limited. On the other hand, our results also suggest the value of preparedness, since for all the models, prepositioning inventory level increases can result in deprivation cost decreases in orders of magnitude.

5.6. Impact of the deprivation cost function

Since there is not constant deprivation cost function that is suitable for all relief items under all socio-economic conditions, this section analyzes the impact of the deprivation cost function on the objective value. In previous sections, the deprivation cost function was defined as $\gamma(t) = \min\{\gamma^{\max}, a\times e^{b\times 48\times t} \text{ if } t \geq 1 \text{ else } 0\}$ where $a = 0.2354, b = 0.1129$, $\gamma^{\max} = 1,000,000$, and t is the deprivation time. In the following, we conduct experiments using deprivation cost functions with $a := a(1+\delta_a), b := b, \gamma^{\max} = 1,000,000$ and $a := a, b := b(1+\delta_b), \gamma^{\max} = 1,000,000$ where $\delta_a \in \{-0.2, -0.1, 0.0, 0.1, 0.2\}$ and $\delta_b \in \{-0.2, -0.1, 0.0, 0.1, 0.2\}$. Similar to Section 5.5, experiments in this section are conducted on the instance 10-03-2, and prepositioning inventory level constraints are also involved, but all the experiments are only conducted using the PRCR model. We illustrate the results in Figure 7. Note that we also conducted experiments with $\gamma^{\max} = 500,000$. However, the results are not significantly different from that of $\gamma^{\max} = 1,000,000$. The similarity between results with $\gamma^{\max} = 500,000$ and $\gamma^{\max} = 1,000,000$ can be explained by the fact that the optimal solutions tend not to incur a deprivation cost as high as the value of life.

Figure 7 reveals that when the prepositioning inventory level is insufficient, i.e., $\rho = 0.25$ and $\rho = 0.50$, the objective value increases with δ_a and δ_b. Furthermore, the difference between curves in Figure 7(a) and Figure 7(b) demonstrates that

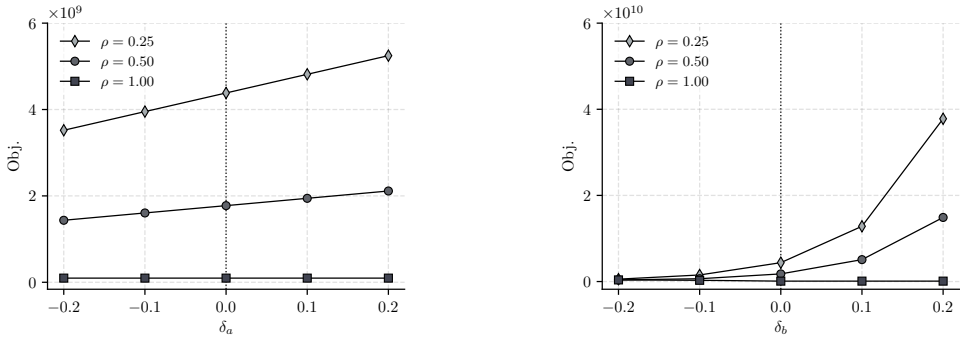

(a) $b = 0.1129, \$1,000,000$ (b) $a = 0.2354, \$1,000,000$

Figure 7: Impact of deprivation cost function parameters

the objective value is more sensitive to δ_b than δ_a. This observation is not surprising as δ_b has exponential impacts on the deprivation cost while δ_a only has linear impacts on the deprivation cost. When the prepositioning inventory level is sufficient, i.e., $\rho = 1.00$, the objective value does not increase with δ_a or δ_b. This observation is intuitive since it is more reasonable to prepare sufficient supplies than to incur deprivation costs. Figure 7(a) shows under lower ρ the objective value grows faster with δ_a ($\rho = 0.25$ versus $\rho = 0.50$). Similar results with δ_b can also be observed in Figure 7(b). Both Figure 7(a) and Figure 7(b) suggest the amplification effect of the limited prepositioning inventory level ρ. Along with the aforementioned similarity between experiments on $\gamma^{\max} = 500,000$ and $\gamma^{\max} = 1,000,000$, following insights are suggested. Firstly, among all the three parameters for deprivation cost function $a, b, \gamma^{\max}$, the objective value is less sensitive to the value of life $\gamma^{\max}$. This observation demonstrates that international humanitarian organizations, which operate globally and provide various types of aid, should focus more on the urgent needs of specific groups of people rather than the value of life of those affected. Secondly, the parameter b is more crucial than a, indicating a need to prioritize urgent demands. For example, medical assistance to injured people usually has higher b than water and food, hence medical assistance should be delivered with higher priority than water and food when transportation resources are limited. Lastly, the value of preparedness is again validated. Sufficiently large ρ makes the objective value not increase with the deprivation cost function parameters a and b. On the contrary, an insufficient prepositioning inventory level would amplify the deprivation cost.

5.7. Case study: climate-related disaster relief in Brazil

In Section 1, we explain that the proposed PRCR system, although inspired by the practices of the PPE industry during the pandemic, is not limited to epidemic or pandemic situations, and can be applied to other unanticipatable hazard events. In this section, we focus on Brazil's disaster relief planning, which is designed to handle various types of disasters. Brazil is the largest nation in South America, and it has a population of over 200 million, which is the fifth in the world. From 2000 to 2022, there are 133 natural hazards recorded in Brazil, among them floods are the most frequent (96 in 133), while droughts result in the most affected people (over 33 million) (CRED, 2022). Weather patterns and consequential disasters exhibit diversity in Brazil, varying according to latitude and topography. The northern regions of the country receive heavy rainfall throughout the year, whereas the central and southern areas experience a distinct wet and dry season. In the central and southern areas, the Andes Mountains create a phenomenon known as the South American Low-Level Jet (SALLJ)[2] (Insel et al., 2010) leading to heavy rainfall during the wet season, which typically occurs from November to March. On the contrary, the dry season typically occurs from May to September when the subtropical high-pressure system moves southward and brings dry air to the region. This results in a decrease in precipitation. Since floods and droughts can be anticipated seasonally, traditionally, Brazil has not been considered one of the most disaster-prone countries. However, global climate change is changing the situation. The La Niña [3] that started in 2020 and lasted until 2022 caused extreme and long-term drought in the La Plata Basin, which includes central and southern Brazil, resulting in the lowest water levels in 77 years. Southern Brazil experienced extremely dry conditions during the wet seasons from 2019 to 2022 compared to 1991 to 2020 (EC-JRC et al., 2023). According to the *WorldRiskIndex*, which has been calculating disaster risk for 193 countries since 2011, Brazil ranked 121st in 2011 and rose to 43rd in 2022 (BEH, 2011, 2022). As global climate change continues to cause more extreme and unanticipatable climate-related disasters, new disaster relief systems, such as PRCR, are required to complement prepositioning. The case study presented in this section analyzes the impact of various factors (i.e., capacity, ability, and unit price) on the overall performance of our disaster relief systems, prior to its implementation in Brazil.

The dataset (Veloso et al., 2022) for our case study consists of two subsets: *national-level* dataset and *state-level* (Santa Catarina) dataset. The data was originally gathered from public sources and official government data portals, from 2003 to 2021. It includes the number of affected people in 5402 Brazilian municipalities by nine types of disasters during 218 months. The national-level and state-level case study datasets are derived from this original data and provided as a spreadsheet. The state of Santa Catarina is considered since it is located in the La Plata Basin, which can be affected by the SALLJ and the La Niña, facing climate-related disaster risks. The most crucial information in the spreadsheet to make our case study reliable and

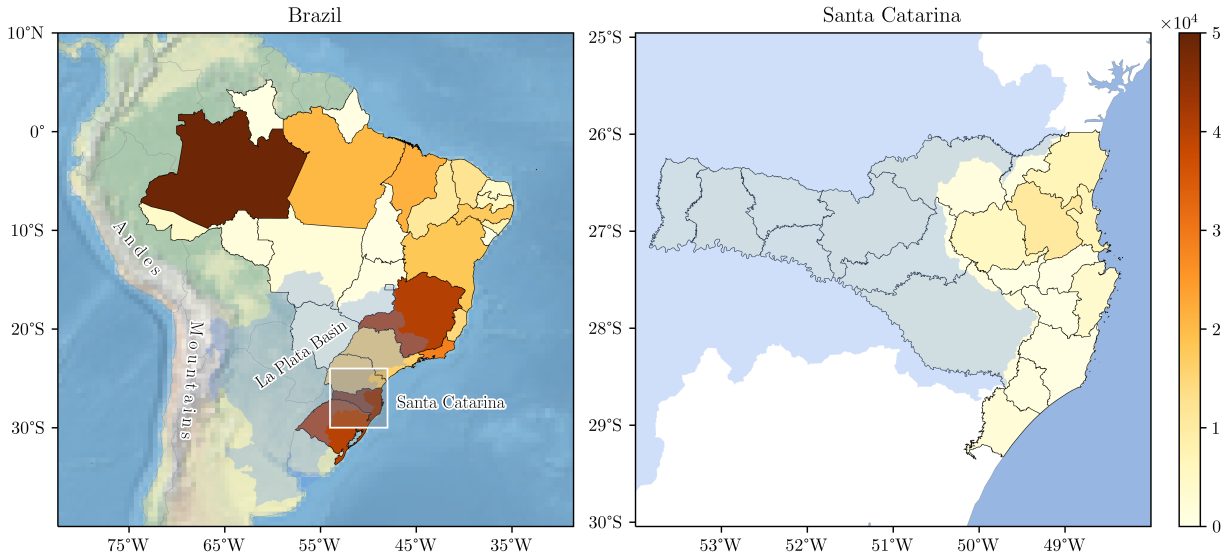

Figure 8: Affected people heatmap of Brazil and Santa Catarina

realistic is the number of affected people, through which the demands, which are used as inputs of our models, can be calculated. Figure 8 [4] depicts the geographical distribution and affected people numbers of the areas of interest, i.e., 26 states (except the Federal District) in Brazil and 20 cities in Santa Catarina. Colors of varying depths are used to represent the expected number of affected people. It is clear that states/cities near the coastline are disaster-prone, and among them, Santa Catarina is one of the most vulnerable. Recall that for each state/city i, our models use d_i^{ts} as a parameter to represent the demand at time t under scenario s. That is the inputted demand should not only be stochastic but also be multi-phase. However, the dataset by Veloso et al. (2022) is stochastic but static. To prepare this dataset for our problem, we assume that during the planning horizon $t \in \{1, 2, \cdots, 5\}$ (one period corresponds to two days) the number of affected people is constant. The demand is calculated from number of affected people as $d_i^{ts} = people_i^s, \forall t \in \{1, 2, \cdots, 5\}$, where $people_i^s$ is the number of affected people in area i under scenario s. There are other sets of parameters required for our models, i.e., capacity-related parameters for facilities, ability-related parameters for suppliers, and cost-related parameters for suppliers. These parameters can vary depending on the context. For instance, even within a specific region, prices may differ based on the time of year. Therefore, it is necessary to analyze how the values of these parameters impact the relief performance and the corresponding overall cost. The methods we use are main effect and interaction effect analysis, which are statistical methods used to identify the primary factors that contribute to an observed outcome. Experiments are conducted by varying one factor at a time while holding all other factors constant, and measuring the effect on the outcome. In the following, we provide the baseline estimation (M) for the factors mentioned earlier, along with their lower-level (L) and higher-level (H) cases.

- *Capacity (capacity of relief facilities and affected areas):* Our models do not involve facility sizing as decision variables but assume facility sizes have been predetermined according to the historical disasters and their impact. Therefore, we set sizes based on demand information. The capacity of the relief facility is considered can meet the demand $\max_{s\in S} \sum_{i\in D} d_i^{ts}$ for one period (two days), two periods (four days), and three periods (six days) in the case L, M, and H, respectively. The capacity of affected areas i is considered can meet their own demand $\max_{s\in S} d_i^{ts}$ for one period (two days), two periods (four days), and three periods (six days) in the case L, M, and H, respectively.
- *Ability (lead time and production capacity of PHCR and PRCR suppliers):* In the case L, the lead time of PHCR and PRCR suppliers are set to two periods, production capacity is assumed to be $0.5 \times \max_{s\in S} \sum_{i\in D} d_i^{ts}$. In the case M, the lead time of PHCR and PRCR suppliers are set to one period, production capacity is assumed to be $\max_{s\in S} \sum_{i\in D} d_i^{ts}$. In the case H, the lead time of PHCR and PRCR suppliers are set to zero, production capacity is assumed to be $2 \times \max_{s\in S} \sum_{i\in D} d_i^{ts}$. We use the deterministic lead time to eliminate the effect of randomness. As we move from case L to H, suppliers' abilities improve.
- *Cost (unit price of prepositioning, PHCR, and PRCR):* The relief item considered is drinking water, which is crucial in humanitarian relief and consistent with previous numerical studies. We use the average unit price \$25 (130 Brazilian reals) estimated by Veloso et al. (2022) as the case M for prepositioning, PHCR, and PRCR. Then 20% is subtracted and added for the case L and H, resulting in \$20 and \$30, respectively. While the capacity-related and ability-related parameters have three cases each, the cost-related parameters have 27 cases. These are determined by $|\{L, M, H\}$ (prepositioning) $\times$ $\{L, M, H\}$ (PHCR) $\times$ $\{L, M, H\}$ (PRCR)$| = 27$.

There are totally $3^5 = 243$ instances generated. The instances with all the factor levels being M can be accessed from https://guo.ph/data/cap_res. All 243 instances share the same demands and deprivation cost function (same as the one used in previous subsections) but have different capacity-related, ability-related, and cost-related parameters. Based on these instances, we set fixed levels for each factor (L, M, and H) and vary the levels of other factors to solve the PRCR models repeatedly. The objective values are recorded to determine the impact of each factor on the overall cost.

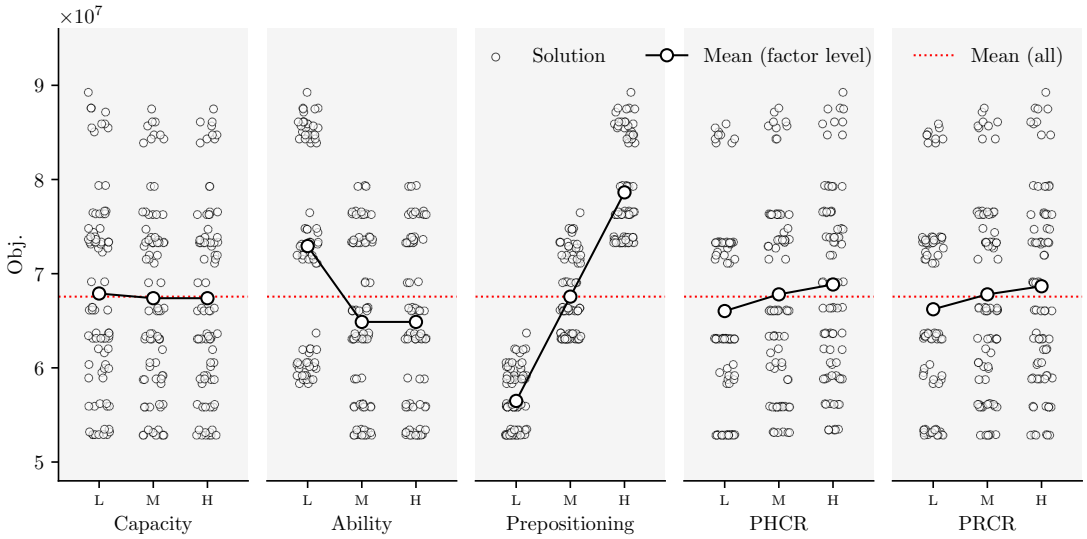

Figure 9: National-level main effects

The main effect plots of the national-level and state-level instances exhibit similarities, as presented in Figure 9 and the supplementary material (they show similar trends, but the scale of objective value differs), leading to several observations. Firstly, the relief facility and affected area capacities have less impact on the overall cost as long as they reach certain thresholds. The L, M, and H levels of capacity-related parameters indicate that facility capacity that meets total demand and affected area capacities that meet their own demand, for at least one period in the worst scenario (case L), is sufficient. Apart from what is presented in Figure 9, experiments with restricted capacities can result in worsened overall cost by several orders of magnitude. Since deprivation cost can be incurred when the prepositioning inventory cannot meet the first period's demand and lead time is nonzero for PHCR and PRCR suppliers. Experiments with restricted capacities are not presented in Figure 9 because extremely large objectives can dim the impact of other factors. The above observation highlights the importance of investing in warehousing before a disaster occurs. However, simply increasing warehouse space does not always result in future cost savings. Decision-makers should consider the worst scenario for determining relief facility size. Secondly, supplier abilities play a crucial role, but the higher ability does not always translate into better performance. When the suppliers are able to provide one period's demand in the worst scenario and the lead time is one period (case M), increased supplier ability cannot significantly enhance overall performance. Although there is a "standard" for supplier ability, selecting the best supplier may not be wise as superior ability often comes with a higher cost. Thirdly, among unit prices of prepositioning, PHCR, and PRCR, the unit prepositioning price has the most significant impact on the overall cost, owing to that a certain part of demand (incurred before PHCR and PRCR deliveries can be made) can only be met by prepositioning inventory. On the contrary, since PHCR and PRCR supplies are interchangeable, a 20% increase in the unit price of PHCR and PRCR results in an overall cost increase far less than 20% on average. It is worth noting that the aforementioned observations are drawn from the average condition (mean values under certain single factor levels, as lines in Figure 9). When discussing the impact of each factor on the overall cost, the levels of other factors are typically neglected. The solutions represented by circles in Figure 9 are typically uniformly distributed on the y-axis in clusters, suggesting that each factor may have interactions with others. In other words, the overall cost is determined by combinations of factors rather than a single factor. Therefore, the interaction effects are analyzed following the main effect analysis.

Interaction effect analysis evaluates the combined effect of two independent variables (factors, e.g., capacity, ability, and unit price) on the dependent variable (objective value). It is used to determine whether the effect of one factor on the outcome depends on the level of another factor. The interaction effect plot is presented in Figure 10(a). In most of the subplots in Figure 10(a), the lines are parallel without intersection, suggesting that no factor has a reverse impact direction on the overall objective value depending on the level of other parameters. Therefore, it is safe to increase only one aspect of the system without causing any harm. However, there are lines with different slopes in PRCR - PHCR and PHCR - PRCR in Figure 10(a). The slope differences suggest that though a higher unit PRCR (or PHCR) price always results in higher overall cost, the increasing speed differs depending on another factor, i.e., unit PHCR (or PRCR) price. For symmetry and simplification, in the following, we only discuss the PHCR - PRCR subplot in Figure 10(a). This subplot says when the unit PRCR price is low, the overall cost is less sensitive to the unit PHCR price, while a higher unit PRCR price results in sensitivity of the overall cost to the unit PHCR price. Also from the PHCR - PRCR subplot, we can conclude that the increase of overall cost with PHCR as in Figure 9 can be mainly interpreted by cases the PRCR level is M or H. Overlaps of lines in the first column, the second column, and the third row in Figure 10(a) also provide valuable information. The first and second columns indicate that there is no significant difference between capacity levels M and H, as well as ability levels M and H. This aligns with the findings from the main effect analysis. The third row indicates that unit prepositioning price is the most significant factor. Since the objective values under certain unit prepositioning price levels are similar, no matter what other factors' levels are. When PHCR and PRCR abilities

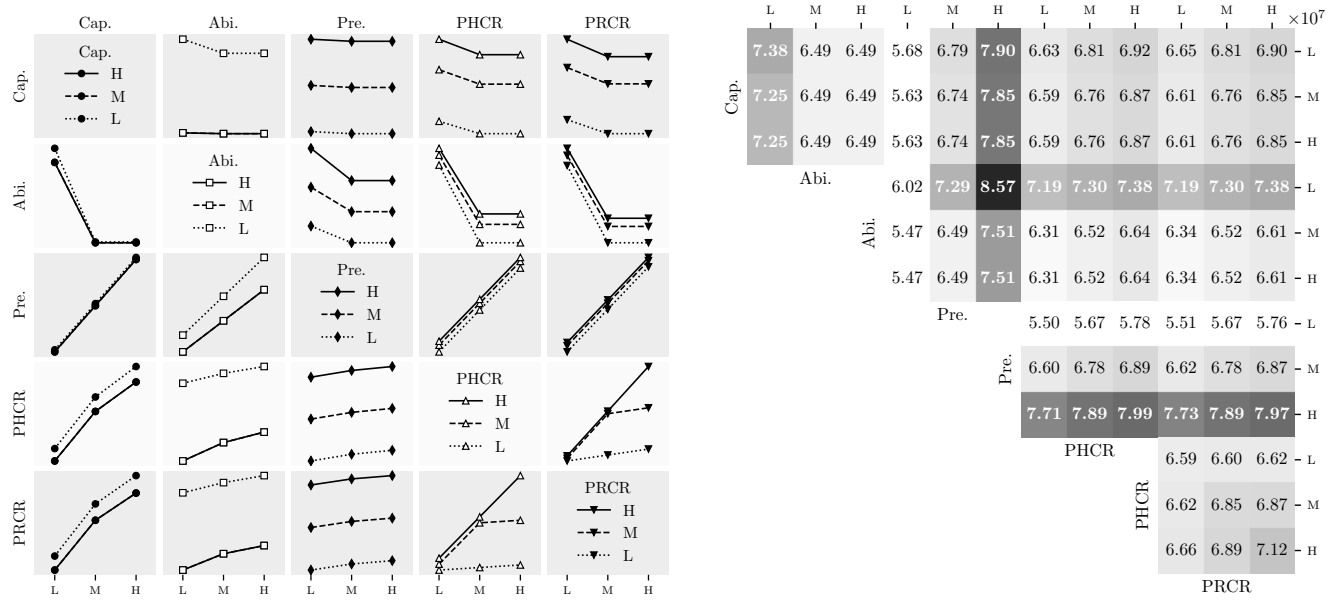

(a) Interaction effect plot

(b) Interaction heatmap

Figure 10: National-level interaction effects

are low, there can be a significant increase in overall cost, compared with ability level being M and H (as in Pre. - Abi.). This highlights the need to enforce specific standards for post-disaster suppliers. Figure 10(b) shows the overall cost under factor level combinations. The highest costs are incurred when either the unit prepositioning price is high, or the supplier's abilities are low. The lowest costs are incurred when the unit prepositioning price is low. These two observations suggest that the overall cost is sensitive to the prepositioning cost, implying that solely relying on prepositioning can be less advisable. On the other hand, it is demonstrated that strengthening the ability of PHCR and PRCR suppliers can lead to cost savings.

Based on the analysis of the main effects and interaction effects using real-world data from Brazil, we can conclude that pre-disaster and post-disaster efforts play different roles in humanitarian relief. Pre-disaster capacity and inventory building are crucial for effective disaster response. However, to continuously improve the efficiency of the relief system, external suppliers must be enhanced to ensure post-disaster supply abilities. Our case study leads to practical guidelines for implementing a capacity reservation enhanced relief system for countries and states that currently use a prepositioning-based relief system. Firstly, it is of great necessity to examine the current ability to respond within the first 48 hours. It is not the right time to implement capacity reservation when prepositioning is even insufficient for the first few days after a disaster strike. Under these conditions, it is more advisable to invest in warehousing and inventory for the first response. When prepositioning meets the requirements and it is decided to involve external suppliers for capacity reservation, decision-makers should prioritize ability over price. This is because ability has a greater impact than price. However, it is not necessary to search for the best supplier in the market. Instead, establishing appropriate supplier standards is more critical.

6. Conclusions

In order to decrease the demand-side suffering and reduce the supply-side monetary cost for humanitarian relief, we study the prepositioning and capacity reservation problem in this work. To trade-off between the pre-disaster procurement cost and post-disaster procurement cost, prepositioning, PHCR, and PRCR are utilized simultaneously. The PRCR is inspired by the practices of the automotive industry, garment industry, etc. for manufacturing PPE during the COVID-19 pandemic. The PRCR is promising for extremely unpredictable events. As far as we know, we are the first that addresses the PRCR in the humanitarian operations management literature. We model the problem with the two-stage stochastic programming where the first stage determines the prepositioning inventory and the second stage determines the order quantity and timing from PHCR suppliers and PRCR suppliers. The stochastic demands and lead time are incorporated into the model. The objective consists of not only the procurement cost but also the deprivation cost which is a measurement of the economic cost of human suffering. Since the nonlinear deprivation cost function is computationally intractable, we introduce the DDCF to tackle it. In order to solve the proposed stochastic programming problem efficiently, we develop an exact solution method based on the LBBD framework. A new type of logic-based Benders cuts, namely logic-based subgradient cuts, are introduced to express the logical relationship between the quantitative variables and the subproblem objective estimators. The coefficients of logic-based subgradient cuts are computed by an efficient heuristics. We also introduce warm-start cuts based on inequalities for stochastic programming to help with finding better feasible solutions in the initial iterations. For humanitarian operations management problems, it is especially desired that the decision is robust in case of unexpected situations, so we use the LHS to improve the out-of-sample performance of stochastic models.

Through extensive numerical studies on designed instances, we conclude the efficiency of the proposed LBBD with logic-based subgradient cuts, heuristics for calculating the cutting coefficients, and warm-start cuts. The LBBD method outperforms the commercial solver in terms of finding the optimal solution and optimality certification. Since the stochastic models are always more challenging than their deterministic counterparts, we validated the value of incorporating stochasticity by the EVPI and VSS indicators. The results confirm the high quality of the stochastic solution and justify the use of stochastic models. We also analyze the out-of-sample performance by increasing the standard deviations of the consumption rate. The results reveal that even with a poor estimation for the stochastic parameters i.e., the estimated standard deviation is lower than the true underlying stochastic distributions, the stochastic models can still (i) approximate the true objective values with relatively small biases and (ii) yield solutions better than the simpler expected value alternatives. After computational performances are analyzed, several managerial insights are derived from findings on further experiments. Firstly, combining capacity reservation with prepositioning can alleviate human suffering significantly, especially when the funds that can be used for prepositioning are limited. This observation not only demonstrates the value of the capacity reservation but also suggests the value of the investment in preparedness. Secondly, we observed that the objective value is less sensitive to changes in the value of life compared to other deprivation function parameters. This suggests that urgent needs should be given greater attention than the value of life of those affected. Thirdly, we find the amplification effect of insufficient prepositioning. That is the curve that the objective function increases with the deprivation cost function parameters can be flattened with a larger prepositioning inventory level. Lastly, a case study on climate-related disaster relief in Brazil offers practical guidelines for nations and states that plan to implement capacity reservation to enhance their relief systems.

This study can be further extended in the following directions. Firstly, since allocation decisions made at the current stage may influence the demands of future stages, exploiting multi-stage stochastic programming to capture this dynamic is a natural extension for this study. Integrating the subgradient cut into nested Benders algorithms, e.g., *stochastic dual dynamic programming*, for multi-stage stochastic programming is also an interesting and promising direction. Secondly, since the PRCR is first introduced to humanitarian operations management literature, some characteristics remain not included in this study. For example, commitment quantity, discount rate, subsidy, and refund for contract design. Thirdly, the proposed subgradient cut can be applied to other problems using the LBBD. For example, for a resource-constrained project scheduling problem that contains both resource investment and scheduling problems, the subgradient cuts can be used to express the relationship between the investment in resources and the results of scheduling.

Notes

[1]Source: https://web.archive.org/web/20220930152255/https://www.southernbeverage.com/anheuser-busch-and-southern-beverage-company-inc-providing-emergency-drinking-water-american-red-cross-relief/, https://web.archive.org/web/20230310115446/https://www.americanbeverage.org/education-resources/blog/post/beverage-industry-mobilizes-in-wake-of-natural-disasters/

[2]The SALLJ is a wind system that is characterized by strong, low-level winds that blow from east to west across the Amazon Basin, the Andes Mountains, and the southern cone of South America. It is most intense during the Southern Hemisphere summer and weaker or absent during the winter months. The SALLJ provides a constant source of moisture and can lead to heavy precipitation and flooding, particularly in the La Plata Basin.

[3]The La Niña is a climate pattern that occurs in the Pacific Ocean, characterized by cooler than normal sea surface temperatures in the central and eastern tropical Pacific. It is the opposite of El Niño, which is a warming of sea surface temperatures in the same region. La Niña events typically occur every three to five years and can last for several months to a year or more. It can lead to changes in global weather patterns, including increased rainfall in some regions and droughts in others.

[4]The following geographical datasets are used for Figure 8: borders and coastline of South America countries (https://web.archive.org/web/20230310211745/https://www.naturalearthdata.com/ through the Python package `Cartopy 0.21.1`), shapes of states in Brazil (https://web.archive.org/web/20221231151516/https://raw.githubusercontent.com/codeforamerica/click_that_hood/master/public/data/brazil-states.geojson), shapes of cities in Santa Catarina (https://web.archive.org/web/20230315194709/https://geodata.lib.utexas.edu/catalog/stanford-pc496bf3938), and border of La Plata Basin (https://web.archive.org/web/20230315195245/https://www.cima.fcen.uba.ar/ClarisLPB/RDA_list.php?ti=ob&su=geo).

Acknowledgments

This work was supported by the National Natural Science Foundation of China (NSFC) [grant number 72071106]. We appreciate the editor and the reviewers for their valuable suggestions, which improved the quality of this paper greatly. We also appreciate Freepik from Flaticon.com for providing the icons used in Figure 1.

References

Acar, M., & Kaya, O. (2022). Inventory decisions for humanitarian aid materials considering budget constraints. *European Journal of Operational Research*, *300*, 95–111. doi:10.1016/j.ejor.2021.07.029.

Aghajani, M., Torabi, S. A., & Heydari, J. (2020). A novel option contract integrated with supplier selection and inventory prepositioning for humanitarian relief supply chains. *Socio-Economic Planning Sciences*, *71*, 100780. doi:10.1016/j.seps.2019.100780.

Akbalik, A., Hadj-Alouane, A. B., Sauer, N., & Ghribi, H. (2017). NP-hard and polynomial cases for the single-item lot sizing problem with batch ordering under capacity reservation contract. *European Journal of Operational Research*, *257*, 483–493. doi:10.1016/j.ejor.2016.07.028.

Akbarpour, M., Ali Torabi, S., & Ghavamifar, A. (2020). Designing an integrated pharmaceutical relief chain network under demand uncertainty. *Transportation Research Part E: Logistics and Transportation Review*, *136*, 101867. doi:10.1016/j.tre.2020.101867.

Alem, D., Bonilla-Londono, H. F., Barbosa-Povoa, A. P., Relvas, S., Ferreira, D., & Moreno, A. (2021). Building disaster preparedness and response capacity in humanitarian supply chains using the Social Vulnerability Index. *European Journal of Operational Research*, *292*, 250–275. doi:10.1016/j.ejor.2020.10.016.

Alem, D., Clark, A., & Moreno, A. (2016). Stochastic network models for logistics planning in disaster relief. *European Journal of Operational Research*, *255*, 187–206. doi:10.1016/j.ejor.2016.04.041.

Angulo, G., Ahmed, S., & Dey, S. S. (2016). Improving the integer L-shaped method. *INFORMS Journal on Computing*, *28*, 483–499. doi:10.1287/ijoc.2016.0695.

Bagirov, A., Karmitsa, N., & Mäkelä, M. M. (2014). Bundle Methods. In A. Bagirov, N. Karmitsa, & M. M. Mäkelä (Eds.), *Introduction to Nonsmooth Optimization: Theory, Practice and Software* (pp. 305–310). Cham: Springer International Publishing. doi:10.1007/978-3-319-08114-4_12.

Balcik, B., & Ak, D. (2014). Supplier selection for framework agreements in humanitarian relief. *Production and Operations Management*, *23*, 1028–1041. doi:10.1111/poms.12098.

Balcik, B., & Beamon, B. M. (2008). Facility location in humanitarian relief. *International Journal of Logistics Research and Applications*, *11*, 101–121. doi:10.1080/13675560701561789.

Balcik, B., Silvestri, S., Rancourt, M.-E., & Laporte, G. (2019). Collaborative prepositioning network design for regional disaster response. *Production and Operations Management*, *28*, 2431–2455. doi:10.1111/poms.13053.

Baloch, G., & Gzara, F. (2020). Strategic network design for parcel delivery with drones under competition. *Transportation Science*, *54*, 204–228. doi:10.1287/trsc.2019.0928.

Barzanji, R., Naderi, B., & Begen, M. A. (2020). Decomposition algorithms for the integrated process planning and scheduling problem. *Omega*, *93*, 102025. doi:10.1016/j.omega.2019.01.003.

BEH (2011). *World Risk Report 2011*. Technical Report Bündnis Entwicklung Hilft.

BEH (2022). *World Risk Report 2022*. Technical Report Bündnis Entwicklung Hilft.

Benders, J. F. (1962). Partitioning procedures for solving mixed-variables programming problems. *Numerische Mathematik*, *4*, 238–252. doi:10.1007/BF01386316.

Birge, J. R. (1982). The value of the stochastic solution in stochastic linear programs with fixed recourse. *Mathematical Programming*, *24*, 314–325. doi:10.1007/BF01585113.

Boujemaa, R., Jebali, A., Hammami, S., & Ruiz, A. (2020). Multi-period stochastic programming models for two-tiered emergency medical service system. *Computers & Operations Research*, *123*, 104974. doi:10.1016/j.cor.2020.104974.

Boulaksil, Y., Grunow, M., & Fransoo, J. (2011). Capacity flexibility allocation in an outsourced supply chain with reservation. *International Journal of Production Economics*, *129*, 111–118. doi:10.1016/j.ijpe.2010.09.010.

Caglar Gencosman, B., & Begen, M. A. (2022). Exact optimization and decomposition approaches for shelf space allocation. *European Journal of Operational Research*, *299*, 432–447. doi:10.1016/j.ejor.2021.08.047.

Cantillo, V., Serrano, I., Macea, L. F., & Holguín-Veras, J. (2018). Discrete choice approach for assessing deprivation cost in humanitarian relief operations. *Socio-Economic Planning Sciences*, *63*, 33–46. doi:10.1016/j.seps.2017.06.004.

Çelik, M., Ergun, Ö., Johnson, B., Keskinocak, P., Lorca, Á., Pekgün, P., & Swann, J. (2012). Humanitarian Logistics. In *2012 TutORials in Operations Research* (pp. 18–49). INFORMS. doi:10.1287/educ.1120.0100.

Cheaitou, A., & Cheaytou, R. (2019). A two-stage capacity reservation supply contract with risky supplier and forecast updating. *International Journal of Production Economics*, *209*, 42–60. doi:10.1016/j.ijpe.2018.01.019.

Chen, J., Liang, L., & Yao, D.-Q. (2017). Pre-positioning of relief inventories for non-profit organizations: A newsvendor approach. *Annals of Operations Research*, *259*, 35–63. doi:10.1007/s10479-017-2521-4.

Chu, Y., & Xia, Q. (2004). Generating Benders cuts for a general class of integer programming problems. In J.-C. Régin, & M. Rueher (Eds.), *Integration of AI and OR Techniques in Constraint Programming for Combinatorial Optimization Problems* Lecture Notes in Computer Science (pp. 127–141). Berlin, Heidelberg: Springer. doi:10.1007/978-3-540-24664-0_9.

Codato, G., & Fischetti, M. (2006). Combinatorial Benders' cuts for mixed-integer linear programming. *Operations Research*, *54*, 756–766. doi:10.1287/opre.1060.0286.

CRED (2022). Centre for Research on the Epidemiology of Disasters: Emergency Events Database (EM-DAT). https://public.emdat.be/. Accessed 2022-05-09.

Das, R., & Hanaoka, S. (2014). Relief inventory modelling with stochastic lead-time and demand. *European Journal of Operational Research*, *235*, 616–623. doi:10.1016/j.ejor.2013.12.042.

Delorme, M., Iori, M., & Martello, S. (2017). Logic based Benders' decomposition for orthogonal stock cutting problems. *Computers & Operations Research*, *78*, 290–298. doi:10.1016/j.cor.2016.09.009.

Devi Prasad Patra, T., & Jha, J. K. (2022). Bidirectional option contract for prepositioning of relief supplies under demand uncertainty. *Computers & Industrial Engineering*, *163*, 107861. doi:10.1016/j.cie.2021.107861.

Dore, M. H. I., & Singh, R. G. (2013). Economic Valuation of Life. In P. T. Bobrowsky (Ed.), *Encyclopedia of Natural Hazards* Encyclopedia of Earth Sciences Series (pp. 240–242). Dordrecht: Springer Netherlands. doi:10.1007/978-1-4020-4399-4_173.

EC-JRC, CEMADEN, CIMA, SISSA, & WMO (2023). *Extreme and Long-Term Drought in the La Plata Basin: Event Evolution and Impact Assessment until September 2022*. Technical Report.

ECLAC (2020). *Sectors and Businesses Facing COVID-19: Emergency and Reactivation: Special Report COVID-19 No. 4*. Technical Report United Nations Economic Commission for Latin America and the Caribbean. doi:10.18356/9789210054683.

Eftekhar, M., Jeannette Song, J.-S., & Webster, S. (2022). Prepositioning and local purchasing for emergency operations under budget, demand, and supply uncertainty. *Manufacturing & Service Operations Management*, *24*, 315–332. doi:10.1287/msom.2020.0956.

Elçi, Ö., & Hooker, J. (2022). Stochastic planning and scheduling with logic-based Benders decomposition. *INFORMS Journal on Computing*, . doi:10.1287/ijoc.2022.1184.

Enayaty-Ahangar, F., Rainwater, C. E., & Sharkey, T. C. (2019). A logic-based decomposition approach for multi-period network interdiction models. *Omega*, *87*, 71–85. doi:10.1016/j.omega.2018.08.006.

Erbeyoğlu, G., & Bilge, Ü. (2020). A robust disaster preparedness model for effective and fair disaster response. *European Journal of Operational Research*, *280*, 479–494. doi:10.1016/j.ejor.2019.07.029.

Fachini, R. F., & Armentano, V. A. (2020). Logic-based Benders decomposition for the heterogeneous fixed fleet vehicle routing problem with time windows. *Computers & Industrial Engineering*, *148*, 106641. doi:10.1016/j.cie.2020.106641.

Falasca, M., & Zobel, C. W. (2011). A two-stage procurement model for humanitarian relief supply chains. *Journal of Humanitarian Logistics and Supply Chain Management*, *1*, 151–169. doi:10.1108/20426741111188329.

Fazel-Zarandi, M. M., & Beck, J. C. (2012). Using logic-based Benders decomposition to solve the capacity- and distance-constrained plant location problem. *INFORMS Journal on Computing*, *24*, 387–398. doi:10.1287/ijoc.1110.0458.

Fazel-Zarandi, M. M., Berman, O., & Beck, J. C. (2013). Solving a stochastic facility location/fleet management problem with logic-based Benders' decomposition. *IIE Transactions*, *45*, 896–911. doi:10.1080/0740817X.2012.705452.

FEMA (2022). Advanced Contracting for Goods and Services. https://www.fema.gov/businesses-organizations/doing-business/advanced-contracts. Accessed 2022-05-09.

Fernandez Pernett, S., Amaya, J., Arellana, J., & Cantillo, V. (2022). Questioning the implication of the utility-maximization assumption for the estimation of deprivation cost functions after disasters. *International Journal of Production Economics*, *247*, 108435. doi:10.1016/j.ijpe.2022.108435.

Fischetti, M., Ljubić, I., & Sinnl, M. (2017). Redesigning benders decomposition for large-scale facility location. *Management Science*, *63*, 2146–2162. doi:10.1287/mnsc.2016.2461.

Gedik, R., Rainwater, C., Nachtmann, H., & Pohl, E. A. (2016). Analysis of a parallel machine scheduling problem with sequence dependent setup times and job availability intervals. *European Journal of Operational Research*, *251*, 640–650. doi:10.1016/j.ejor.2015.11.020.

Geoffrion, A. M. (1972). Generalized Benders decomposition. *Journal of Optimization Theory and Applications*, *10*, 237–260. doi:10.1007/BF00934810.

Ghavamifar, A., Torabi, S. A., & Moshtari, M. (2022). A hybrid relief procurement contract for humanitarian logistics. *Transportation Research Part E: Logistics and Transportation Review*, *167*, 102916. doi:10.1016/j.tre.2022.102916.

Guo, C., Bodur, M., Aleman, D. M., & Urbach, D. R. (2021). Logic-based Benders decomposition and binary decision diagram based approaches for stochastic distributed operating room scheduling. *INFORMS Journal on Computing*, *33*, 1551–1569. doi:10.1287/ijoc.2020.1036.

Haraguchi, M., She, W., & Taniguchi, M. (2022). *Conversion as an Adaptation Strategy for Supply Chain Resilience to the COVID- 19 Pandemic*. Technical Report United Nations Office for Disaster Risk Reduction.

Heching, A., Hooker, J. N., & Kimura, R. (2019). A logic-based Benders approach to home healthcare delivery. *Transportation Science*, *53*, 510–522. doi:10.1287/trsc.2018.0830.

Hein, C., Behrens, F., & Lasch, R. (2020). Insights on the costs of humanitarian logistics a case study analysis. *Logistics Research*, *13*. doi:10.23773/2020_3.

Holguin-Veras, J., Amaya-Leal, J., Cantillo, V., Van Wassenhove, L. N., Aros-Vera, F., & Jaller, M. (2016). Econometric estimation of deprivation cost functions: A contingent valuation experiment. *Journal of Operations Management*, *45*, 44–56. doi:10.1016/j.jom.2016.05.008.

Holguín-Veras, J., Pérez, N., Jaller, M., Van Wassenhove, L. N., & Aros-Vera, F. (2013). On the appropriate objective function for post-disaster humanitarian logistics models. *Journal of Operations Management*, *31*, 262–280. doi:10.1016/j.jom.2013.06.002.

Hooker, J. N. (2007). Planning and scheduling by logic-based Benders decomposition. *Operations Research*, *55*, 588–602. doi:10.1287/opre.1060.0371.

Hooker, J. N. (2019). Logic-based Benders decomposition for large-scale optimization. In J. M. Velásquez-Bermúdez, M. Khakifirooz, & M. Fathi (Eds.), *Large Scale Optimization in Supply Chains and Smart Manufacturing: Theory and Applications* Springer Optimization and Its Applications (pp. 1–26). Cham: Springer International Publishing. doi:10.1007/978-3-030-22788-3_1.

Hooker, J. N., & Ottosson, G. (2003). Logic-based Benders decomposition. *Mathematical Programming*, *96*, 33–60. doi:10.1007/s10107-003-0375-9.

Hooshmand, F., Amerehi, F., & MirHassani, S. A. (2020). Logic-based Benders decomposition algorithm for contamination detection problem in water networks. *Computers & Operations Research*, *115*, 104840. doi:10.1016/j.cor.2019.104840.

Hou, J., Zeng, A. Z., & Sun, L. (2017). Backup sourcing with capacity reservation under uncertain disruption risk and minimum order quantity. *Computers & Industrial Engineering*, *103*, 216–226. doi:10.1016/j.cie.2016.11.011.

Hsu, S. S. (2007). Tons of food spoiled as FEMA ran out of space. https://www.nbcnews.com/id/wbna18084847. Accessed 2022-05-09.

Hu, S., & Dong, Z. S. (2019). Supplier selection and pre-positioning strategy in humanitarian relief. *Omega*, *83*, 287–298. doi:10.1016/j.omega.2018.10.011.

Hu, S., Dong, Z. S., & Lev, B. (2022). Supplier selection in disaster operations management: Review and research gap identification. *Socio-Economic Planning Sciences*, *82*, 101302. doi:10.1016/j.seps.2022.101302.

Hu, S.-L., Han, C.-F., & Meng, L.-P. (2017). Stochastic optimization for joint decision making of inventory and procurement in humanitarian relief. *Computers & Industrial Engineering*, *111*, 39–49. doi:10.1016/j.cie.2017.06.029.

Hu, Z., Tian, J., & Feng, G. (2019). A relief supplies purchasing model based on a put option contract. *Computers & Industrial Engineering*, *127*, 253–262. doi:10.1016/j.cie.2018.12.015.

Insel, N., Poulsen, C. J., & Ehlers, T. A. (2010). Influence of the Andes Mountains on South American moisture transport, convection, and precipitation. *Climate Dynamics*, *35*, 1477–1492. doi:10.1007/s00382-009-0637-1.

Ismail, I. (2021). A possibilistic mathematical programming model to control the flow of relief commodities in humanitarian supply chains. *Computers & Industrial Engineering*, *157*, 107305. doi:10.1016/j.cie.2021.107305.

Jamali, A., Ranjbar, A., Heydari, J., & Nayeri, S. (2021). A multi-objective stochastic programming model to configure a sustainable humanitarian logistics considering deprivation cost and patient severity. *Annals of Operations Research*, . doi:10.1007/s10479-021-04014-2.

John, L., & Gurumurthy, A. (2021). Are quantity flexibility contracts with discounts in the presence of spot market procurement relevant for the humanitarian supply chain? An exploration. *Annals of Operations Research*, . doi:10.1007/s10479-021-04058-4.

John, L., Gurumurthy, A., Mateen, A., & Narayanamurthy, G. (2020). Improving the coordination in the humanitarian supply chain: Exploring the role of options contract. *Annals of Operations Research*, . doi:10.1007/s10479-020-03778-3.

Kaut, M., & Wallace, S. W. (2007). Evaluation of scenario-generation methods for stochastic programming. *Pacific Journal of Optimization*, *3*, 257–271. doi:http://www.ybook.co.jp/online2/oppjo/vol3/p257.html.

Keshvari Fard, M., Ljubić, I., & Papier, F. (2022). Budgeting in international humanitarian organizations. *Manufacturing & Service Operations Management*, *24*, 1261–1885. doi:10.1287/msom.2021.1016.

Kloimüllner, C., & Raidl, G. R. (2017). Full-load route planning for balancing bike sharing systems by logic-based Benders decomposition. *Networks*, *69*, 270–289. doi:10.1002/net.21736.

Kůdela, J., & Popela, P. (2017). Warm-start cuts for generalized Benders decomposition. *Kybernetika*, *53*, 1012–1025. doi:10.14736/kyb-2017-6-1012.

Laporte, G., & Louveaux, F. V. (1993). The integer L-shaped method for stochastic integer programs with complete recourse. *Operations Research Letters*, *13*, 133–142. doi:10.1016/0167-6377(93)90002-X.

Lee, M., Ma, N., Yu, G., & Dai, H. (2021). Accelerating generalized Benders decomposition for wireless resource allocation. *IEEE Transactions on Wireless Communications*, *20*, 1233–1247. doi:10.1109/TWC.2020.3031920.

Leutwiler, F., & Corman, F. (2022). A logic-based Benders decomposition for microscopic railway timetable planning. *European Journal of Operational Research*, (p. S0377221722001643). doi:10.1016/j.ejor.2022.02.043.

Li, M. K., Sodhi, M. S., Tang, C. S., & Yu, J. J. (2022a). Preparedness with a system integrating inventory, capacity, and capability for future pandemics and other disasters. *Production and Operations Management*, . doi:10.1111/poms.13887.

Li, Y., Côté, J.-F., Callegari-Coelho, L., & Wu, P. (2022b). Novel formulations and logic-based Benders decomposition for the integrated parallel machine scheduling and location problem. *INFORMS Journal on Computing*, *34*, 671–1304. doi:10.1287/ijoc.2021.1113.

Liang, L., Wang, X., & Gao, J. (2012). An option contract pricing model of relief material supply chain. *Omega*, *40*, 594–600. doi:10.1016/j.omega.2011.11.004.

Lin, Y. H., & Tian, Q. (2021). Branch-and-cut approach based on generalized Benders decomposition for facility location with limited choice rule. *European Journal of Operational Research*, *293*, 109–119. doi:10.1016/j.ejor.2020.12.017.

Linderoth, J., Shapiro, A., & Wright, S. (2006). The empirical behavior of sampling methods for stochastic programming. *Annals of Operations Research*, *142*, 215–241. doi:10.1007/s10479-006-6169-8.

Liu, R., & Xie, X. (2021). Weekly scheduling of emergency department physicians to cope with time-varying demand. *IISE Transactions*, *53*, 1109–1123. doi:10.1080/24725854.2021.1894656.

Liu, Y., Tian, J., & Feng, G. (2021). Pre-positioning strategies for relief supplies in a relief supply chain. *Journal of the Operational Research Society*, (pp. 1–17). doi:10.1080/01605682.2021.1920343.

Liu, Y., Tian, J., Feng, G., & Hu, Z. (2019). A relief supplies purchasing model via option contracts. *Computers & Industrial Engineering*, *137*, 106009. doi:10.1016/j.cie.2019.106009.

Lombardi, M., Milano, M., Ruggiero, M., & Benini, L. (2010). Stochastic allocation and scheduling for conditional task graphs in multi-processor systems-on-chip. *Journal of Scheduling*, *13*, 315–345. doi:10.1007/s10951-010-0184-y.

Loree, N., & Aros-Vera, F. (2018). Points of distribution location and inventory management model for post-disaster humanitarian logistics. *Transportation Research Part E: Logistics and Transportation Review*, *116*, 1–24. doi:10.1016/j.tre.2018.05.003.

Macea, L. F., Cantillo, V., & Arellana, J. (2018). Influence of attitudes and perceptions on deprivation cost functions. *Transportation Research Part E: Logistics and Transportation Review*, *112*, 125–141. doi:10.1016/j.tre.2018.02.007.

Madansky, A. (1960). Inequalities for stochastic linear programming problems. *Management Science*, *6*, 197–204. doi:10.1287/mnsc.6.2.197.

Mak, W.-K., Morton, D. P., & Wood, R. K. (1999). Monte Carlo bounding techniques for determining solution quality in stochastic programs. *Operations Research Letters*, *24*, 47–56. doi:10.1016/S0167-6377(98)00054-6.

Mäkelä, M. (2002). Survey of bundle methods for nonsmooth optimization. *Optimization Methods and Software*, *17*, 1–29. doi:10.1080/10556780290027828.

Martínez, K. P., Adulyasak, Y., & Jans, R. (2022). Logic-based Benders decomposition for integrated process configuration and production planning problems. *INFORMS Journal on Computing*, (p. ijoc.2021.1079). doi:10.1287/ijoc.2021.1079.

McLoughlin, D. (1985). A framework for integrated emergency management. *Public Administration Review*, *45*, 165–172. doi:10.2307/3135011.

Moreno, A., Alem, D., Ferreira, D., & Clark, A. (2018). An effective two-stage stochastic multi-trip location-transportation model with social concerns in relief supply chains. *European Journal of Operational Research*, *269*, 1050–1071. doi:10.1016/j.ejor.2018.02.022.

Moshtari, M., Altay, N., Heikkilä, J., & Gonçalves, P. (2021). Procurement in humanitarian organizations: Body of knowledge and practitioner's challenges. *International Journal of Production Economics*, *233*, 108017. doi:10.1016/j.ijpe.2020.108017.

Naderi, B., & Roshanaei, V. (2020). Branch-Relax-and-Check: A tractable decomposition method for order acceptance and identical parallel machine scheduling. *European Journal of Operational Research*, *286*, 811–827. doi:10.1016/j.ejor.2019.10.014.

Naderi, B., & Roshanaei, V. (2022). Critical-path-search logic-based benders decomposition approaches for flexible job shop scheduling. *INFORMS Journal on Optimization*, *4*, 1–28. doi:10.1287/ijoo.2021.0056.

NDRC (2021). *Outline of the 14th Five-Year Plan (2021-2025) for National Economic and Social Development and Vision 2035 of the People's Republic of China*. Technical Report National Development and Reform Commission (NDRC).

Ni, W., Shu, J., & Song, M. (2018). Location and emergency inventory pre-positioning for disaster response operations: Min-max robust model and a case study of yushu earthquake. *Production and Operations Management*, *27*, 160–183. doi:10.1111/poms.12789.

Nikkhoo, F., Bozorgi-Amiri, A., & Heydari, J. (2018). Coordination of relief items procurement in humanitarian logistic based on quantity flexibility contract. *International Journal of Disaster Risk Reduction*, *31*, 331–340. doi:10.1016/j.ijdrr.2018.05.024.

Noham, R., & Tzur, M. (2018). Designing humanitarian supply chains by incorporating actual post-disaster decisions. *European Journal of Operational Research*, *265*, 1064–1077. doi:10.1016/j.ejor.2017.08.042.

Norkin, V. I., Pflug, G. C., & Ruszczyński, A. (1998). A branch and bound method for stochastic global optimization. *Mathematical Programming*, *83*, 425–450. doi:10.1007/BF02680569.

OCHA (2018). Allocation process. https://www.unocha.org/sudan/allocation-process. Accessed 2022-03-26.

Park, S. I., & Kim, J. S. (2014). A mathematical model for a capacity reservation contract. *Applied Mathematical Modelling*, *38*, 1866–1880. doi:10.1016/j.apm.2013.10.005.

Paul, J. A., & Wang, X. J. (2019). Robust location-allocation network design for earthquake preparedness. *Transportation Research Part B: Methodological*, *119*, 139–155. doi:10.1016/j.trb.2018.11.009.

Paul, J. A., & Zhang, M. (2019). Supply location and transportation planning for hurricanes: A two-stage stochastic programming framework. *European Journal of Operational Research*, *274*, 108–125. doi:10.1016/j.ejor.2018.09.042.

Perez-Rodriguez, N., & Holguin-Veras, J. (2016). Inventory-allocation distribution models for postdisaster humanitarian logistics with

explicit consideration of deprivation costs. *Transportation Science*, *50*, 1261–1285. doi:10.1287/trsc.2014.0565.

Polyakovskiy, S., & M'Hallah, R. (2021). Just-in-time two-dimensional bin packing. *Omega*, *102*, 102311. doi:10.1016/j.omega.2020.102311.

Pradhananga, R., Mutlu, F., Pokharel, S., Holguín-Veras, J., & Seth, D. (2016). An integrated resource allocation and distribution model for pre-disaster planning. *Computers & Industrial Engineering*, *91*, 229–238. doi:10.1016/j.cie.2015.11.010.

Rafiei, R., Huang, K., & Verma, M. (2022). Cash versus in-kind transfer programs in humanitarian operations: An optimization program and a case study. *Socio-Economic Planning Sciences*, *82*, 101224. doi:10.1016/j.seps.2022.101224.

Rahmaniani, R., Crainic, T. G., Gendreau, M., & Rei, W. (2017). The Benders decomposition algorithm: A literature review. *European Journal of Operational Research*, *259*, 801–817. doi:10.1016/j.ejor.2016.12.005.

Raiffa, H., & Schlaifer, R. (1961). *Applied Statistical Decision Theory*. (1st ed.). Boston: Harvard University Press.

Rawls, C. G., & Turnquist, M. A. (2010). Pre-positioning of emergency supplies for disaster response. *Transportation Research Part B: Methodological*, *44*, 521–534. doi:10.1016/j.trb.2009.08.003.

Restrepo, M. I., Gendron, B., & Rousseau, L.-M. (2018). Combining Benders decomposition and column generation for multi-activity tour scheduling. *Computers & Operations Research*, *93*, 151–165. doi:10.1016/j.cor.2018.01.014.

Riedler, M., & Raidl, G. (2018). Solving a selective dial-a-ride problem with logic-based Benders decomposition. *Computers & Operations Research*, *96*, 30–54. doi:10.1016/j.cor.2018.03.008.

Riise, A., Mannino, C., & Lamorgese, L. (2016). Recursive logic-based Benders' decomposition for multi-mode outpatient scheduling. *European Journal of Operational Research*, *255*, 719–728. doi:10.1016/j.ejor.2016.06.015.

Roshanaei, V., Booth, K. E. C., Aleman, D. M., Urbach, D. R., & Beck, J. C. (2020). Branch-and-check methods for multi-level operating room planning and scheduling. *International Journal of Production Economics*, *220*, 107433. doi:10.1016/j.ijpe.2019.07.006.

Roshanaei, V., Luong, C., Aleman, D. M., & Urbach, D. (2017). Propagating logic-based Benders' decomposition approaches for distributed operating room scheduling. *European Journal of Operational Research*, *257*, 439–455. doi:10.1016/j.ejor.2016.08.024.

Roshanaei, V., & Naderi, B. (2021). Solving integrated operating room planning and scheduling: Logic-based Benders decomposition versus Branch-Price-and-Cut. *European Journal of Operational Research*, *293*, 65–78. doi:10.1016/j.ejor.2020.12.004.

Sabbaghtorkan, M., Batta, R., & He, Q. (2020). Prepositioning of assets and supplies in disaster operations management: Review and research gap identification. *European Journal of Operational Research*, *284*, 1–19. doi:10.1016/j.ejor.2019.06.029.

Sakiani, R., Seifi, A., & Khorshiddoust, R. R. (2020). Inventory routing and dynamic redistribution of relief goods in post-disaster operations. *Computers & Industrial Engineering*, *140*, 106219. doi:10.1016/j.cie.2019.106219.

Salmerón, J., & Apte, A. (2010). Stochastic optimization for natural disaster asset prepositioning. *Production and Operations Management*, *19*, 561–574. doi:10.1111/j.1937-5956.2009.01119.x.

Sanci, E., & Daskin, M. S. (2019). Integrating location and network restoration decisions in relief networks under uncertainty. *European Journal of Operational Research*, *279*, 335–350. doi:10.1016/j.ejor.2019.06.012.

Serel, D. A., Dada, M., & Moskowitz, H. (2001). Sourcing decisions with capacity reservation contracts. *European Journal of Operational Research*, *131*, 635–648. doi:10.1016/S0377-2217(00)00106-5.

Shao, J., Wang, X., Liang, C., & Holguín-Veras, J. (2020). Research progress on deprivation costs in humanitarian logistics. *International Journal of Disaster Risk Reduction*, *42*, 101343. doi:10.1016/j.ijdrr.2019.101343.

Shapiro, A. (2013). Sample average approximation. In S. I. Gass, & M. C. Fu (Eds.), *Encyclopedia of Operations Research and Management Science* (pp. 1350–1355). Boston, MA: Springer US. doi:10.1007/978-1-4419-1153-7_1154.

Shapiro, A., Dentcheva, D., & Ruszczynski, A. (2021). *Lectures on Stochastic Programming: Modeling and Theory*. MOS-SIAM Series on Optimization (3rd ed.). Society for Industrial and Applied Mathematics. doi:10.1137/1.9781611976595.

Thomas, A., & Mizushima, M. (2005). Logistics training: Necessity or luxury? *Forced Migration Review*, *22*, 60. doi:https://www.fmreview.org/education-emergencies/thomas-mizushima.

Torabi, S. A., Shokr, I., Tofighi, S., & Heydari, J. (2018). Integrated relief pre-positioning and procurement planning in humanitarian supply chains. *Transportation Research Part E: Logistics and Transportation Review*, *113*, 123–146. doi:10.1016/j.tre.2018.03.012.

Tran, T. T., Araujo, A., & Beck, J. C. (2016). Decomposition methods for the parallel machine scheduling problem with setups. *INFORMS Journal on Computing*, *28*, 83–95. doi:10.1287/ijoc.2015.0666.

UNDRR (2022). *Global Assessment Report on Disaster Risk Reduction 2022*. Technical Report United Nations Office for Disaster Risk Reduction.

UNICEF (2021). *Extraordinary Operation at Scale*. Supply Annual Report 2020 United Nations Children's Fund.

Van Slyke, R. M., & Wets, R. (1969). L-shaped linear programs with applications to optimal control and stochastic programming. *SIAM Journal on Applied Mathematics*, *17*, 638–663. doi:10.1137/0117061.

Veloso, R., Cespedes, J., Caunhye, A., & Alem, D. (2022). Brazilian disaster datasets and real-world instances for optimization and machine learning. *Data in Brief*, *42*, 108012. doi:10.1016/j.dib.2022.108012.

Wang, X., Li, F., Liang, L., Huang, Z., & Ashley, A. (2015). Pre-purchasing with option contract and coordination in a relief supply chain.

International Journal of Production Economics, *167*, 170–176. doi:10.1016/j.ijpe.2015.05.031.

Wang, X. J., & Paul, J. A. (2020). Robust optimization for hurricane preparedness. *International Journal of Production Economics*, *221*, 107464. doi:10.1016/j.ijpe.2019.07.037.

WFP (2020). *WFP Supply Chain Annual Report 2019 in Review*. Technical Report World Food Programme.

Wheatley, D., Gzara, F., & Jewkes, E. (2015). Logic-based Benders decomposition for an inventory-location problem with service constraints. *Omega*, *55*, 10–23. doi:10.1016/j.omega.2015.02.001.

Yu, L., Yang, H., Miao, L., & Zhang, C. (2019). Rollout algorithms for resource allocation in humanitarian logistics. *IISE Transactions*, *51*, 887–909. doi:10.1080/24725854.2017.1417655.

Yu, L., Zhang, C., Yang, H., & Miao, L. (2018). Novel methods for resource allocation in humanitarian logistics considering human suffering. *Computers & Industrial Engineering*, *119*, 1–20. doi:10.1016/j.cie.2018.03.009.

Zhang, C., Li, Y., Cao, J., & Wen, X. (2022a). On the mass COVID-19 vaccination scheduling problem. *Computers & Operations Research*, *141*, 105704. doi:10.1016/j.cor.2022.105704.

Zhang, L., Lu, J., & Yang, Z. (2021a). Optimal scheduling of emergency resources for major maritime oil spills considering time-varying demand and transportation networks. *European Journal of Operational Research*, *293*, 529–546. doi:10.1016/j.ejor.2020.12.040.

Zhang, L., Tian, J., Fung, R. Y. K., & Dang, C. (2019). Materials procurement and reserves policies for humanitarian logistics with recycling and replenishment mechanisms. *Computers & Industrial Engineering*, *127*, 709–721. doi:10.1016/j.cie.2018.11.013.

Zhang, Y., Lin, W.-H., Huang, M., & Hu, X. (2021b). Multi-warehouse package consolidation for split orders in online retailing. *European Journal of Operational Research*, *289*, 1040–1055. doi:10.1016/j.ejor.2019.07.004.

Zhang, Y., Richter, A. R., Shanthikumar, J. G., & Shen, Z.-J. M. (2022b). Dynamic inventory relocation in disaster relief. *Production and Operations Management*, *31*, 1052–1070. doi:10.1111/poms.13594.

Zhang, Z., Song, X., Huang, H., Zhou, X., & Yin, Y. (2022c). Logic-based Benders decomposition method for the seru scheduling problem with sequence-dependent setup time and DeJong's learning effect. *European Journal of Operational Research*, *297*, 866–877. doi:10.1016/j.ejor.2021.06.017.

Zhu, L., Gong, Y., Xu, Y., & Gu, J. (2019). Emergency relief routing models for injured victims considering equity and priority. *Annals of Operations Research*, *283*, 1573–1606. doi:10.1007/s10479-018-3089-3.

Supplementary material: Capacity reservation for humanitarian relief: A logic-based Benders decomposition method with subgradient cut

S.1. Notations

Table S1: Notations

Sets	
R	Set of relief facilities.
D	Set of affected areas.
T	Set of discrete time periods, $T = \{1, 2, 3, \cdots, t_{\max}\}$.
S	Set of scenarios.
K	Set of PHCR suppliers.
K'	Set of PRCR suppliers.
Parameters	
u	Unit acquisition cost for prepositioning inventory.
w_i	Population of affected area $i \in D$.
d_i^{ts}	Demand of affected area $i \in D$ at $t \in T$ under scenario $s \in S$.
v_j, v_i	Capacity of relief facility $j \in R$ and affected area $i \in D$.
$\gamma(\cdot)$	Deprivation cost function.
M	A sufficiently large number.
ϵ	A sufficiently small number.
$\gamma(dt)$	Value of deprivation cost function with deprivation time $dt \in T$.
p_k	Unit cost for acquiring relief item from supplier $k \in K \cup K'$.
(α_k, β_k)	Parameters for the quantity-flexibility contract of $k \in K$.
η_k	Production capacity of supplier $k \in K \cup K'$.
L_k^s	Lead time of supplier $k \in K'$ for the first order under scenario $s \in S$.
L_k	Lead time of supplier $k \in K$ and supplier $k \in K'$ for orders after the first one.
Decision variables	
SPIP decision variables:	
r_j	Quantity of prepositioned inventory at $j \in R$.
y_j^{ts}, y_i^{ts}	Quantity of inventory at $j \in R$ and $i \in D$ at $t \in T$ under scenario $s \in S$.
f_{ji}^{ts}	Quantity of relief items transported from $j \in R$ to $i \in D$ at $t \in T$ under scenario $s \in S$.
ω_i^{ts}	Binary variable indicate whether inventory at $i \in D$ at least meet the demand at $t \in T$ under scenario $s \in S$, $\omega_i^{ts} = 1$ if $y_i^{ts} \geq d_i^{ts}$ else $\omega_i^{ts} = 0$.
ϕ_i^{ts}	Binary variable that indicates whether a delivery is made to $i \in D$ at $t \in T$ under scenario $s \in S$.
l_i^{ts}	The most recent time that $i \in D$ consumed relief items before $t \in T$ under scenario $s \in S$.
DDCF decision variables:	
$\pi_i^{ts}(dt)$	Binary indicator variable that denotes whether the deprivation time of $i \in D$ at $t \in T$ under scenario $s \in S$ is $dt \in T$.
$\pi_i^{'t_{\max}s}(dt)$	Binary indicator variable that denotes whether the deprivation time of $i \in D$ at $t_{\max}$ under scenario $s \in S$ is $dt \in T$.
Γ_i^{ts}	Continuous variable that denotes the deprivation cost incurred for $i \in D$ at $t \in T$ under scenario $s \in S$.
$\Gamma_i^{'t_{\max}s}$	Continuous variable that denotes the deprivation cost incurred for $i \in D$ at $t_{\max}$ under scenario $s \in S$.
PHCR decision variables:	
λ_k^{nts}	Binary variable that indicates whether an order in quantity of o_k^{ns} is placed from $k \in K$ at $t \in T$ under scenario $s \in S$, $q_k^{-ts} = o_k^{ns}$ if $\lambda_k^{nts} = 1$.
ψ_k^{ns}	Binary variable that controls the length of quantity series under the quantity-flexibility contract.
o_k^{ns}	Quantity of relief item under the quantity-flexibility contract. $[o_k^{0s}, o_k^{1s}, \cdots, o_k^{ns}](n \leq t_{\max})$ denotes a quantity series under the quantity-flexibility contract.
q_k^{-ts}	Quantity of order placed from $k \in K$ at $t \in T$ under scenario $s \in S$.
q_k^{ts}	Quantity of order delivered from $k \in K$ at $t \in T$ under scenario $s \in S$.
$f_{kj}^{'ts}$	Quantity of relief items transported from $k \in K$ to $j \in R$ at $t \in T$ under scenario $s \in S$.
PRCR decision variables:	
q_k^{-ts}	Quantity of order, which is not the first one, placed from $k \in K'$ at $t \in T$ under scenario $s \in S$.
t_{0k}^s	Time when the first order is placed from $k \in K'$ under scenario $s \in S$.
$q_k^{-t_{0k}^s s}$	Quantity of the first order placed from $k \in K'$ under scenario $s \in S$.
g_k^{ts}	Quantity of order delivered from $k \in K'$ at $t \in T$ by the first order placement under scenario $s \in S$.
q_k^{ts}	Quantity of order delivered from $k \in K'$ at $t \in T$ under scenario $s \in S$.
$f_{kj}^{'ts}$	Quantity of relief items transported from $k \in K'$ to $j \in R$ at $t \in T$ under scenario $s \in S$.

S.2. Illustrative example for the deprivation cost

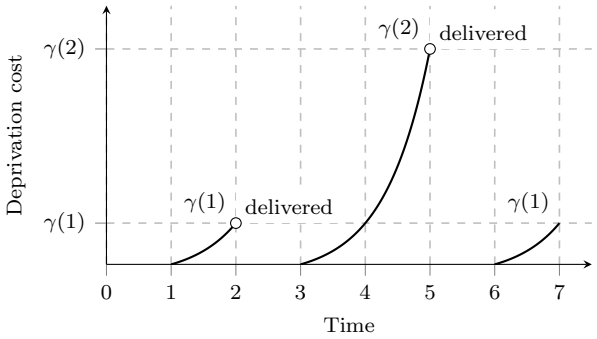

variables \ t	0	1	2	3	4	5	6	7
(delivery) ϕ^t		0	1	0	0	1	0	0
(consumption) l^t	0	1	1	3	3	3	6	6
(sufficiency) ω^t	1	0	1	0	0	1	0	0
$1-\omega^{t-1}$		0	1	0	1	1	0	1
$t-l^{t-1}$		1	1	2	1	2	3	1
(2.1)	$\gamma(1)+\gamma(2)+\gamma(1)$							

Figure S1: Deprivation cost function

Figure S1 provides an illustrative example for calculating deprivation cost with one affected area and six response periods (range from one to seven), assuming that the quantity of relief items delivered meets the demand for the next period and that these items are consumed during this period. The response action begins at $t = 1$ when the disaster strikes. From $t = 0$ to $t = 1$, no relief item is required, thus no deprivation cost is incurred. From $t = 1$ to $t = 7$, there are two deliveries that are made at $t \in \{2, 5\}$. Note that there is no delivery at $t = 7$. The values of ϕ^t, ω^t, and l^t can be obtained according to the left part of Figure S1, and they are presented in the right table in Figure S1. The overall deprivation cost can be calculated by substituting the values of ϕ^t, ω^t, and l^t to (2.1). The resulting deprivation cost is $2\gamma(1) + \gamma(2)$. Note that for $t = 7$, which is the last period of the planning horizon, $\phi^7(1-\omega^6)\gamma(7-l^6) = 0$ and $(1-\omega^7)\gamma(7-l^7) = \gamma(1)$ correspond the first and the second term of (2.1). This reflects that though there is not any delivery made at $t = 7$, since $t = 7$ is the end of the planning horizon, the deprivation cost incurred from $t = 6$ to $t = 7$ should be considered. Figure S1 also provides a more intuitive explanation than the mathematical formulation (2.1). At the beginning of the response period $t = 1$, there is no initial inventory, thus the deprivation cost begins to increase, and human suffering is incurred from $t = 1$ to $t = 2$. After the first delivery that exactly meets the demand of the following period ($t = 2$ to $t = 3$) is made at $t = 2$, there is no deprivation cost incurred till relief items are exhausted at $t = 3$. Then the deprivation cost continues to increase till the second delivery is made at $t = 5$, which meets demand from $t = 5$ to $t = 6$. Finally, at $t = 7$, though no delivery is made here, deprivation cost incurred from $t = 6$ to $t = 7$ must be considered. This explains the purpose of the second term of (2.1). In summary, (2.1) and Figure S1 reveal that for a particular affected area through the planning horizon, the deprivation cost increases continually till delivery is made. After this delivery, the deprivation cost is reset to zero, and the deprivation cost is added to the summation only when there is a delivery or at the end of the planning horizon.

S.3. Illustrative example for quantity-flexibility-contract constraints

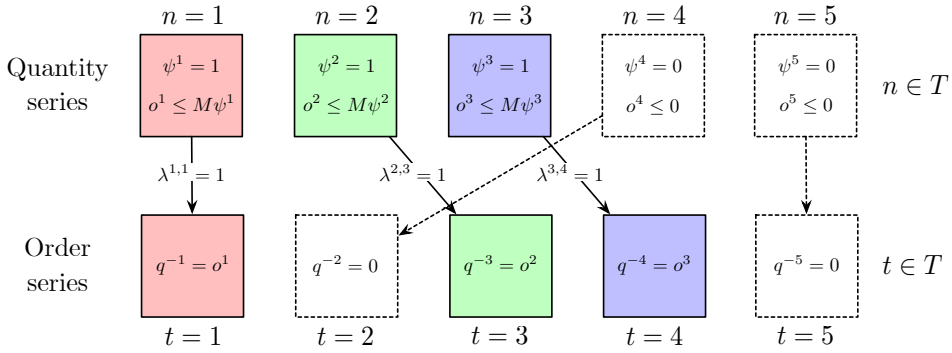

Figure S2: Quantity-flexibility contract

To model the contract, besides q_k^{-ts}, variables $\psi_k^{ns} \in \{0,1\}, o_k^{ns} \in \mathbb{Z}_0^+$, and $\lambda_k^{nts} \in \{0,1\}, \forall k \in K, n \in T, t \in T, s \in S$ are introduced. In the following, we omit the subscript k and superscript s for ease of presentation. Since it is possible that at a certain time period (e.g., $t = 2$ in Figure S2) there is not an order placed, the quantity-flexibility constraint $(1-\alpha)q^{-t} \leq q^{-t'} \leq (1+\beta)q^{-t}$ cannot be directly applied to variables q^{-t} ("order series" in Figure S2). Our idea to tackle this is to introduce an auxiliary "quantity series" (as in Figure S2), which satisfies the quantity-flexibility constraint, then assign items in the quantity series to the actual order series. Among variables associated with the quantity series, $\psi^n \in \{0,1\}, \forall n \in T$ control the length of the quantity series by (4.2) and (4.3). $o^n, \forall n \in T$ are quantities. Then $\lambda^{nt}, \forall n \in T, t \in T$ assign quantities to orders by (4.6), (4.7), and (4.8). To avoid crossing of solid arrows in Figure S2, which can violate quantity-flexibility constraint, (4.9) is introduced. The order series satisfies the quantity-flexibility constraint as long as the quantity series satisfies (4.4) and (4.5).

S.4. Linearization for conditional statement

(4.11), (5.2), (5.3), and (5.4) that contain the if statements are linearized in this section. Firstly, (4.11) is rewritten as

$$q_k^{ts} = \sum_{t' \in \{T | t' < t, t' + L_k = t\}} q_k^{-t's} = \sum_{t' \in \{1,\dots,t\}} \begin{cases} q_k^{-t's}, & \text{if } t' + L_k = t \\ 0, & \text{otherwise} \end{cases}.$$

Then we introduce a set of auxiliary parameter $\tau_k^{t't} \in \{0,1\} \forall t \in T, t' \in \{1,\dots t\}, k \in K, s \in S$ that denotes whether the order placed at t' is delivered exactly at time t with the lead time being L_k, i.e., $\tau_k^{t't} = 1$ if and only if $t' + L_k = t$ otherwise $\tau_k^{t't} = 0$. With the $\tau_k^{t't}$ we can calculate the quantity of relief item delivered at t (ordered at any time before t) as $q_k^{ts} = \sum_{t' \in \{1,\dots,t\}} \tau_k^{t't} q_k^{-t's}$, where $\tau_k^{t't} q_k^{-t's} \in \{0, q_k^{-t's}\}$ denotes the quantity of relief item ordered at t' and delivered at t. The constraint with if statement has been transformed into accumulating of binary parameter products continuous variable, which is linear. (4.11) is equivalent to

$$q_k^{ts} = \sum_{t' \in \{1,\dots,t\}} \tau_k^{t't} q_k^{-t's} = \sum_{t' \in T} \tau_k^{t't} q_k^{-t's}, \qquad \forall k \in K, t \in T, s \in S. \tag{S1}$$

This equality holds because it is impossible to deliver an order before it is placed, i.e., $\tau_k^{t't} = 0, \forall t' > t$.

It is more involved to linearize (5.2) - (5.4). similar to linearization for (4.11), let $\tau_k^{'t'ts}$ be a set of binary parameter that indicates whether the first order received by $k \in K'$ at $t' \in T$ is delivered exactly at $t \in T$, and $\tau_k^{t't}$ be binary parameters that indicate whether orders after the first one placed at $t' \in T$ is delivered at $t \in T$. Furthermore, let $q_k^{'-t's}$ denotes the quantity of the first order placed at $t' \in T$, in other words, for each (k,s) pair, for all $t' \in T$ there is at most one t' such that $q_k^{'-t's} > 0$. Then, recall that q_k^{-ts} denotes the quantity of an order after the first one, $q_k^{-ts} \le M \cdot \sum_{t' \in \{0,1,\cdots,t-1\}} q_k^{'-t's}$ holds since the second, third, etc. order must be made after the first one. Finally, a set of auxiliary binary variables that indicate whether the first order is placed at $t' \in T$ is denoted as $\zeta_k^{t's}$. (5.2) - (5.5) are reformulated to

$$\sum_{t' \in T} \zeta_k^{t's} \le 1, \qquad \forall k \in K', s \in S \tag{S2.1}$$

$$\epsilon \zeta_k^{t's} \le q_k^{'-t's} \le M \zeta_k^{t's}, \qquad \forall k \in K', t' \in T, s \in S \tag{S2.2}$$

$$q_k^{-ts} \le M \sum_{t' \in \{0,1,\cdots,t-1\}} q_k^{'-t's}, \qquad \forall k \in K', t \in T, s \in S \tag{S2.3}$$

$$q_k^{ts} = \sum_{t' \in T} \tau_k^{'t'ts} q_k^{'-t's} + \sum_{t' \in T} \tau_k^{t't} q_k^{-t's}, \qquad \forall k \in K', t \in T, s \in S \tag{S2.4}$$

$$q_k^{'-t's} \le \eta_k, \qquad \forall k \in K', t' \in T, s \in S \tag{S2.5}$$

$$\zeta_k^{t's} \in \{0,1\}, \qquad \forall k \in K', t' \in T, s \in S \tag{S2.6}$$

$$q_k^{'-t's} \in \mathbb{Z}_0^+, \qquad \forall k \in K', t' \in T, s \in S \tag{S2.7}$$

(S2.1) ensures there is at most one point of time at which the first order is placed. (S2.2) ensures the first order quantity is incurred and only incurred when the first order is placed. (S2.3) makes sure other orders are only made after the first one. (S2.4) calculates delivered order quantity at $t \in T$ by adding up the first order delivered at $t \in T$ and other orders delivered at $t \in T$. Note that in (S2.4), $\tau_k^{'t'ts}$ is scenario-dependent while $\tau_k^{t't}$ is scenario-independent, which reflects that only the first lead time is uncertain in the PRCR model. (S2.5) limits the maximum order quantity by the capacity of $k \in K$. (S2.6) and (S2.7) are domains of auxiliary decision variables.

S.5. Transformation for subgradient cuts using indicator constraints

Conditional statement in (9.1) and (9.2) is not supported directly by off-the-shelf solvers. We transform (9.1) and (9.2) into an equivalent form (S3.1) - (S3.5) using indicator constraints. By introducing binary indicator variables $h^{s(v)} \in \{0,1\}$, such that $\sum_{j \in R} r_j \ge \sum_{j \in R} \bar{r}_j$ if and only if $h^{s(v)} = 1$ and $\sum_{j \in R} r_j \le \sum_{j \in R} \bar{r}_j - 1$ if and only if $h^{s(v)} = 0$, we have

$$h^{s(v)} = 1 \Rightarrow \sum_{j \in R} r_j \ge \sum_{j \in R} \bar{r}_j \tag{S3.1}$$

$$h^{s(v)} = 0 \Rightarrow \sum_{j \in R} r_j \le \sum_{j \in R} \bar{r}_j - 1 \tag{S3.2}$$

$$h^{s(v)} = 1 \Rightarrow \theta_s \ge \hat{Q}(\bar{X}, \xi_s) - \nabla_1^s \cdot \sum_{j \in R} (r_j - \bar{r}_j) \tag{S3.3}$$

$$h^{s(v)} = 0 \Rightarrow \theta_s \ge \hat{Q}(\bar{X}, \xi_s) + \nabla_2^s \cdot \sum_{j \in R} (\bar{r}_j - r_j) \tag{S3.4}$$

$$h^{s(v)} \in \{0,1\}. \tag{S3.5}$$

(S3.1) and (S3.3) are derived from $h^{s(v)} = 1 \Leftrightarrow \sum_{j \in R} r_j \ge \sum_{j \in R} \bar{r}_j$ and (9.1). Similarly, (S3.2) and (S3.4) are derived from $h^{s(v)} = 0 \Leftrightarrow \sum_{j \in R} r_j \le \sum_{j \in R} \bar{r}_j - 1$ and (9.2).

S.6. Proof for validity of Benders cuts

Substitute $\nabla_1^s = \max\{\max_{k\in K\cup K'} p_k, \nu^s\}$ and $\nabla_2^s = 0$ into (9.1) and (9.2) respectively we have

$$\sum_{j\in R} r_j \geq \sum_{j\in R} \bar{r}_j \Rightarrow \theta_s \geq \hat{Q}(\bar{X}, \xi_s) - \max\left\{\max_{k\in K\cup K'} p_k, \nu^s\right\} \cdot \sum_{j\in R}(r_j - \bar{r}_j) \tag{S4.1}$$

$$\sum_{j\in R} r_j \leq \sum_{j\in R} \bar{r}_j - 1 \Rightarrow \theta_s \geq \hat{Q}(\bar{X}, \xi_s). \tag{S4.2}$$

Property (i): (S4.1) and (S4.2) exclude the current master problem solution if it is not globally optimal.

Let $(\bar{r}_j, \bar{\theta}_s)$ denotes a master problem solution that is not globally optimal, it is implied that $\bar{\theta}_s < \hat{Q}(\bar{X}, \xi_s)$ (the condition for adding cuts). If $(\bar{r}_j, \bar{\theta}_s)$ is obtained again in a future iteration, substitute $(\bar{r}_j, \bar{\theta}_s)$ to (S4.1) and (S4.2) we have $\bar{\theta}_s \geq \hat{Q}(\bar{X}, \xi_s)$, which contradicts $\bar{\theta}_s < \hat{Q}(\bar{X}, \xi_s)$. Thus property (i) holds.

Property (ii): There exists a ν^s that let (S4.1) and (S4.2) do not remove any globally optimal solution.

Let ν^s be a sufficiently large constant such that the inequality $Q(X, \xi_s) \leq \max\{\max_{k\in K\cup K'} p_k, \nu^s\} \cdot \sum_{j\in R}(r_j - \bar{r}_j)$ holds for all values of $X = \{r_j\}$. Since θ_s is nonnegative, (S4.1) and (S4.2) become

$$\sum_{j\in R} r_j \geq \sum_{j\in R} \bar{r}_j \Rightarrow \theta_s \geq 0 \tag{S5.1}$$

$$\sum_{j\in R} r_j \leq \sum_{j\in R} \bar{r}_j - 1 \Rightarrow \theta_s \geq \hat{Q}(\bar{X}, \xi_s). \tag{S5.2}$$

Let (r_j^*, θ_s^*) be the optimal solution and assume it is excluded by (S5.1) and (S5.2), one of the following cases must holds

$$\sum_{j\in R} r_j^* \geq \sum_{j\in R} \bar{r}_j \bigwedge \theta_s^* < 0 \tag{S6.1}$$

$$\sum_{j\in R} r_j^* \leq \sum_{j\in R} \bar{r}_j - 1 \bigwedge \theta_s^* < \hat{Q}(\bar{X}, \xi_s). \tag{S6.2}$$

Since θ_s is nonnegative, it is clear that (S6.1) does not hold. Considering that $\hat{Q}(\bar{X}, \xi_s)$ is the minimum $Q(\cdot)$ with the given $\bar{X} = \{\bar{r}_j\}$ and $Q(\cdot)$ is monotonically decreasing with $\sum_{j\in R} r_j$, i.e., if $\sum_{j\in R} r_j^* \leq \sum_{j\in R} \bar{r}_j - 1$ holds then $\theta_s^* \geq \hat{Q}(\bar{X}, \xi_s)$ must holds. Thus, (S6.2) also does not hold, which makes property (ii) holds by contradiction. In summary, property (i) and (ii) hold for (9), there is a ν^s that let (9) be a valid logic-based Benders cut (Theorem 1).

S.7. Instance parameters

Table S2: Instance parameters

Parameters	Description	Value
Variable parameters		
$\|D\|$	Number of affected area	{5, 10}
$\|T\|$	Number of time period	{3, 5} ({6 days , 10 days})
$\mathcal{C}$	Patterns of consumption rate	{0, 1, 2}
Stochastic parameters		
$\mathcal{C}_0(t)$	Increasing consumption rate (per person per period)	$\mathcal{C}_0(t) \sim N(1.75/(1+e^{-0.4t}) - 0.75, 0.05^2)$
$\mathcal{C}_1(t)$	Decreasing consumption rate (per person per period)	$\mathcal{C}_1(t) \sim N(1.50/(1+e^{0.6t}) + 0.25, 0.05^2)$
$\mathcal{C}_2(t)$	Steady consumption rate (per person per period)	$\mathcal{C}_2(t) \sim N(0.5, 0.05^2)$
d_i^{ts}	Demand of relief item (per period)	$d_i^{ts} = w_i \mathcal{C}_*(t)$
L_k^s	Lead time for the first order of PRCR supplier	$L_k^s \sim U(2, 4)$
Deterministic parameters		
Affected area:		
v_i	Capacity of affected area	$2 \times w_i \left(\max_{t\in T} \mathbb{E}\mathcal{C}_*^s(t) + 3\sigma_*\right)$
w_i	Population of affected area	$U(5000, 100000)$
Deprivation cost function:		
$\gamma(t)$	Deprivation cost function	\$ $\min\{\gamma^{\max}, 0.2354 \times e^{0.1129\times 48\times t}$ if $t \geq 1$ else $0\}$
$\gamma^{\max}$	Value of life	\$ 1,000,000
Local distribution cnter:		
u	Unit prepositioning acquiring cost	\$ 100
v_j	Capacity of facility	$2 \times \|T\| \sum_{i\in D} w_i \left(\max_{t\in T} \mathbb{E}\mathcal{C}_*^s(t) + 3\sigma_*\right) / \|R\|$
PHCR supplier:		
p_k	Unit PHCR acquiring cost	\$ 60
α_k, β_k	Quantity-flexibility contract parameters	0.2, 0.2
η_k	Maximum production capacity	$2 \times \sum_{i\in D} w_i \left(\max_{t\in T} \mathbb{E}\mathcal{C}_*^s(t) + 3\sigma_*\right) / \|K\|$
L_k	Lead time	1
PRCR supplier:		
p_k	Unit PRCR acquiring cost	\$ 50
η_k	Maximum production capacity	$4 \times \sum_{i\in D} w_i \left(\max_{t\in T} \mathbb{E}\mathcal{C}_*^s(t) + 3\sigma_*\right) / \|K\|$
L_k	Lead time for orders after the first one	1

[1] U: integer uniform distribution; $N(\mu, \sigma^2)$: normal distribution truncated at $\mu - 3\sigma$ and $\mu + 3\sigma$.

S.8. Illustration for the consumption rate

Figure S3 shows the expected values of $\mathcal{C}_0(t)$, $\mathcal{C}_1(t)$, and $\mathcal{C}_2(t)$ as lines, while the shaded areas represent the range within three standard deviations from the mean ($[\mathbb{E} - 3\sigma, \mathbb{E} + 3\sigma]$).

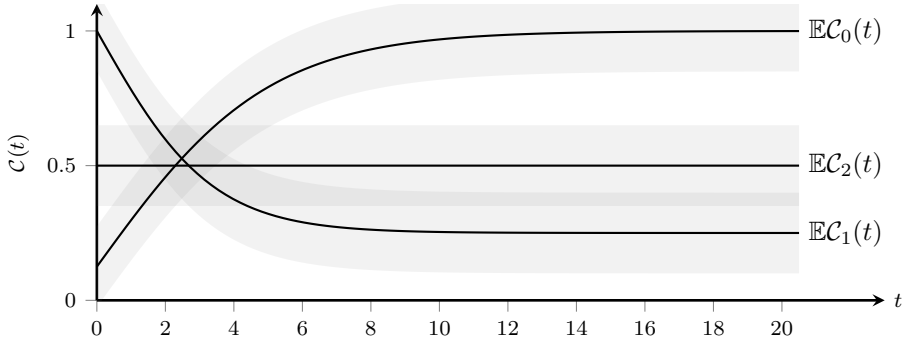

Figure S3: Consumption rate

S.9. State-level main effects and interaction effects

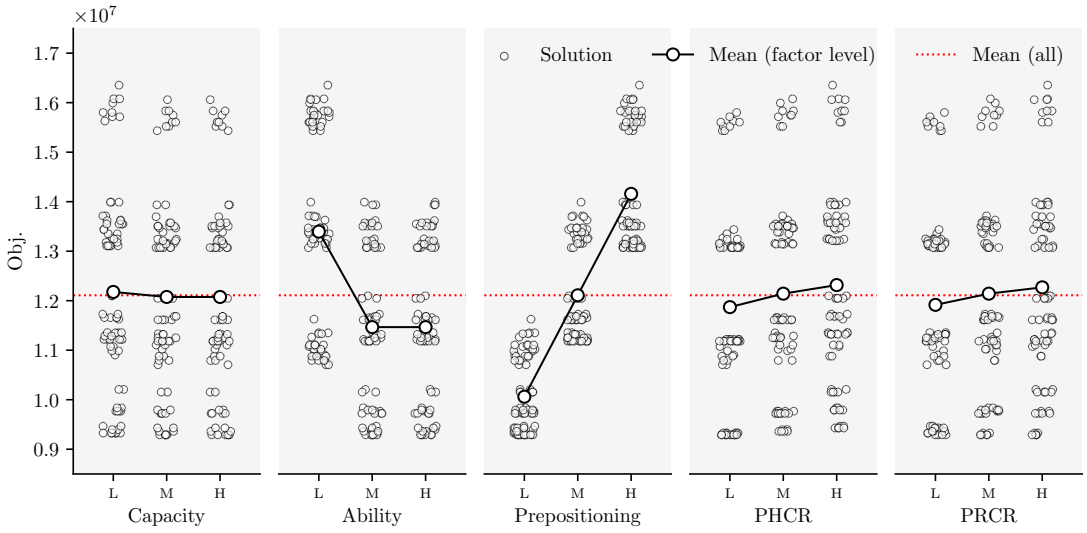

Figure S4: State-level main effects

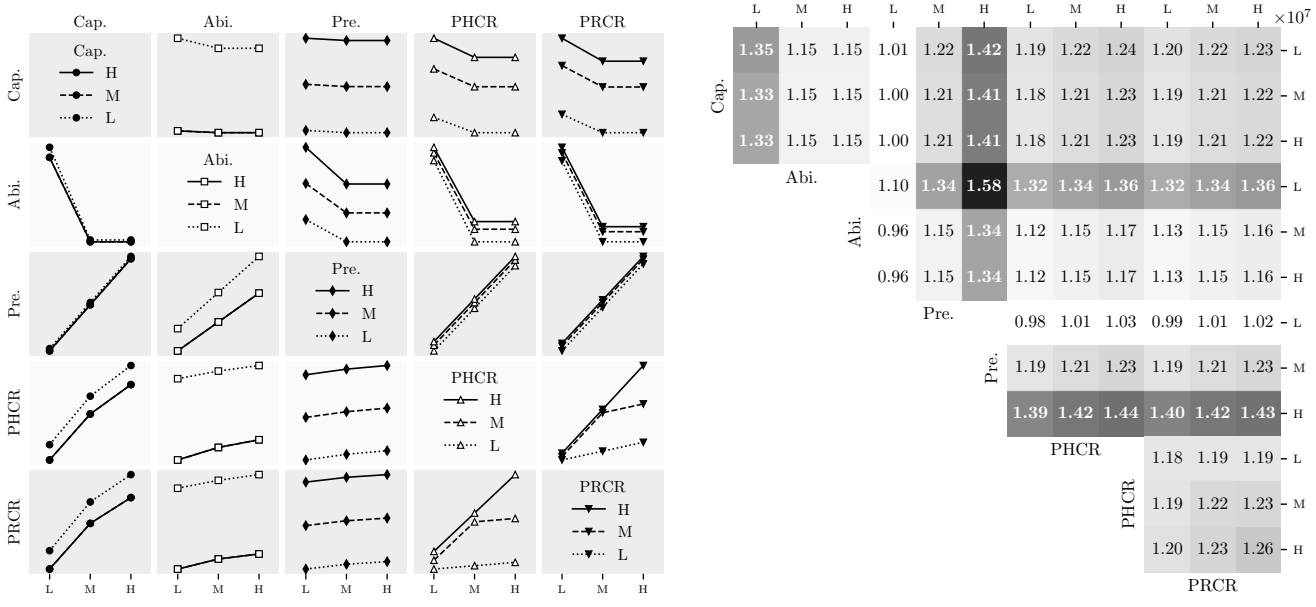

(a) Interaction effect plot

(b) Interaction heatmap

Figure S5: State-level interaction effects